PALEOMAGNETISM AND TECTONICS OF NORTHERN MUNESSA, ETHIOPIA

A Thesis submitted to School of Graduate studies of Addis Ababa University in Partial fulfillment for the requirements of the Degree of Master of Science in Earth Sciences (Structural Geology and Tectonics).

By: DIRIBA ALEMAYEHU GURMU

June, 2012

ADDIS ABABA UNIVERSITY

SCHOOL OF GRADUATE STUDIES

PALEOMAGNETISM AND TECTONICS OF NORTHERN MUNESSA, ETHIOPIA

BY:

DIRIBA ALEMAYEHU GURMU

DEPARTMENT OF EARTH SCIENCES

APPROVED BY:

Dr. Sefu Kebede……

Chairperson

Dr. Tesfaye Kidane……..

Advisor

Dr. Bekele Abebe……

Examiner

Dr. Girma W/Tensae …….

Examiner

ABSTRACT

The paleomagnetic investigation is carried out in the eastern part of lake langano-ziway, Main Ethiopian Rift. The aim of this paleomagnetic study is to quantify vertical axis rotation.A total of 11 paleomagnetic samples were sampled from outcrop of basalt, ignimbrites and rhyolite flows ranging in age from 2ma to 0.1ma. The paleomagnetic specimens are subjected to progressive alternating field demagnetization, thermal demagnetization and impulse magnetization. In general, the directional analysis showed either one or two components of Natural Remanent Magnetization (NRM) to characterize the wholemeasurements. The low stability components are removed by alternating fields up to 15mt or by heating up to 300^{o}C. The high stability components are isolated above those steps and vector is directed towards origin, and it represented by Characteristic Remanent Magnetization (ChRM). The principal component analysis and site mean directions calculation yielded normal and reversed polarities. An overall mean direction calculated from individual site mean directions are Ds=354.1^{o}, Is=8.3^{o}, N=11, K =22, α_{95}=10^{o}, with an angular difference of -7.8 ± 8.24 and the negative value indicate the rotation is counter clock wise.The comparison of this result with the mean expected reference dipole geomagnetic field direction (Ds=1.9, Is=13.5, N=32, K=105.6, andα_{95} =2.5), from the apparent polar wander path reference curve for Africa at 1.5 ma (Besse&Courtillot 2003), found to be statistically different. This would imply that the area is at the contact of central and rift margins with small rotation. These results indicate that the late Pliocene-Pleistocene rocks of the MER in the study area show small vertical axis rotation, argue transtensional and seafloor-spreading-transform kinematic models. It is therefore, suggested that large offset faults, produce the right stepping, en echelon magmatic segments of the MER, which is at the transition from continental to oceanic extensionrather thanmagma intrusion.

Contentspage

List of Index

List of figures

List of Tables

List of Symbols and abbreviations

AF= Alternating Field

APWP= Apparent Polar Wander Path

ChRM= Characteristics Remnant Magnetization

D= Declination

EARS= East African Rift System

GAD= Geocentric Axial Dipole

GPTS= Geomagnetic Polarity Time Scale

I= Inclination

IRM= Induced Remnant Magnetization

MAD= Maximum Angular Deviation

MD= Multi Domain

MER= Main Ethiopian Rift

mT= mili Tesla

NRM= Natural Remnant Magnetization

PCA= Principal Component Analysis

SD= Single Domain

TRM= Thermal Remnant Magnetization

WFB= Wonji Fault Belt

VRM= Viscous Remnant Magnetization

1. INTRODUCTION

1.1 Paleomagnetism and Tectonics

The geology of east Africa was affected by voluminous flood basalt eruptions 30Ma ago and later break up, between Africa and Arabian plates and led to the formation of east African rift system (EARS), (Hoffman et al. 1997).

According to Boccaletti M., et al., (1997) the Ethiopian rift is roughly NE oriented segment of the east African rift system and it extends about 1000km in a NE-SW to N-S from afar to southern Ethiopia (fig.1.1). It represents an area of crucial geological interest since it is a segment of the EARS that connects the afar depression, at the Red sea-Gulf of Aden junction, with the Gulf of Aden ridge (see fig.1.1).It is a magmatic rift of the different stages of rift evolution, i.e. from rift initiation to break up and developing oceanic spreading (e.g. Ebinger, 2005, Corti, G., 2009), and marking the initial boundary between Nubia and Somalia plates. Based on either plate tectonics kinematics or structural and geological studies, the tectonic evolution of Ethiopian rift were NW-SE with pure extension(Bonini et al., 1997).

On the basis of structural features the Ethiopian Rift is divided into the N-E oriented northern ER (NER), and the central and southern Ethiopian Rift, both oriented NNE–SSW, and it cuts the NW oriented Turkana depression in the south and connects to the Afar depression in the north. Accordingly, the NER is linked to the Red Sea and Gulf of Aden rifts and thus to the global oceanic rift system at the Afar triple junction (R–R–R). The development of the EARS (the formation of magmatic provinces, plateau uplift, crustal thinning and rifting) is attributed to one or several Paleocene mantle plumes (Schilling et al., 1992; Ebinger and Sleep, 1998). The northern ER is one of the few areas in the world where the crust is in a transitional stage from continental to oceanic.

The regional fault distribution is very complex, but it permits a general structural subdivision of the ER into two main segments: the Main Ethiopian Rift (MER) and the Southwestern Ethiopian Rift (SER).

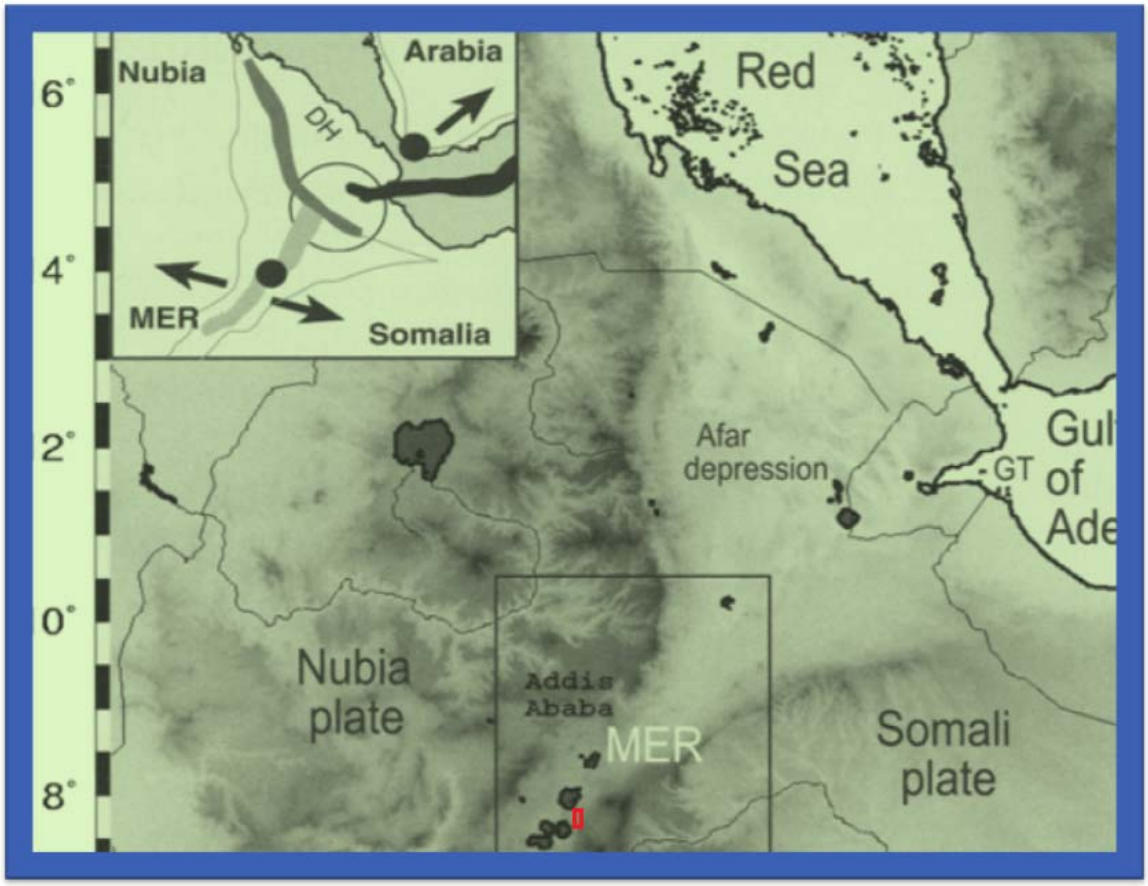

Fig.1.1 Elevation model diagram of the East African rift system (after T. Kidane et al., 2006).

The Main Ethiopian Rift (MER) forms the northernmost sector of the East African rift system stretching from Lake Abay in the south to Gabilema volcano in the north where it forms the third arm of the Afar-triple junction (Fig. 1.1.).

Hoffman et al.,(1997) suggested the MER is 700 km-long, 80km-wide and volcanically active rift situated between the Ethiopian and Somalian plateaus, which are covered by Oligocene-Miocene lavas. It is one of the few places in the worldwhere one can observe the process of continentalrifting and study the patterns of faulting and eruptivevolcanic centers prior to continentalbreak-up.

Diriba A. Paleomagnetism and Tectonics of Northern Munesa, 2012. MSc thesis, Tel: +251-910-66-7446, email: nabekdiriba@hotmail.com, Addis Ababa; Ethiopia

Geological field observations andhistoric-recent seismic activity be evidence of ongoingextension in the MER (Gouin 1979; Asfaw 1992).

According to Bastow et al. (2005); Kendall et al. (2005), low seismic velocities and lowdegree of seismic anisotropy recorded beneath therift and indicate the existence of melt.

Two main fault systems have been distinguished in the MER: a N30^{o}E-N40^{o}Etrending fault system which characterizes mainly the rift borders, and a N-S to N20^{o}Etrending fault system, the Wonji Fault Belt (WFB) of Mohr (1962, 1967, 1987), which exhibits a number of sigmoidal, overlapping, right-stepping en-echelon fault zones obliquely cutting the rift floor.

The MER attains a width of about 100 km in the central sector, between Fonko and the Langano Lake area, but narrows southward in the Abaya region, where it is bifurcated by the N-Sstriking Amaro horst. This in fact separates the Ganjuli basin in the west, from the Gelana depression in the east. Distribution of volcanic rocks along the MER boundary faults show a discontinuous sequence ranging in age from the Late Eocene up to the Plio-Quaternary (Mohr, 1970; WoldeGabriel et al., 1990, 1991; Ebinger et al., 1993). Late Pliocene- Quaternary volcanism is mainly localized in the rift floor, although volcanic activity is also present in the Ambo area (WoldeGabriel et al., 1990) and in Southern Ethiopia (Davidson, 1983). The whole volcanic successions exposed along the border faults of both margins indicate a bimodal magma system of acidic and basic associations (WoldeGabriel et al., 1990; Alula et al., 1992; Boccaletti et al., 1995). E-W to WNW-ESEtrending cross-rift oblique slip transfer faults transects the rift floor and Quaternary volcanic centers are commonly located along them (Davidson and Rex, 1980; WoldeGabriel et al., 1990; Ebinger et al., 1993; Hayward and Ebinger, 1996). At places, cross-rift structures are overprinted by the WFB volcanotectonic axis (WoldeGabriel et al., 1990).

The several sub parallel Quaternary fault belts (WFB) give rise to a widespread deformation affecting the MER floor and, in the interior of the rift, making angles of 20^{o} with respect to the main direction of the margin.

The gently curved s-shaped adjustment of these fault zones with the $N30^{o}E$-$N40^{o}E$ oriented border faults, as well as their right-stepping en-echelon arrangement, implies the existence of a sinistral shear component along the Main Ethiopian Rift, as suggested by some authors (Mohr, 1968; Gibson, 1969; Gibson and Tazieff, 1970; Kazmin, 1980; Boccaletti et al., 1992). According to Di Paola (1972); and Casey et al. (2006), along the margins of the rift, large offset border faults are characterized by rift ward en echelon right-stepping normal faults with a dominant orientation of NNE-SSW to NE-SW, having characteristic structural styles on the eastern and western margins.

According to Boccaletti et al., (1994); Abebe, (1993); Bonini et al., (1997) recent structural investigations in the Assela and Adama area are consistent with a change in extension direction from NW-SE to E-W during the Quaternary with implications for vertical axis block rotations. However, paleomagnetic results from the same region indicated an absence of vertical axis rotations (Kidane et al., 2006). The structural grain of the MER, including the orientation of the border faults, shows significant along-strike variations.

Paleomagnetism studies help to know the direction and intensity of earth's magnetic field through geologic time, and are useful for determining the movement of rocks both on a large and small scale. On a large scale, Paleomagnetism studies show how the continental and oceanic plates have drifted relative to the earth's spin axis and to one another. On a small scale, it helps to determine the movement of crustal blocks in continents, particularly vertical axis rotation.Oligocene-Recent volcanic rocks including basalts, ignimbrites and rhyolites crop out along the rift margin and also cover the floor of the MER (fig.3.2).

In some places, these flows form thick piles, making them suitable for paleomagnetic investigations and providing a good opportunity to study the geology, tectonic evolution as well as features of the geomagnetic field which are the main purpose of assigning this research.

1.2 Description of the study area

1.2.1 Location and accessibility

The study area is located about 250km south of Addis Ababa in the north-east Lake Langano and segmented with in the MER (fig.1.2). The area is accessible for study and good weather for extensive field work. Geographically the area is bounded between 830000m N to 890000m Nand 470000m E to 520000m E.

This rift area is manifested faulted blocks with relatively steep scarps that form local horst and graben structures and cinder cones which constitute very rugged topography.

Diriba A. Paleomagnetism and Tectonics of Northern Munesa, 2012. MSc thesis, Tel: +251-910-66-7446, email: nabekdiriba@hotmail.com, Addis Ababa; Ethiopia

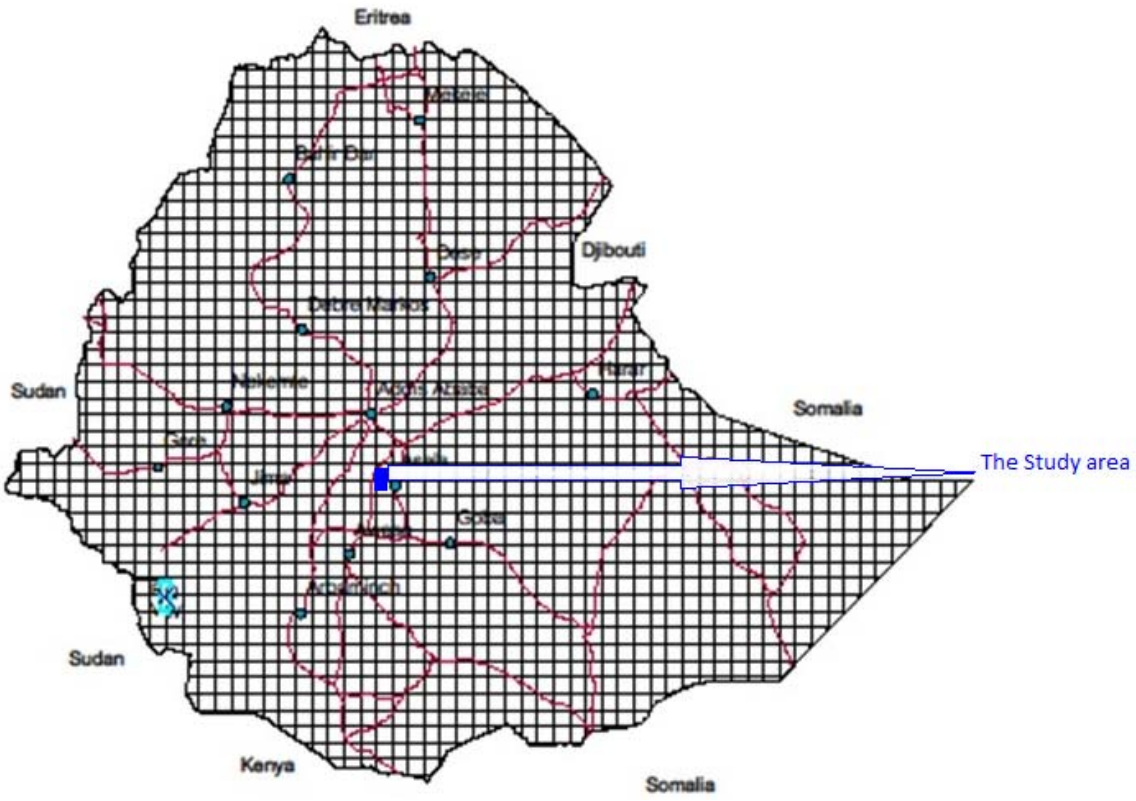

Fig.1.2Location map of the conducted area.

1.2.2 Physiography and drainage

The study area is generally characterized by the existence of both mountainous at the margins and flat topography at the center and rectangular drainages. The area is extended and relatively narrow extension fractures and different volcanic structures such as brecciated lava flows, lava domes, cinder cones, crater and calderas are the most notable features with in the study area and the surrounding.

1.2.3 Objectives

Diriba A. Paleomagnetism and Tectonics of Northern Munesa, 2012. MSc thesis, Tel: +251-910-66-7446, email: nabekdiriba@hotmail.com, Addis Ababa; Ethiopia

The general objective of the study is to quantify crustal block rotation to rift overlap and propagation in the rift floor, which is significant to paleomagnetic methods, with respect to vertical axis.

The Specific objectives include the following:

- Determining vertical axis tectonic rotation;
- Determining average direction and the paleomagnetic pole for MER;
- Determining ferromagnetic minerals;
- Describing tectonic setting in the area;
- Determining way of extension in the future in the area;
- Lithological and structural mapping.

Therefore to address the objectives the following methods, materials and procedures are used.

1.3 METHODS, MATERIALS AND PROCEDURES

The scientific approach involves the steps outlined below:

1.3.1. Pre-field Works

At the first steps of the study, different available information about the area and previous works are gathered and evaluated. This section includes reading and organizing all published and unpublished reports on geology, and applications of Paleomagnetism to

Diriba A. Paleomagnetism and Tectonics of Northern Munesa, 2012. MSc thesis, Tel: +251-910-66-7446, email: nabekdiriba@hotmail.com, Addis Ababa; Ethiopia

tectonics and related activities, and analyzing topographic, and geological and structural maps of the area at large (1:50,000) and small scales (1:250,000).

Preliminary field work was conducted for ten days from 20/11/2010 to 29/11/2010 with Japanese researcher around Kesem area of the Main Ethiopian Rift. Sampling and drilling of oriented core samples were performed to get familiar with field techniques.

1.3.2. Field Activities

The objective of the field work is to collect samples for paleomagnetic analysis, and geological mapping and identifications. During field activities 11 paleomagnetic sites were collected in one season that is at the beginning of March 2011 and a total of 95 cores were collected for paleomagnetic analysis and they oriented using both magnetic and sun compass.

Mostly fissural basalt (mafic lava flow) and welded ignimbrite (felsic pyroclastics flows) are taken as paleomagnetic sites and there is very weak rhyolite with ash and obsidian. The general paleomagnetic sampling scheme were described in the following (fig.1.3).

A **rock unit:** This is an exposed sequence of beds in a sedimentary sequence or cooling units in an igneous complex, usually a member of a geological formation, an entire formation, or even a sequence of formations (fig.1.3). The rock units during field work (volcanic rock) were cropped out along fault scarps, road cuts and river valley exposure.

A **site:** itis an outcropped of a particular bed in a sedimentary sequence or a cooling unit in an igneous complex (i.e., a lava flow or dike) (fig.1.3) in which paleomagnetic samples are collected. Multiple sites within a given rock unit are needed to provide adequate time sampling of the geomagnetic field fundamental to most paleomagnetic applications.

During the field work about 11 paleomagnetic sites conducted from basalts, ignimbrites and rhyolite exposed in the area. From these paleomagnetic sites seven sites are from ignimbrite, three from basalt, and one from rhyolite (which is not good for paleomagnetic interpretation because of poor magnetization content).

Samples: are separately oriented pieces of rock that are collected from the selected paleomagnetic sites (fig.1.3). Totally 95 samples were collected from eleven sites during field studies and six to ten separately oriented samples from each sites spread over 5 to 10m of outcrop. Comparison of NRM directions from sample to sample within a site allows within-site homogeneity of the NRM to be evaluated. Because of the flat-lying of the bedding at each site, the orientation of the bedding are not collected and as a result there is no structural correction take place and the geographic coordinates are the same with the stratigraphic coordinates.

Specimens: are pieces of samples prepared to appropriate dimensions for measurement of NRM. Multiple specimens may be prepared from an individual sample, and this procedure can provide additional checks on homogeneity of the NRM and experimental procedures. Often only a single specimen is prepared from a particular sample, and little is gained by preparing more than three specimens from a sample; at the starting of laboratory activities.The prepared specimens have volume $10cm^3$ in average similar with standard specimens.

Diriba A. Paleomagnetism and Tectonics of Northern Munesa, 2012. MSc thesis, Tel: +251-910-66-7446, email: nabekdiriba@hotmail.com, Addis Ababa; Ethiopia

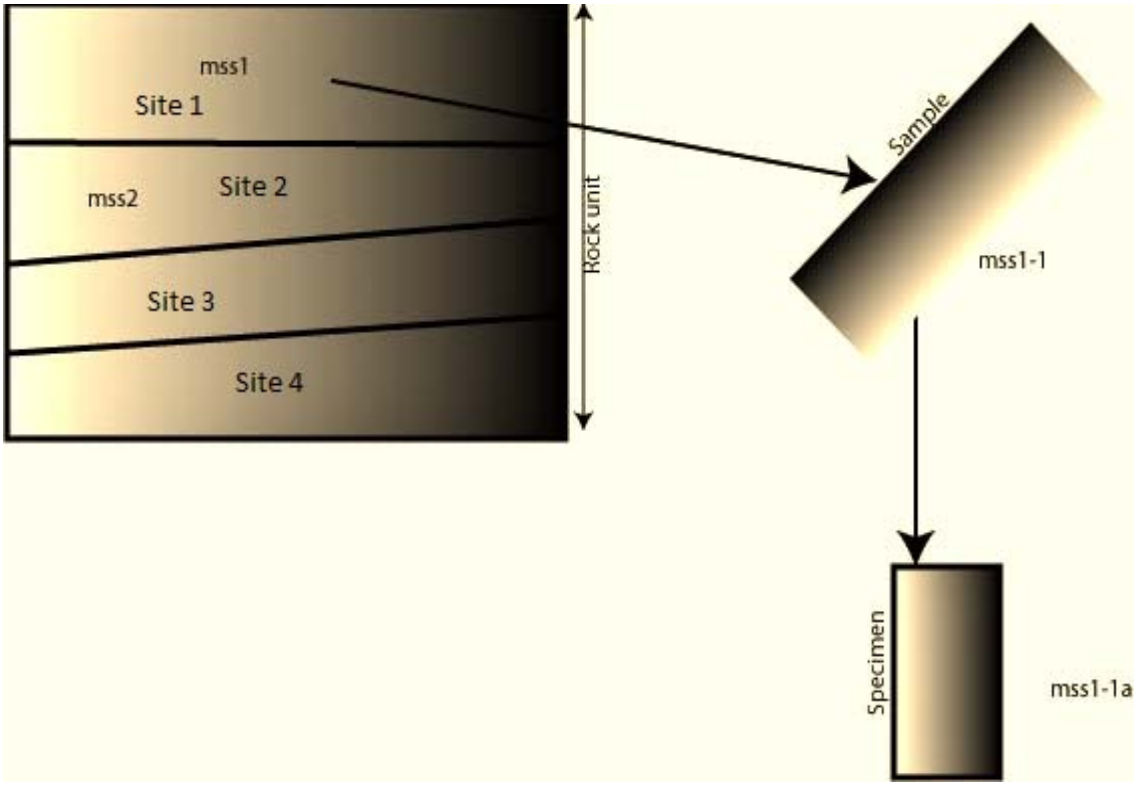

Fig.1.3. Paleomagnetic sampling scheme. Multiple sampling sites are collected within the rock unit; multiple samples are collected from each site; specimens for laboratory measurements are prepared from samples.

Diriba A. Paleomagnetism and Tectonics of Northern Munesa, 2012. MSc thesis, Tel: +251-910-66-7446, email: nabekdiriba@hotmail.com, Addis Ababa; Ethiopia

2. Paleomagnetic Sampling and analysis

Sampling sites were selected to be representative of a single lava flow and pyroclastics rocks, and the location of each site is well-known using GPS and located on fig.4.4. Cores were oriented in the field with both solar and magnetic compass (fig.2.1). The orientation procedure was done in order to obtain accurate geographic orientation of each sample (Butler, 1992). The sun angle and local time are recorded as a check because of possible magnetic disturbances that might affect the magnetic compass reading.

A paleomagnetic investigation involves numerous sites to collect numerous samples within a particular rock unit. These site-mean directions must be averaged to yield either the average ChRM direction or a paleomagnetic pole position from the rock unit using Remasoft and Paleomac program.

Logistics of sample collection dictate strategies for obtaining oriented samples. Basic attributes of the most common sampling methods are samples cored with portable drill, Block samples, and Lake-bottom or sea-bottom core samples. Out of these methods of sampling collections core sampling were used for this research, and discussed below.

1. Samples cored with portable drill. The most common type of paleomagnetic sample is collected by using a gasoline-powered portable drilling apparatus with a water-cooled diamond bit (Fig.2.2a).

The diameter of cores is about 2.5 cm. After coring of the outcrop to a depth of 6 to 12 cm (Fig.2.2b), an orientation stage is slipped over the sample while it is still attached to the outcrop at its base (Fig.2.2c). Orientation stages have an inclinometer for determining inclination (dip) of the core axis and magnetic or sun compass (or both) for determining azimuth of core axis.

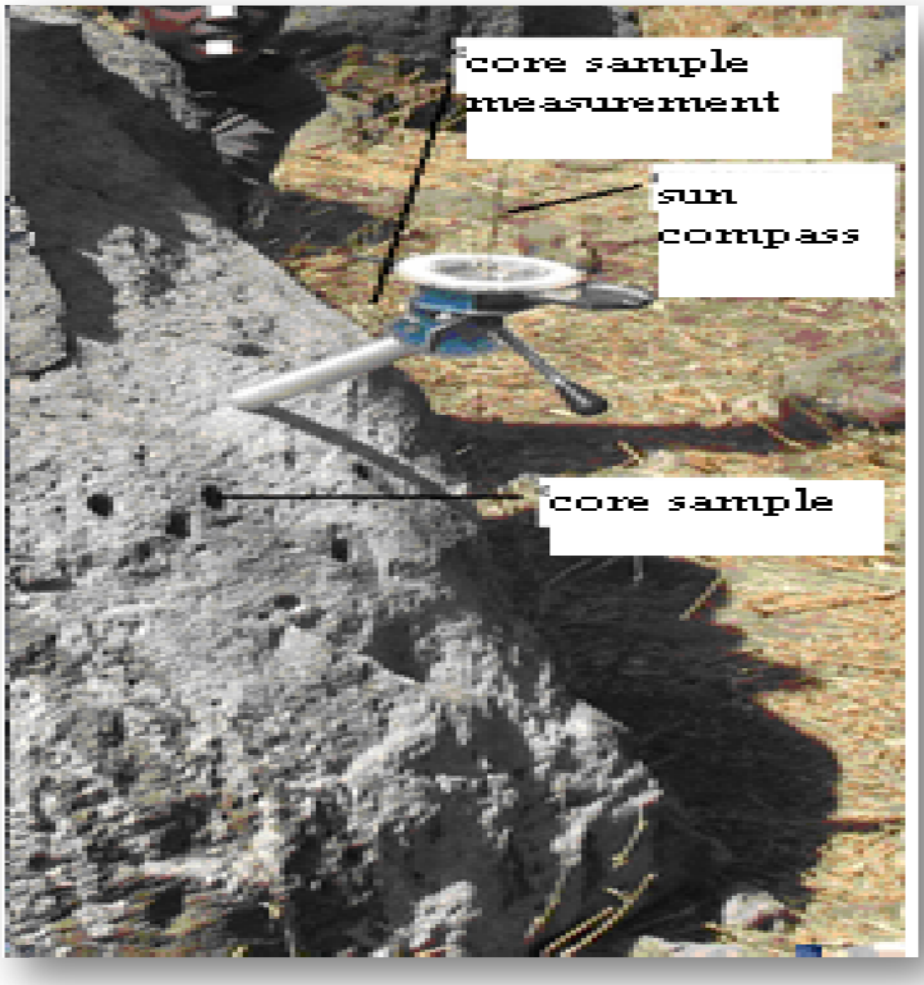

Fig.2.1 Core sample measurements.

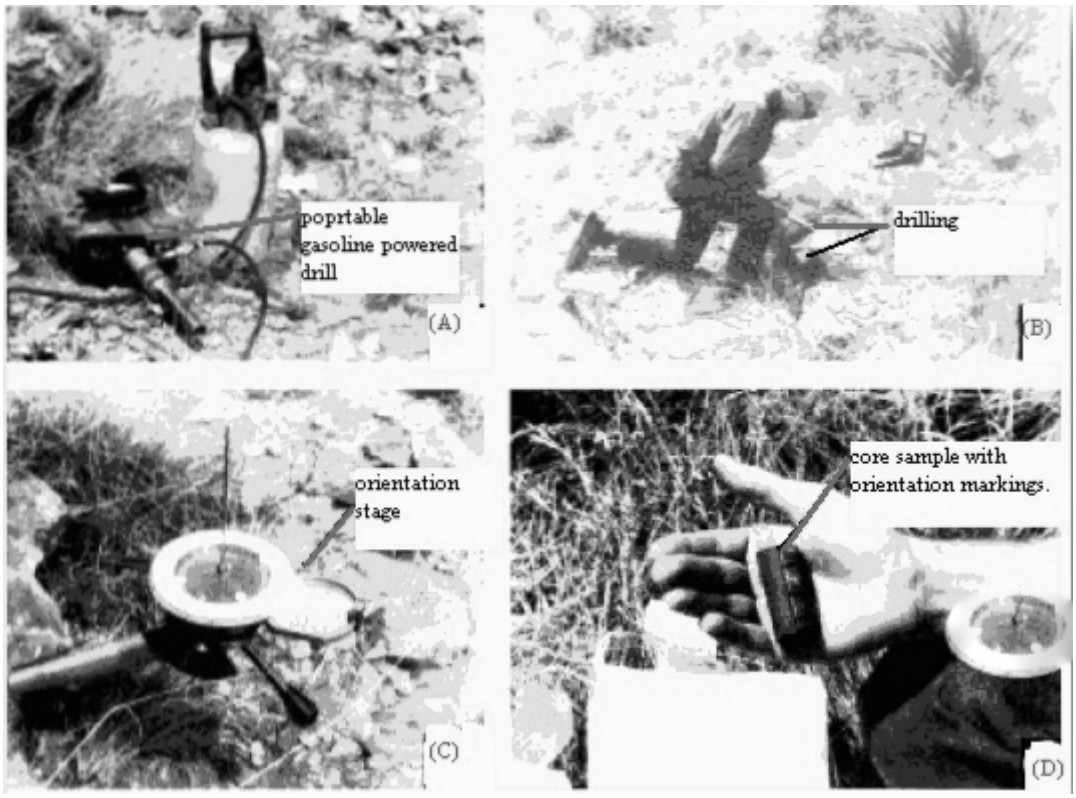

Fig.2.2. Core samples collection procedures. (A) Portable gasoline-powered drill with diamond drilling bit; a pump is used to force cooling water through the drill bit. (B)Drilling a core. (C) Orientation stage placed over in situ core. (D) Core sample with orientation markings.

The samples must be oriented before they are taken from the rock units. If a magnetic compass is used to orient samples in the field, the measured azimuth must be adjusted by the local magnetic declination. A dial with a vertical needle is placed on the horizontal platform. The angle (α) that the sun's shadow makes with the drilling direction is noted as well as the exact time of sampling and the location of the sampling site. With this information and the aid of the Astronomical Almanac or a simple algorithm, it is possible to calculate the desired direction to the reasonable accuracy.

Diriba A. Paleomagnetism and Tectonics of Northern Munesa, 2012. MSc thesis, Tel: +251-910-66-7446, email: nabekdiriba@hotmail.com, Addis Ababa; Ethiopia

After orientation, the core is broken from the outcrop, marked for orientation and identification (Fig.2.2d), and returned to the laboratory. Advantages of the coring technique are the ability to obtain samples from a wide variety of natural or artificial exposures and accurate orientation. Disadvantages include the necessity of transporting heavy fluids (water and gasoline) to the sampling site, dependence on performance of the drilling apparatus (often in remote locations), and herniated disks suffered by inveterate drillers.

2. Block samples. If some locations or particular lithology are not easily drilled, logistics might demand collection of oriented block samples. Joint blocks are often oriented (generally by determining the strike and dip of a surface) and then removed from the outcrop.

3. Lake-bottom or sea-bottom core samples. Numerous devices have been developed to obtain columns of sediment from lake or sea bottom.

The levels of paleomagnetic data analysis at which mean directions calculated are:

The ChRM directions for the multiple specimens must be averaged, then Site mean ChRM direction is calculated from the sample ChRM directions, and site-mean directions was averaged to yield either the average ChRM direction or a paleomagnetic pole position from the rock unit.

Where linear vector components were identified the ChRM is determined using the Principal Components Analysis (P.C.A). From a set of observation, P.C.A. determines the best fitting line through a sequence of data points. In addition, a Maximum Angular Deviation (MAD) is calculated to provide a quantitative measure of the precision with which the best fit line is determined. In average, all the analyzed specimens are gives $MAD \leq 4^0$.

2.1 Laboratory Activities

The main objectives of paleomagnetic laboratory work are to remove secondary NRM. NRM is prior to any laboratory treatment and composed of at least two components; primary NRM acquired during rock formation (TRM, CRM, or DRM) and secondary NRM components (VRM or lighting induced IRM) acquired at some later time.

An initial step is recognition and erasure of secondary components of NRM. As the NRMs of specimens from a rock unit are initially measured, the distribution of NRM often indicates the presence of secondary NRM.

To overcome the objectives of this thesis different paleomagnetic laboratory partial demagnetizations (alternating-Field Demagnetization, thermal demagnetization), and impulse magnetization techniques are used and spinner magnetometer are used to measure magnetic saturation for each procedures.

After the collection of paleomagnetic samples from the paleomagnetic sites during field activities in the study area with the identification of lithology and structural frameworks different paleomagnetic laboratory activities were done. These activities were started from preparation of specimens for other partial demagnetization and magnetization laboratory techniques. The general procedure in progressive demagnetization is to sequentially demagnetize a specimen at progressively higher levels, measuring remaining NRM following each demagnetization steps.

A generally adopted procedure is to apply progressive AF demagnetization to some specimens and progressive thermal demagnetization to other specimens. This procedure allows comparison of results obtained by the two techniques.

The objective is to reveal components of NRM that are carried by ferromagnetic grains within a particular interval of coercivity or blocking temperature.

Diriba A. Paleomagnetism and Tectonics of Northern Munesa, 2012. MSc thesis, Tel: +251-910-66-7446, email: nabekdiriba@hotmail.com, Addis Ababa; Ethiopia

The resistance to demagnetization is described in terms of stability of NRM, with low-stability components easily demagnetized and high-stability components removed only at high levels of demagnetization. Distributions of NRM directions provide information about likely secondary components, while knowledge of ferromagnetic mineralogy can indicate which demagnetization technique is likely to provide isolation of components of NRM and to identify the most ferromagnetic minerals.
These activities were discussed below with detailed procedures.

2.1.1 Alternating-Field Demagnetization and thermal demagnetization

The fundamental AF demagnetization procedure is to expose a specimen to an alternating magnetic field and it is conducted using Alternating-Field demagnetizer (fig.2.3).

Typical instruments allow AF demagnetization to maximum 100mT magnetic fields, sequentially from NRM (0mT), 5mT, 10mT, 15mT, 20mT, 25mT, 30mT, 40mT, 60mT, 80mT, then at 100mT. Most AF demagnetizing instruments use a tumbler apparatus that rotates the sample within several nested gears (Fig.2.3).

AF demagnetization can be used to erase NRM carried by grains with coercivity less than the peak demagnetizing field.

The tumbler is designed to present in sequence all axes of the specimen to the axis of the demagnetizing coil. The tumbler thus allows demagnetization of all axes of the specimen during the course of a single demagnetization treatment.AF demagnetization is often effective in removing secondary NRM and isolating characteristic NRM (ChRM) in rocks with titanomagnetite as the dominant ferromagnetic mineral. In this rock unit secondary NRM is mostly carried by multidomain (MD) grains, while ChRM is retained by single domain (SD) or pseudosingle domain (PSD) grains. As MD grains have hc dominantly ≤20mt, and SD and PSD grains have higher hc. So it can remove a secondary NRM carried by the low hc grains and leave the ChRM unaffected.

AF demagnetization is a convenient technique because of speed and ease of operation and is thus preferred over other techniques when it can be shown to be effective.

The procedure for thermal demagnetization involves heating a specimen to an elevated temperature (Tdemag) below the Curie temperature of the constituent ferromagnetic minerals, then cooling to room temperature in zero magnetic fields.

The followed temperature values for thermal demagnetization are $120c^o$, $200c^o$, $250c^o$, $300c^o$, $350c^o$, $400c^o$, $430c^o$, $460c^o$, $490c^o$, $520c^o$, $540c^o$, $560c^o$, $580c^o$, $600c^o$, $620c^o$, $640c^o$, $660c^o$, $680c^o$.

This causes all grains with blocking temperature (TB) $\leq$ Tdemag to acquire a "thermoremanent magnetization" in H = 0, thereby erasing the NRM carried by these grains. In other words, the magnetization of all grains for which TB $\leq$ Tdemag is randomized, as low hc grains during AF demagnetization.

The effectiveness of thermal demagnetization in erasing Viscous remnant magnetization (VRM) can be understood by realizing that thermal demagnetization to Tdemag $\geq$ TB of grains carrying VRM will selectively erase VRM, leaving unaffected the ChRM carried by grains with longer t (= higher TB).

AF demagnetization generally fails to remove secondary NRM components from hematite-bearing rocks. The property common to grains carrying secondary NRM in hematite-bearing rocks is low t resulting from low product v. hc. Grains with high hc but small volume, v, can carry secondary NRM. But these grains would not be erased by AF demagnetization because their coercive force could easily exceed the maximum available field H_{AF}. Therefore, in rocks with hematite as the dominant ferromagnetic mineral, removal of VRM invariably requires thermal demagnetization.

Diriba A. Paleomagnetism and Tectonics of Northern Munesa, 2012. MSc thesis, Tel: +251-910-66-7446, email: nabekdiriba@hotmail.com, Addis Ababa; Ethiopia

The end product of a progressive demagnetization experiment is a set of measurements of NRM remaining after increasing demagnetization levels. Analyses of these data require procedures for displaying the progressive changes in both direction and magnitude of NRM.

At each demagnetization levels the spinner magnetometer is used to measure the saturation magnetization. This spinner magnetometer involve the spinning shaft on which a rock specimen is rotated and a magnetic field sensor to detect the oscillating magnetic field produced by the rotating magnetic moment of the specimens. The signal from the sensor is passed to a phase-sensitive detector designed to amplify signals at the rotation frequency of the spinning shaft. With the development of effective phase-sensitive detectors and digital summing circuits, sensitivity of spinner magnetometers and speed of measurement have been greatly improved. The measurements are made of components (mx, my, mz) of magnetic moment of the specimens (in sample coordinates), then the data were fed into a computer that contains orientation data for the sample and calculation of the best-fit direction of NRM in sample coordinate in geographic coordinates is performed using Remasoft. The paleomagnetic directions are described interms of inclination (I), (with respect to horizontal at the collecting location) and declination (D), (with respect to geographic north).

Results of progressive demagnetization experiments are now displayed by Zijderveld diagram (fig.6.1). The power of the vector component diagram is its ability to display directional and intensity information on a single diagram by projecting the vector onto two orthogonal planes. However, an initial investment of time and concentration is required to understand these diagrams. Almost all research articles on Paleomagnetism that have been published within the past decade contain at least one vector component diagram.

Paleomagnetic instruments that are used during laboratory works are showed below.

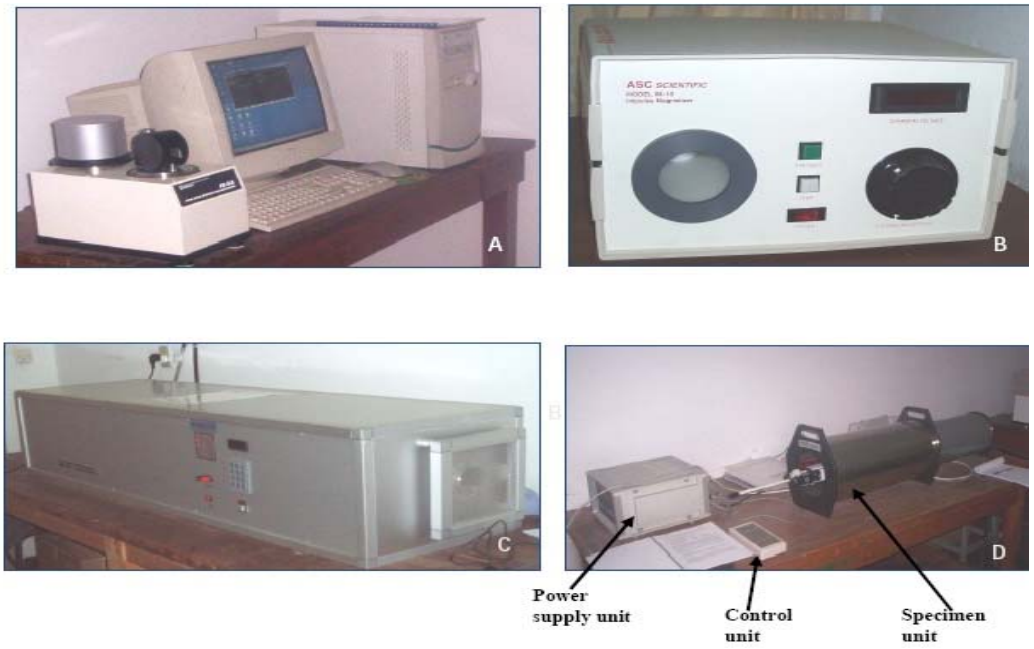

E 

Fig.2.3Paleomagnetic Instruments used in laboratory.A)Spinner magnetometer. B) Impulse magnetizer. C) Thermal demagnetizer. D) alternating-field demagnetizer. E)Cutter.

Diriba A. Paleomagnetism and Tectonics of Northern Munesa, 2012. MSc thesis, Tel: +251-910-66-7446, email: nabekdiriba@hotmail.com, Addis Ababa; Ethiopia

3. GEOLOGY OF THE MAIN ETHIOPIAN RIFT (MER)

3.1 Geology and Geochronology of the MER

The main Ethiopian rift (MER) is a symmetrical graben with uplifted flanks and steep border faults; it lies between 5^{o}-9^{o}N lat. and 37 ^{o} 30'-40 ^{o}long. The MER divides the 1,000km wide uplifted Ethiopian volcanic province asymmetrically into the northwest - southeast plateaus. Volcanic sequences that cover an area several hundred kilometers across are more voluminous and widespread on the northwest plateau than on the opposite side.

According to WoldeGabriel et al., (1990); Hofmann et al., (1997) the Ethiopian Rift developed within an Eocene-Oligocene flood basalt province. In the northern MER two pre-rift flood basalt episodes (predominantly transitional to tholeiitic) occurred by 24–23 Ma and 11–8 Ma (the latter characterized by less alkali basaltic shield volcanism). Extension, basin subsidence and rift-flank uplift began during or after the second flood-basalt phase (Ebinger et al., 1993). The MER propagated into the Afar depression after 11 Ma (WoldeGabriel et al., 1990; Wolfenden et al., 2004). Bimodal volcanism (basalt-rhyolite) appeared by 7 Ma and continued to recent times (Chernet et al., 1998). In the late Miocene and during the Pliocene intra-rift marginal aligned silicic center developed.

During the Plio-Quaternary, volcanism was concentrated within the rift floor, and felsic products constitute 80% of the exposed Plio-Quaternary rocks in the MER. The oldest (pre2 Ma) and youngest (post 0.6 Ma) intra-rift units are characterized by bimodal compositions (alkali basalts and rhyolites, mainly pantelleritic), whereas in the intervening period (1.6–0.6 Ma) units occur with unimodal characteristics (pantelleritic) (WoldeGabriel et al., 1990).

Diriba A. Paleomagnetism and Tectonics of Northern Munesa, 2012. MSc thesis, Tel: +251-910-66-7446, email: nabekdiriba@hotmail.com, Addis Ababa; Ethiopia

It is assumed that the bimodal compositions indicate a period of increased extension (Boccaletti et al., 1999). Recent basalts (post-0.6 Ma) are essentially fissural and have geochemical signatures characteristic of mid oceanic ridge basalt (MORB).

According to Benoit et al., (2003); Bastow et al., (2005), the Main Ethiopian Rift system developed within an Oligocene flood basalt province, and it overlies a broad region of anomalously low velocity mantle. A synthesis of 40Ar/39Ar data shows that a 1–2km thickness of mainly flood basalts erupted to form the Ethiopian and Yemen plateaus between 31–30Ma or 29Ma (e.g. Hofmann et al., 1997; Pik et al., 2003). The main outpouring of the Ethio-Yemen trap series is linked genetically to the Afro-Arabian continental breakup.

However, some volcanism persisted and extended over large areas outside the developing rifts until 11Ma (e.g.Wolfenden et al., 2005), when the bulk of volcanism was localized within the developing rift valley. Less voluminous volcanic products of that age extend several hundredkilometers further to the north (e.g. Kenea et al., 2001). An earlier probably related volcanic phase between 45–39Ma affected southwest Ethiopia (e.g. Ebinger et al., 2000), though evidence of earlier faulting is non-existent.

In general, WoldeGabriel et al., (1990) subdivided the volcanic products of the whole Ethiopian rift into six main tectonomagmatic chronozones since Eocene to Oligocene. These groups were described from the oldest to the youngest as the following:

3.1.1. Kella basalt (26-32Ma): this is the oldest volcanic unit in the central sector of MER and is found at Agereselam, Ambo and Kella. These rocks are dominated by basalt with localized rhyolite and sedimentary strata.

3.1.2. Shebele trachyte (12-17Ma): the rocks of this unit are exposed along some deep canyons of Omo River and Wabi Shebele. This group is dominated by intermediate and acidic volcanic rocks such as trachyte, phonolite, and rhyolite and intercalated volcanoclastic strata.

3.1.3. Guraghe Basalt (8.3-10.6Ma): basalts and subordinate silicic flows of this unit are found at Hawasa, guraghe and Omo river canyon. In Omo river canyon, these 10.6Ma old basalts are underlain by several undated basalt flows and middle Miocene shebele trachyte. At Hawasa and guraghe, the base of correlative unites is not exposed.

3.1.4. Butajira Ignimbrite (3-4.2Ma): voluminous silicic pyroclastics material and subordinate basalt flows of this unit were erupted from the Hawasa caldera, the wegebta caldera complex and a major caldera probably buried beneath the Ziway- Langano-Abijata basin. Petrologically these groups of rhyolite rocks are distinguished from those of the quaternary Wonji group as being transitional or mildly per alkaline while the Wonji group is per alkaline.

3.1.5. Chilalo trachyte (1.6-3.5Ma): this group includes the product of Pliocene centers of the eastern and western shoulder of the rift and compositionally correlative units from the Hawasa caldera. It includes trachyte, silicic rocks and basalt that overlie units of either Shebele trachyte or Butajira ignimbrite.

3.1.6. Wonji Group (<1.6Ma): this group is confined to the Wonji Fault Belt (WFB), along the entire MER and also includes the young basalts. This group consists of the diverse quaternary lava, pyroclastics rocks and volcanoclastic strata younger than 1.6Ma.

3.2 Structural Framework of MER and Its Evolution

The East African Rift System (EARS) is a Miocene-quaternary intercontinental extensional system, divided into eastern and western branches and composed of several interacting segments from Mozambique to Afar (Davidson and Rex, 1980). At Afar, the EARS join the Gulf of Aden and Red Sea Rifts, both characterized by a more advanced extension stage (McKenzie et al., 1970; Ebinger and Hayward, 1996).

The oblique rifting deformations induces also a high sinistral shear gradient close to the eastern border of the MER responsible for the occurrence of transtensional structures, like rhomb-shaped features and pull apart (Boccaletti et al., 1992). The occurrence of a component of dextral displacement along some N-S to N20^{o}E trending faults of the WFB, which suggests a roughly NW to NNW direction of extension (Chorowicz et al., 1994), however, does not necessarily contrast with the regional E-W oriented extension.

The pre-Quaternary deformation was possibly associated with the N30^{o}E -N40^{o}E striking major normal faults, which were active principally since the Middle Miocene (Ebinger et al., 1993). The onset of the oblique rifting could also be related with the change in the magmatic activity at around 1.6 Ma, which matches with both the development of the WFB (Meyer et al., 1975) and the eruption of the volcanic rocks of the Wonji Group (WoldeGabriel et al., 1990). Moreover, the uprising of the Quaternary basaltic magmas appears to be strongly controlled by the en-echelon N-S to N20^{o}E trending fault system of the WFB, since their distribution follows this trend.As Boccaletti et al., (1994) suggest, the Quaternary E-Wtrending direction of extension, therefore, would reactivate, in the Ethiopian Rift; suitably oriented structures related either to earlier stage of rifting deformation or to basement weakness zones.

For understanding, Boccaletti et al., 1997, compile the category ofthe MER into the rift floor, the western margin and the eastern margin which are the rift border.

The eastern margin is well developed and it is defined by a more or less continuous system of boundary faults and it is high angle W dipping N30^{o}E-N40^{o}E trending border faults which separate the MER from the southwestern plateau, whereas the western border is marked by only a few major faults of the Mt. Guraghe area and high angle ENE dipping N35^{o}E-N40^{o}E trending at north and N-S to N20^{o}E striking faults at the south of the margin. The rift floor faults have steep scarps and constitute a right-stepping arrangement of en-echelon N-S to N20^{o}E trending faults (WFB), which began to develop around 1.6 Ma (Meyer et al., 1975). The Late Pliocene-Quaternary volcanic and sedimentary rocks of the rift floor are affected by this fault system that, therefore, reflects Quaternary tectonics.

During Pliocene and quaternary, the MER progressively deepened, involving through the sequence of interacting half graben segments marking the boundary between the Nubia and Somalia plates (Hayward and Ebinger, 1996). The MER limited by discontinuous boundary faults, active from Miocene (WoldeGabriel et al., 1990). Structurally the MER is categorized into southern, central and northern sectors.

Corti et al., (2012) further suggest the three MER sectors reveal a variation in the extension direction between the rift margins (N105°- 110°E) and the rift floor (N90°-95°E). The N90°-95°E trending extension is similar to the ~N100°E regional extension related to the Nubia-Somalia kinematics. This is likely because the enhanced tectono-magmatic weakening of the rift floor is expected to allow the faults to respond more efficiently to the regional stress; conversely, boundary faults may be influenced by a local reorientation of the regional stress directions controlled by the reactivation of deep seated inherited fabrics.

The variations in extension direction across the rift suggest a slip partitioning between in rift WFB faults and the boundary faults during oblique rifting.

4. Geology and Geochronology of the Study area

To address the objective of the research, the major activities conducted during field work are identifications of lithology and structural frameworks, geological and structural mapping of the area at the scale of 1:50,000, and collections of paleomagnetic samples from each paleomagnetic sites. The paleomagnetic samples were collected mostly from the ignimbrite and basalt, conducted as paleomagnetic sites, through paleomagnetic sampling schemes (fig. 1.3). Thusthe followings are an identification and mapping of the lithology and structures of the study area.

4.1 Lithology

4.1.1 Basalt: this rock unit is outcropped mostly at the northern part of the lake Langano and northwestern of the area (fig.4.2), including recent rift floor scoracies basalts and relatively older vesicular basalts. This basalt is generally of fissural type and outcropped through NE trending open extension fractures. Compositionally, it is plagioclase with some pyroxene and olivine. In some part of the area this basalt shows pahoehoe type, and there is up to 8m thickness of outcropped due to NE trending faults and taken as paleomagnetic sites to collect paleomagnetic samples.

4.1.2 Ignimbrite: This unit was covers large area in the eastern and central part of the study area (fig.4.2) and exposed due to faulting. The maximum thickness (about 10m) of this unit has been exposed along the main bounder fault escarpments, north east of Golja. According to WoldeGabriel et al., (1990), the radiometric age available on this unit is 1.66Ma. Compositionally it is pantelleritic and fiamme rich ignimbrites exhibiting different textural characters due to the grade of welding. It is characterized by medium welded, more or less fresh with different lithic fragments, like pumice and basalt. As observed in the central part of the study area the welding degree of this rock unit and the presence of lithic fragments (fiamme) have been increased. Most of the paleomagnetic sites were conducted on this rock mainly at the northern part of the study area.

4.1.3 Rhyolites: This rock unit is out cropped at western part of the study area. It is highly weathered and intercalated with the volcanic ash and obsidian. This outcrop shows surface layering features (banding) which exist due to slow flows during its formation (fig.4.1).

Fig.4.1.Surface layering (banding) features of rhyolite.

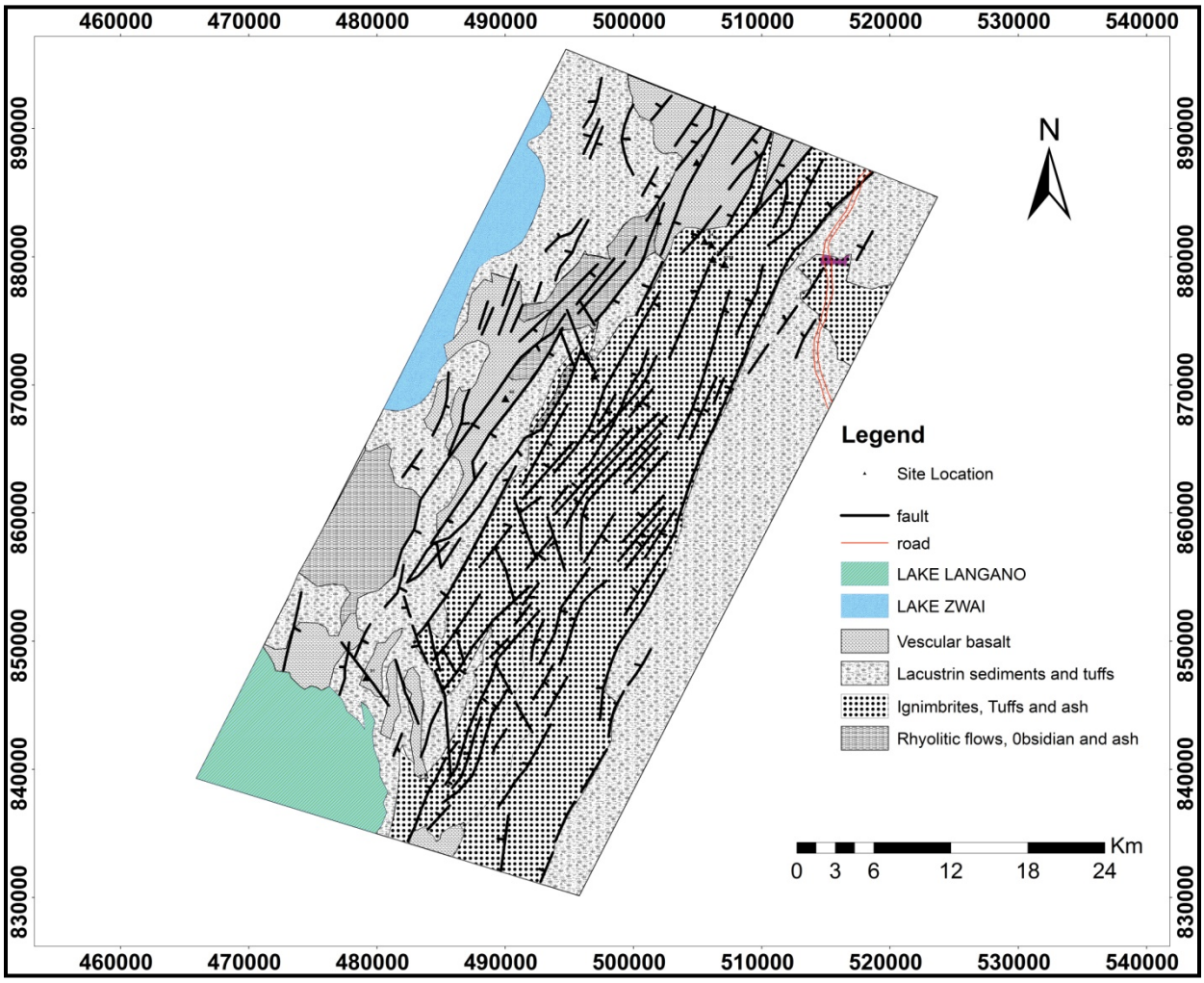

Fig.4.2Detailed geological map of the area**.**

Diriba A. Paleomagnetism and Tectonics of Northern Munesa, 2012. MSc thesis, Tel: +251-910-66-7446, email: nabekdiriba@hotmail.com, Addis Ababa; Ethiopia

4.2 Structural interpretation of the area

As sketched on the structural map of the study area (fig.4.4), different geological structures were observed and described in terms of their orientation and morphologies as indicated below.

4.2.1 Faults

Faults are fracture surfaces along which appreciable displacement of the layering has taken place. Normal faults are the most well developed structures in rift zones. The geological structures observed in the study area are part of the brittle deformation and they are oriented similar to the orientation of the central MER which is NE direction (fig.4.4). The study area is part of the central sector of the MER mainly part of the eastern margin and it is a symmetrical rift, mainly characterized by well-defined synthetic rift margins having variable throws along the strike of the boundary faults.

In the eastern part of the area, which is affected by Wonji Fault Belt (WFB), the rift-in-rift (graben-horst) (fig.4.3) structures usually run parallel to each other. Faults and joints are relatively concentrated on the central and eastern part of the area near to the main Assela-munesa escarpment (eastern escarpment) of the rift.

Fig.4.3. Rift-in-Rift structure.

Diriba A. Paleomagnetism and Tectonics of Northern Munesa, 2012. MSc thesis, Tel: +251-910-66-7446, email: nabekdiriba@hotmail.com, Addis Ababa; Ethiopia

The down throw direction of the faults is variable but more commonly to the west associated with tensional fractures.

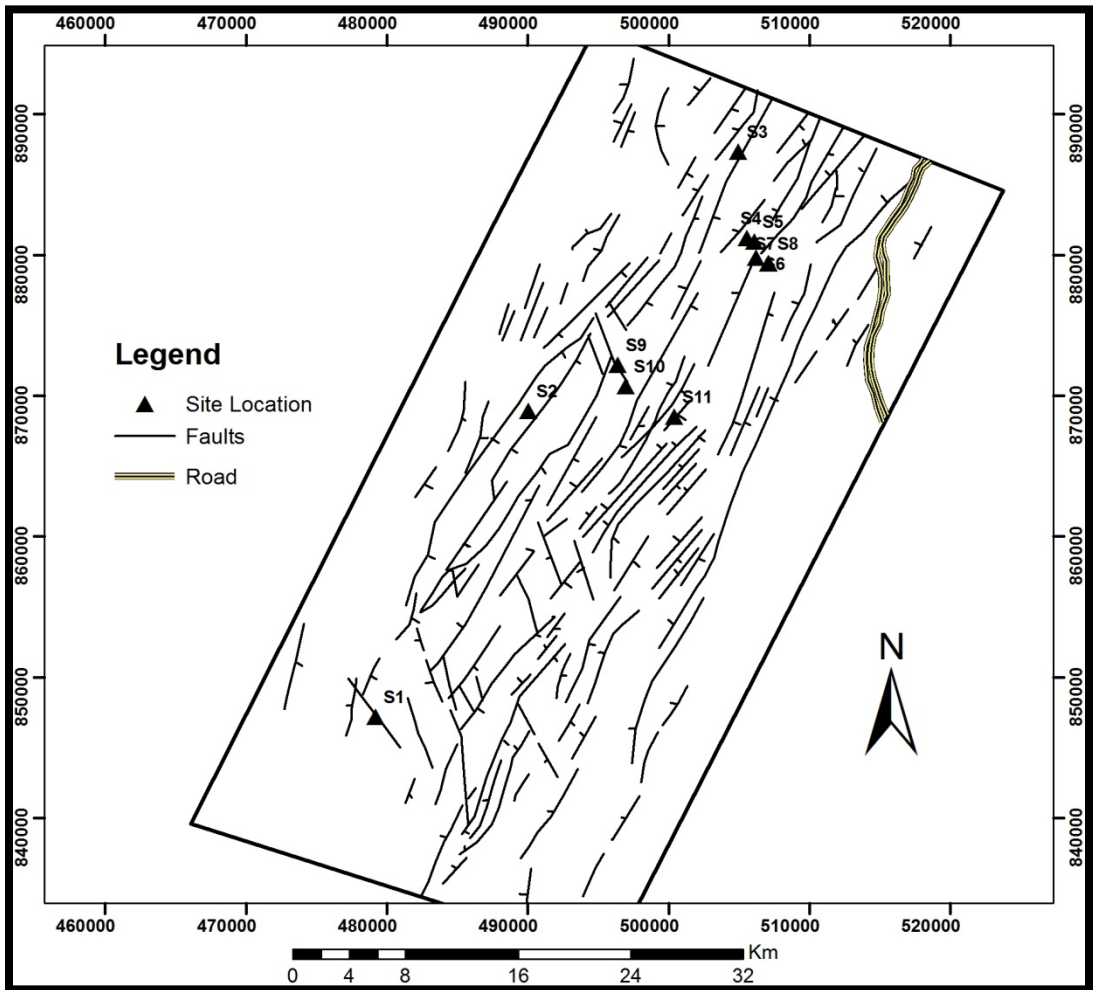

Fig.4.4 Map ofthe geological structures of the area.

Mostly the faults in the study area were terminated due to contacts of major faults which is transtensional faults and it forms rely ramp structures (fig.4.5). Also dies out with in pyroclastics material at the end of the lava cone (fig.4.6), at the northern part of the area. At the contact of these faults the block rotations were expected. So the objectives of this study is to quantify these block rotations significant to paleomagnetic methods.

Diriba A. Paleomagnetism and Tectonics of Northern Munesa, 2012. MSc thesis, Tel: +251-910-66-7446, email: nabekdiriba@hotmail.com, Addis Ababa; Ethiopia

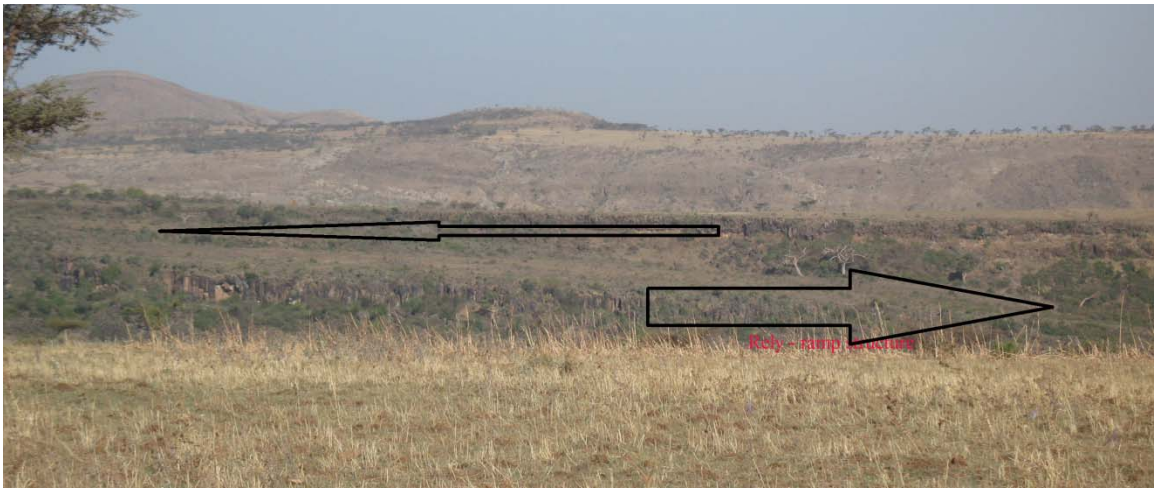

Fig.4.5 Rely ramp structure.

Morphologically, these faults are characterized by steep and high escarpments at the centre and change into simple fractures along strike or die out. In the figure below the rhyolite dome is crossed by NNE to SSW oriented fault and the rhyolite cone exposed along this fault. So the rhyolite dome could be formed before the fault exists.

Fig.4.6Rhyolites crossed and erupted along the fault.

In general, the faults within the study area are running with an approximate strike of N25^{o}E, and having significant vertical displacement and dipping to west.

Diriba A. Paleomagnetism and Tectonics of Northern Munesa, 2012. MSc thesis, Tel: +251-910-66-7446, email: nabekdiriba@hotmail.com, Addis Ababa; Ethiopia

4.2.2 Joints

Joints are seen to be continuous and through-going planar fractures, commonly on the scale of centimeters to tens or hundreds of meters in length. There has been imperceptible "pull-apart" movement more or less perpendiculars to the fracture surface are observed along the joints.

The Columnar joints (not well developed) are exposed in basalt which is produced by a fracturing that accommodates contraction during congealing shrinking of the flows as it cools and it tends to be polygonal in the same way that mud cracks resulting from shrinkage of mud are polygonal.

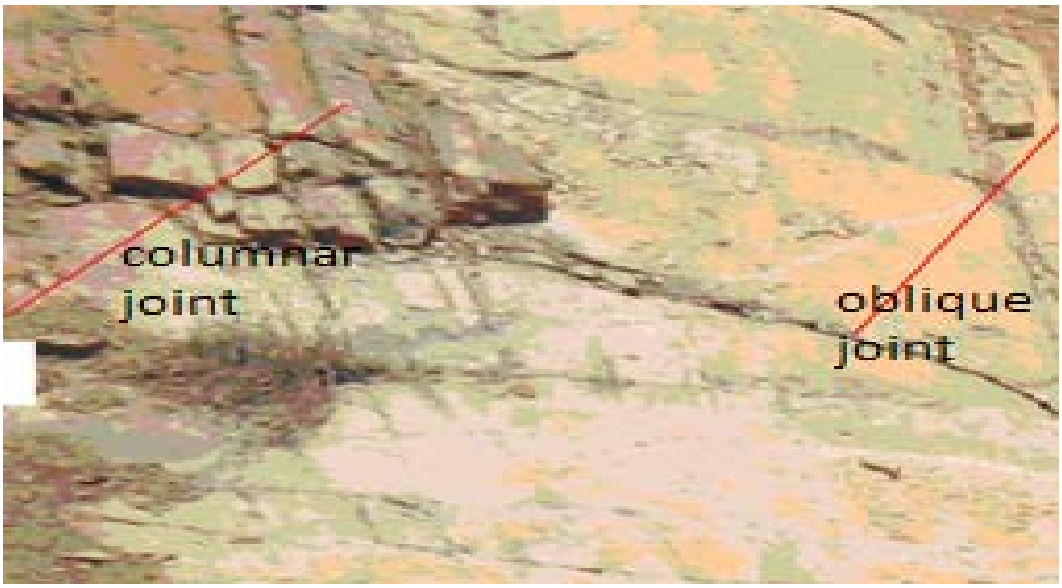

Fig.4.7 Observed joint systems (columnar, polygonal and oblique joints).

Diriba A. Paleomagnetism and Tectonics of Northern Munesa, 2012. MSc thesis, Tel: +251-910-66-7446, email: nabekdiriba@hotmail.com, Addis Ababa; Ethiopia

5. Ferromagnetic Rock Minerals

The ferromagnetic minerals identification in a rock is used to associate a particular component of NRM (identified from partial demagnetization) with a particular ferromagnetic mineral (identified from acquisition data). From this data it is possible to determine whether a characteristic NRM is primary or secondary. There are three techniques used to identify ferromagnetic minerals: such as; microscopy techniques including optical microscopy, electron microprobe, and SEM; determination of Curie temperature; and coercivity spectrum analysis. In this study coercivity spectrum analysis followed by Curie temperature were conducted to identify ferromagnetic minerals. The usual procedure conducted in coercivity spectrum analysis is to induce isothermal remnant magnetization (IRM) by exposing the specimen to a magnetizing field, H, using impulse magnetizer; measurement of the result IRM using spinner magnetometer, then repeat the procedure using the stronger magnetizing field with the following magnetizing levels 15mt, 50mt, 66mt, 83mt, 168mt, 253mt, 337mt, 504mt, 666mt, 831mt, 994mt and 1154mt.

Titanomagnetite has saturation magnetization, Js, up to 480 G and microscopic coercive force, hc ≤300 mT, and hematite has only 2–3 G but can have hc 1T.

A sample containing only titanomagnetite (or ferromagnetic titanohematite) acquires IRM in H 300 mT, but no additional IRM is acquired in higher H. If only hematite (or goethite) is present, IRM is gradually acquired in H up to 3T. Samples containing both titanomagnetite and hematite (or goethite) rapidly acquire IRM in H 300 mT, followed by gradual acquisition of additional IRM in stronger magnetizing fields. This procedure allows detection of small amounts of hematite (or goethite) even when coexisting with more strongly ferromagnetic titanomagnetite. The saturation magnetizations are obtained at magnetic field of 253mt which is carried by titanomagnetite and magnetite that is primary ChRM.

Thermal demagnetization was conducted following the IRM acquisition experiment for each specimen. The IRM decreases during thermal demagnetization as blocking temperatures are reached. Decreasing in IRM during thermal demagnetization is important to estimate Curie temperatures because maximum blocking temperatures are always slightly less than the Curie temperature.

An example of coercivity spectrum analysis obtained from laboratory was shown below (fig.5.1 a, and b). A Curie temperature of 580°C is evident, but there is no indication of a 680°C Curie temperature due to hematite in basalt.

From the figure 5.1 the NRM curve are steeply increased up to 200mT and become saturated around 300mT, which shows the ferromagnetic mineral is magnetite. Also some sulphide minerals show these properties, and to know the exact ferromagnetic minerals the thermal demagnetization was conducted and proves the ferromagnetic mineral is magnetite.

Thermal demagnetization of acquired IRM for this rock is illustrated in Figure 5.1 c and d. Most IRM is removed by thermal demagnetization to the 580°C Curie temperature of magnetite.

The first two graphs show acquisition of IRM by sample of basalt and ignimbrite, indicating the dominant ferromagnetic minerals are magnetite and titanomagnetite, which attain magnetic saturation upto 300mt.

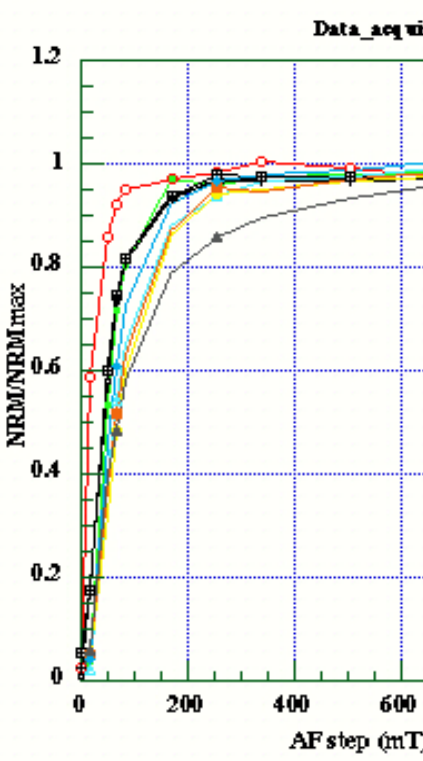

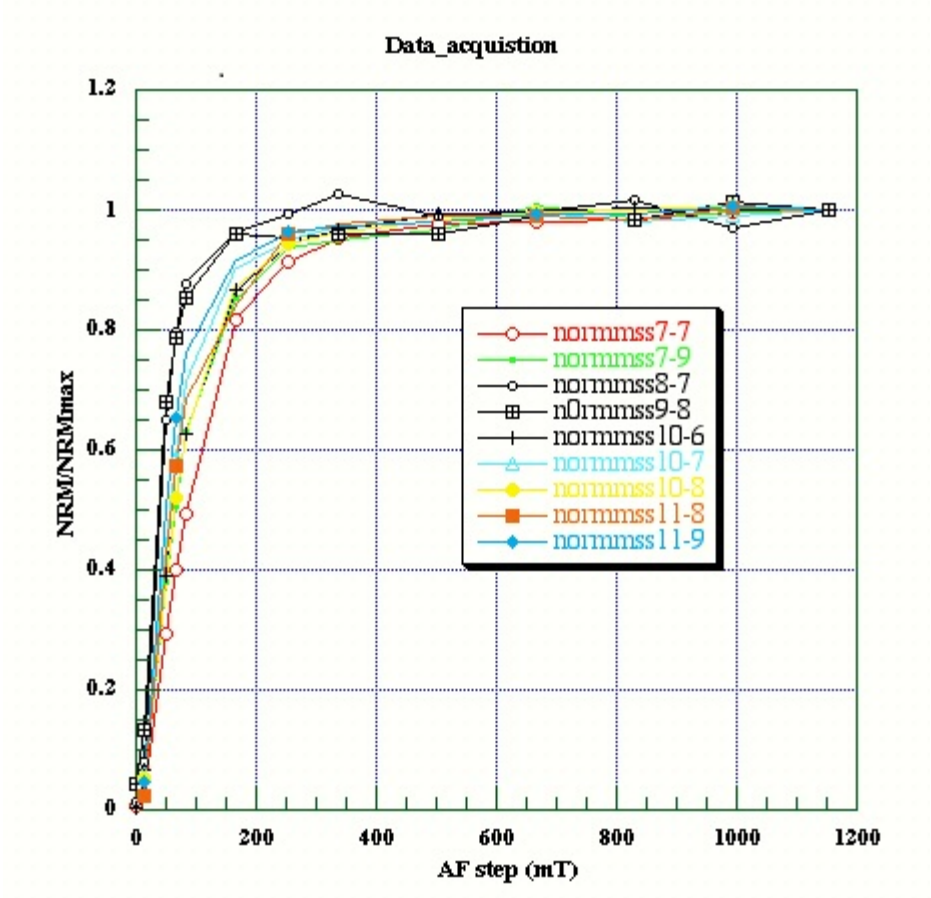

Diriba A. Paleomagnetism and Tectonics of Northern Munesa, 2012. MSc thesis, Tel: +251-910-66-7446, email: nabekdiriba@hotmail.com, Addis Ababa; Ethiopia

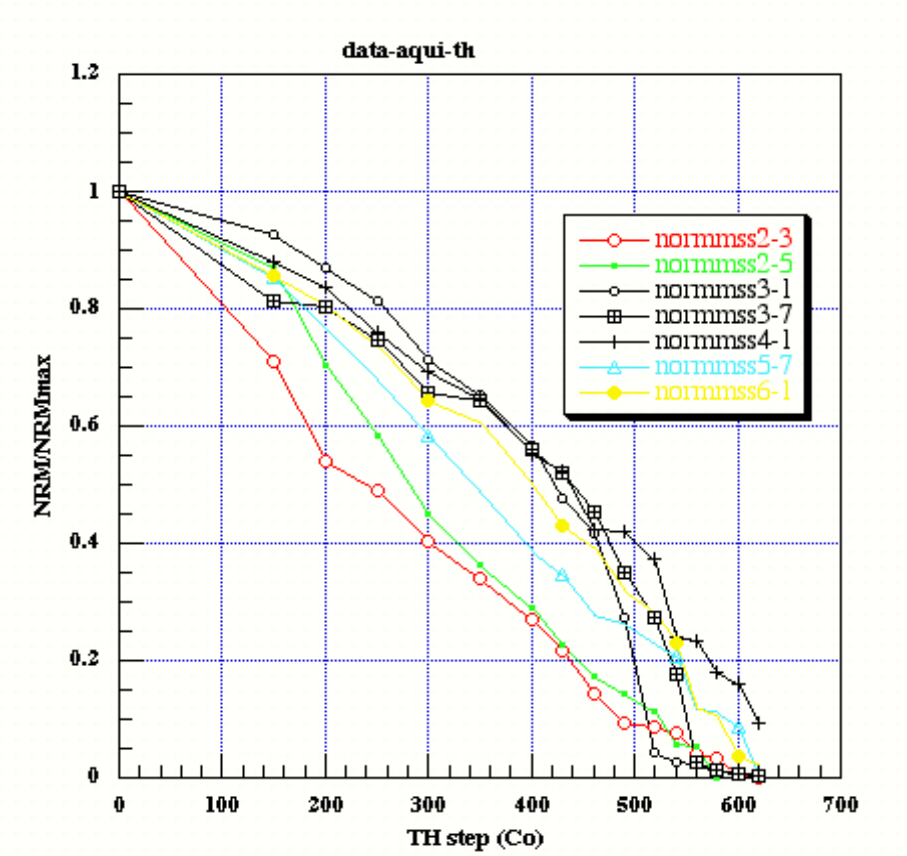
data-aqui-th
NRM/NRMmax
TH step (Co)
1.2
1
0.8
0.6
0.4
0.2
0
0
100
200
300
400
500
600
700
normmss2-3
normmss2-5
normmss3-1
normmss3-7
normmss4-1
normmss5-7
normmss6-1

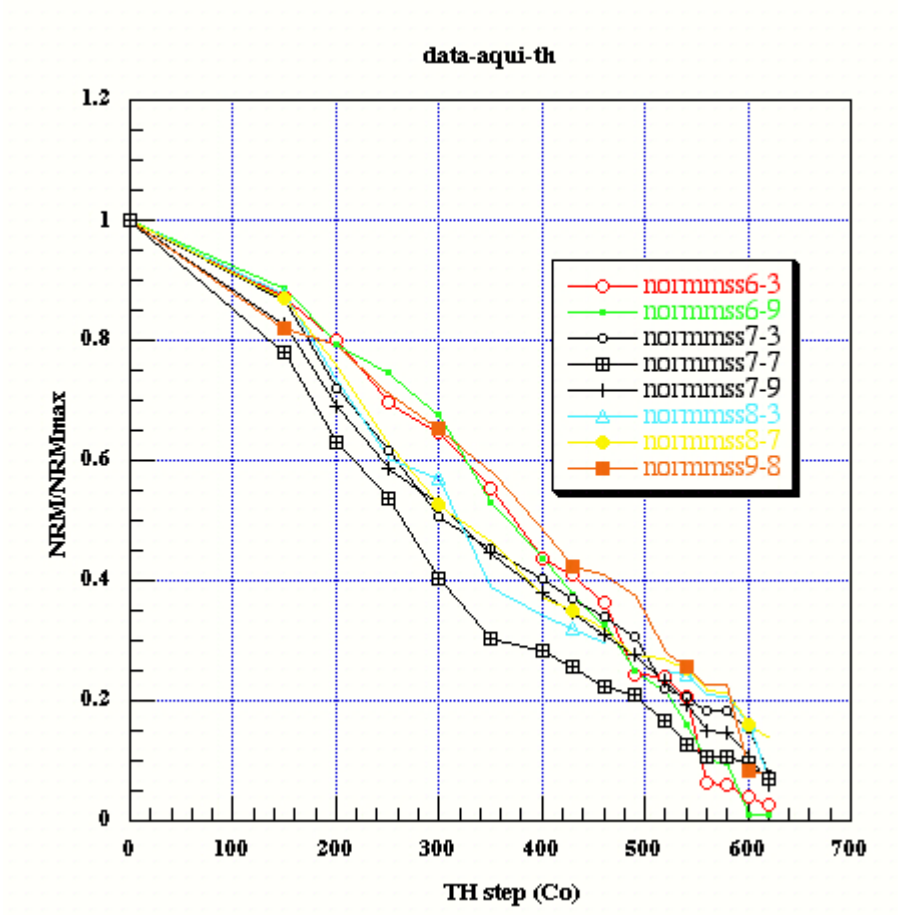

Fig.5.1. Typical example for acquisition of IRM by sample of basalt and ignimbrite, where saturated above 300mt (a,& b) and thermal demagnetization of acquired IRM, mostly becomes zero at 620°C (c & d). The y-axis values are saturation magnetization and the x-axis values are the level of magnetization and demagnetization.

Diriba A. Paleomagnetism and Tectonics of Northern Munesa, 2012. MSc thesis, Tel: +251-910-66-7446, email: nabekdiriba@hotmail.com, Addis Ababa; Ethiopia

6. Paleomagnetic Resultsand Analysis

From the segmented rift floor in eastern part of Lake Langano and Lake Ziway, 11 paleomagnetic sites were collected in March, 2011. Mostly fissural basalt (mafic lava flow) and welded ignimbrites were taken as paleomagnetic sites and only one site was collected from rhyolite rocks which exposed with ash and obsidian. From these rocks types about 11 sites were marked mss1-1 to mss11-10. The rock units cropped out along fault scarps, road cuts, and river valley exposures. During sampling, care was taken to collect cores from the central part of the flow in order to avoid the possibility that the sample had been remagnetized during emplacement of the next flow. A total of about 98 cores were collected for paleomagnetic analysis and they oriented using both magnetic and sun compass. All the samples were collected from sub horizontal to horizontal rock units and there thickness range from 5m to 20m. For each core samples alpha-sol, alpha-mag, and beta with their time of measurement are documented during field work.

Natural remnant magnetization (NRM) is remnant magnetization present in a rock prior to laboratory treatment and formed depending on the geomagnetic field and geological processes during rock formation and history of the rock. Therefore, it consist two components that formed during rock formation (primary NRM) and subsequent to rock formation (secondary NRM). Samples collected from basalt, ignimbrites and rhyolites are subjected to progressive alternating field demagnetization with 11 steps and thermal demagnetization with at 15-18 steps.

Most of the core samples were assigned for 2-3 specimens. One of the specimen was demagnetized with alternative field demagnetization, the second specimen was demagnetized thermally, and the third one 23 specimens was for ferromagnetic rock mineral identification conducted by impulse demagnetizer then by thermal demagnetization. Mostly the samples collected from basalts and ignimbrites are analyzed further and samples collected from rhyolites are not good for paleomagnetic data, because it has poor magnetization.

Diriba A. Paleomagnetism and Tectonics of Northern Munesa, 2012. MSc thesis, Tel: +251-910-66-7446, email: nabekdiriba@hotmail.com, Addis Ababa; Ethiopia

The results from laboratory analysis indicated that the AF treatment identified two components of remnant magnetization (primary NRM and secondary NRM). Generally an AF of between 0-40mt isolates the first components (fig.6.1a).

The component of remnant magnetization isolated above 40mt in most of the samples directed towards the origins of the plot with straight line segment and it is interpreted as characteristic remnant magnetization (ChRM) acquired during rock formation.

During AF demagnetization to peak fields in the 0-40mt interval, vector end points define a trajectory toward the origin with no significant change in direction of remaining NRM. These observation shows that ChRM is isolated by AF demagnetization to 40mt.

Diriba A. Paleomagnetism and Tectonics of Northern Munesa, 2012. MSc thesis, Tel: +251-910-66-7446, email: nabekdiriba@hotmail.com, Addis Ababa; Ethiopia

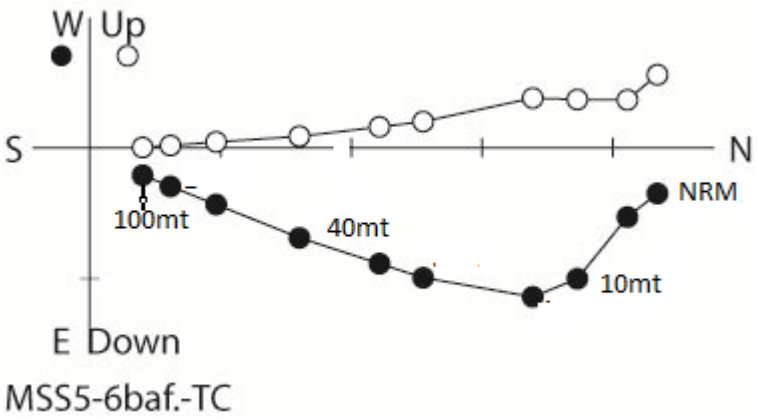
W Up
S
N
NRM
100mt
40mt
10mt
E Down
MSS5-6baf.-TC

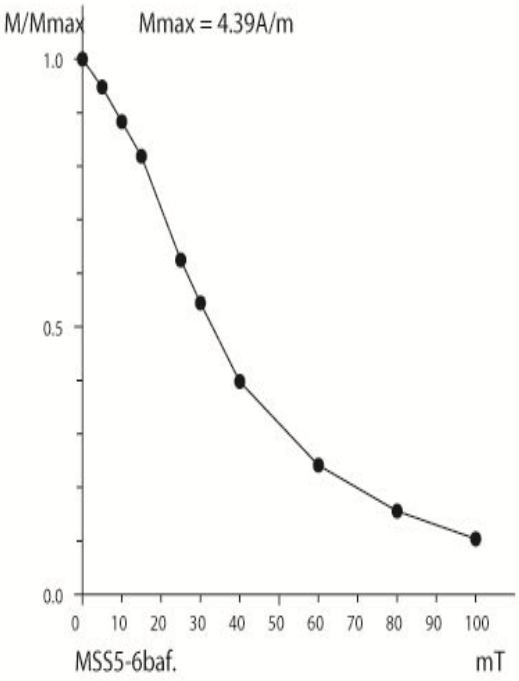
M/Mmax
Mmax = 4.39A/m
1.0
0.5
0.0
0
10
20
30
40
50
60
70
80
90
100
MSS5-6baf.
mT

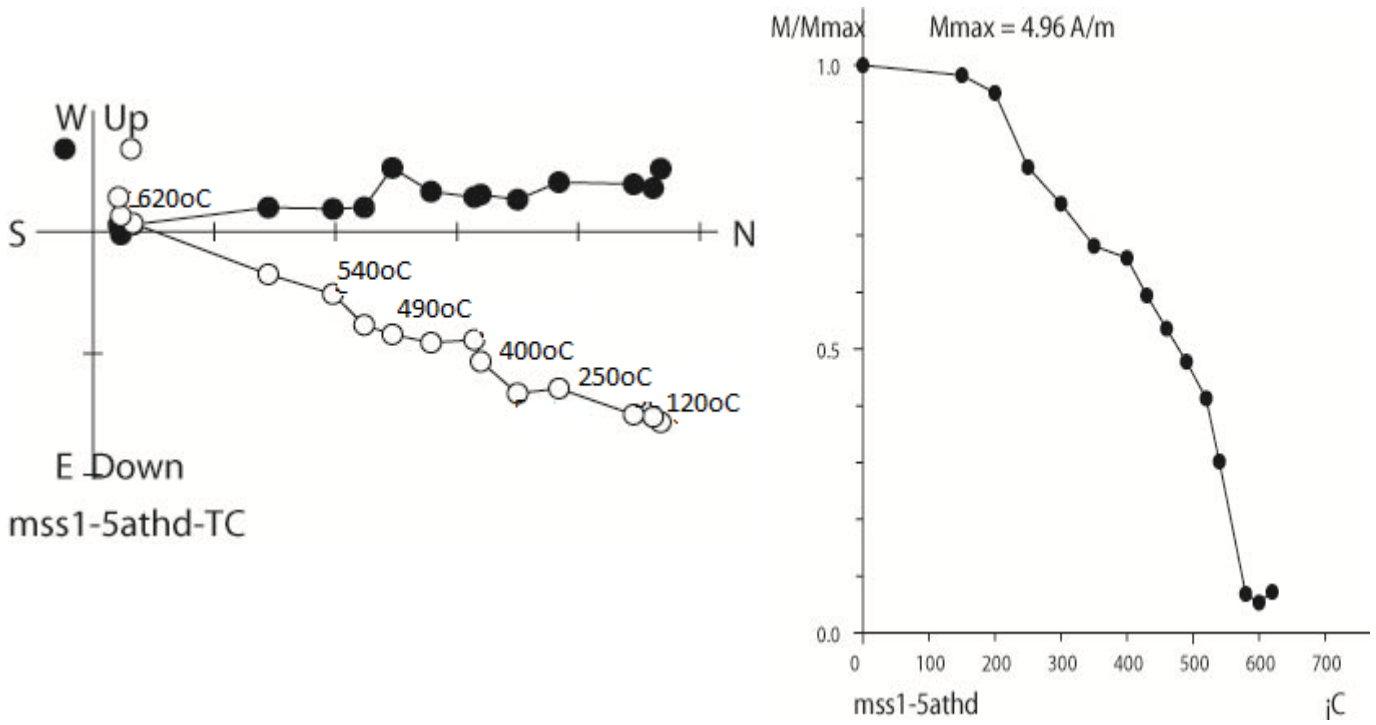

Fig.6.1 Vector component diagrams were done by thermal demag, normal polarity and AF, reverse polarity. In all diagrams, solid data points indicate projection onto the horizontal plane represents by N-E-S-W plane representing declination, and open data points indicate projection onto the vertical plane represents by up-down-east-west plane representing inclination. Werea,(Zijderveld diagram) and b (moment) are progressive AF demagnetization of sample of ignimbrite, and c and d indicate thermal demagnetization of sample of basalt.

Diriba A. Paleomagnetism and Tectonics of Northern Munesa, 2012. MSc thesis, Tel: +251-910-66-7446, email: nabekdiriba@hotmail.com, Addis Ababa; Ethiopia

Additionally, sample from these sites were thermally demagnetized following isolation of the ChRM by AF demagnetization to 40mt peak field, in Addis Ababa University paleomagnetic laboratory. The results obtained in this laboratory indicate the removal of the secondary components is by heating the specimens at temperature of between 0-400^{o}c(fig.6.1c.). For some samples, secondary components are persist up to a temperature of 490^{o}c and the demagnetization is complete by 620^{o}c and stepwise heating went until a temperature of 680^{o}c, to check the existence of significant amount of titanohematite or hematite.

In average the samples directed towards the origins of the plot with straight line segment after the thermal demagnetization level of 400^{o}c and it is interpreted as characteristic remnant magnetization (ChRM).

For demagnetization temperatures from 400^{o}c to 620^{o}c, the trajectory of vector end points is mostly along a linear trend toward the origin. This ChRM points almost directly to origin with no significant directional change in the 400^{o}c to 620^{o}c interval of demagnetization temperatures. Similar directions were observed during progressive demagnetization of other samples from this collecting area. The ChRM constitutes a significant portion of total NRM, and there is a substantial interval of demagnetization temperatures over which the ChRM can be observed. From the laboratory results thermal demagnetization to any temperature from 490^{o}c to 620^{o}c would effectively remove the low-stability component, revealing the high-stability ChRM.

Diriba A. Paleomagnetism and Tectonics of Northern Munesa, 2012. MSc thesis, Tel: +251-910-66-7446, email: nabekdiriba@hotmail.com, Addis Ababa; Ethiopia

7. Paleomagnetic Direction

The ChRM values determined at the specimen level then were used to calculate the core and site (flow) averages using Fischer (1953) statistics for combined analysis of remagnetization circles and stable linear segments.

With Paleomagnetism, we can detect only motions with respect to a paleomagnetic pole; purely longitudinal motions cannot be detected because of the geocentric axial dipole nature of the geomagnetic field.

For most applications, we want to determine motion of a crustal block with respect to a continental interior. The apparent polar wander (APW) path of the continent indicates how that continent has moved with respect to the rotation axis. The set of paleomagnetic poles that make up the APW path also serve as reference poles for determining motions of crustal blocks. Each reference pole was determined by paleomagnetic analysis of rocks of a particular age from the continental interior. So in principle the reference pole can be used to calculate the expected paleomagnetic direction for rocks of that age at any point on the continent.

Because all determinations of crustal block motion are with respect to a reference paleomagnetic pole (or expected direction calculated from the reference pole), accuracy of the reference pole is crucial. Inaccuracy in the reference pole leads directly to inaccurate estimates of motion of the crustal block.

Development of APW paths (reference poles) for continents is an ongoing process. New data and new methods of analysis sometimes result in significant changes to APW paths. So evaluation of reference poles is equal in importance to evaluation of paleomagnetic data from a crustal block.

On the orthogonal vector diagram, where linear vector components are identified, the ChRM is determined by least square technique (Kirchvink, 1980). Remagnetization circles (great circle) (Halls, 1976, 1978) are used to deal with samples for which ChRM cannot be isolated directly because of overlapping blocking temperature spectra (coercivity spectra) or lightning strikes. I.e. if two specimens give different and complex results, great circle used to show mixed average of the two.

Both AF and TH partial demagnetization revealed two components of NRM. The low stability component mostly has been removed by imposing an alternating field of 10–15mT or by heating above a temperature of 250^{o}C; the high stability component represents the Characteristic Remnant Magnetization (ChRM). Fig.6-1 and 6-2 gives representative Zijderveld diagrams by ignimbrite and basalt units of twin specimens treated by both AF and TH techniques from normal and reversed polarities. The directions of the ChRM component or the principal component analysis are determined by using the best-fitting line of least square technique passing through the origin (Kirchvink, 1980). The maximum angular deviation (MAD) for most of the ChRM is less than 4^{o} and no specimens had MAD $\leq$4◦. A few specimens from some sites did not have stable end points and linear segments could not be isolated.

The ChRM components determined at specimen level then were used to calculate the sample and site (flow) averages using Fisher (1953) statistics or McFadden and McElhinny (1988) statistics for combined analysis of remagnetization circles and stable linear segments. The paleomagnetic data analyses from principal component determination to calculate overall mean direction was done using the Paleomac software (Cogné, 2003).

In general, the procedure conducted to calculate the overall mean directions for several levels of paleomagnetic data are:

1. As the specimen are prepared more than one from the sample, then ChRM direction for the multiple specimens has been averaged;
2. A site-mean direction is calculated from the sample ChRM direction;
3. A paleomagnetic investigation involves numerous sites with a particular rock unit. These site-mean direction averaged to yield the average ChRM direction (paleomagnetic pole position) (table 7.1).

The figure below (fig. 7.2) roughly shows the pattern of concordant paleomagnetic declinations observed in the study area. As Kidane (2006) observed the paleomagnetic declination in the Assela area, similarly there is no significant vertical block rotation to paleomagnetic investigations but statistically the two directions are different and shows small amount of block rotation as the area exposed along the contact of central and rift margin.

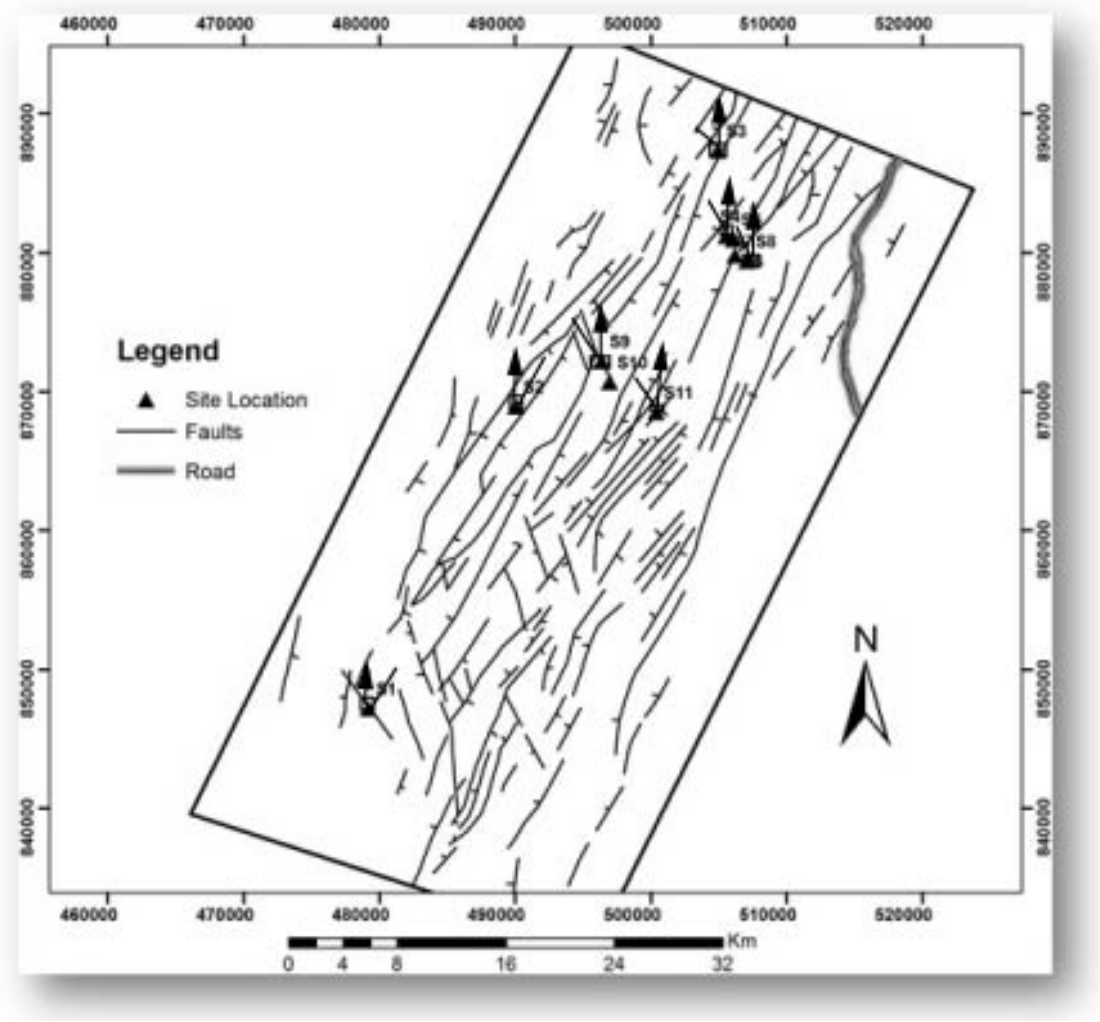

Fig.7.1. expected and observed paleomagnetic declinations are compared at sites of each volcanic rock units. Expected declinations are shown by the north-directed line, and observed declinations are shown by arrows.

Diriba A. Paleomagnetism and Tectonics of Northern Munesa, 2012. MSc thesis, Tel: +251-910-66-7446, email: nabekdiriba@hotmail.com, Addis Ababa; Ethiopia

The site averages calculated for all the 11 paleomagnetic sites are reported in Table 7.1 below.

Table7.1. paleomagnetic site mean directions with the expected direction.

Site Name	Coordinates		N	Ds	Is	K	α_{95}
	lat.	Long.					
MSS1	7.6641	38.8111	8	352.8	19.9	121.5	5
MSS 2 Mean 2	7.8612	38.9094	3	352	-4.2	120.1	13.3
MSS 4	7.9723	39.0502	14	169.9	-18.9	59.9	5.2
MSS 5	7.9697	39.0549	16	6.1	6.6	41.7	5.8
MSS 6	7.9594	39.0562	6	2.2	12	22.1	14.6
MSS 7	7.9558	39.0642	5	13.4	-6.2	54	10.5
MSS 8	7.9558	39.0644	6	348.1	6.9	25.8	13.4
MSS 9	7.8906	39.9669	5	2.6	-0.2	17.7	18.7
MSS 10	7.8767	38.9723	4	5.4	14.7	728.5	3.4
MSS 11	7.8574	39.0032	9	80.2	23.2	17.9	12.5
All mean			11	354.1	8.3	22	10
Exp.direction			32	1.9	13.5	105.5	2.5

Remark: Site name; location coordinates (latitude and longitude); N, number of samples; Ds and Is, declination and inclination in stratigraphic coordinates; K, Fischer precision parameter; $\alpha_{95,\ 95\%}$ confidence interval.

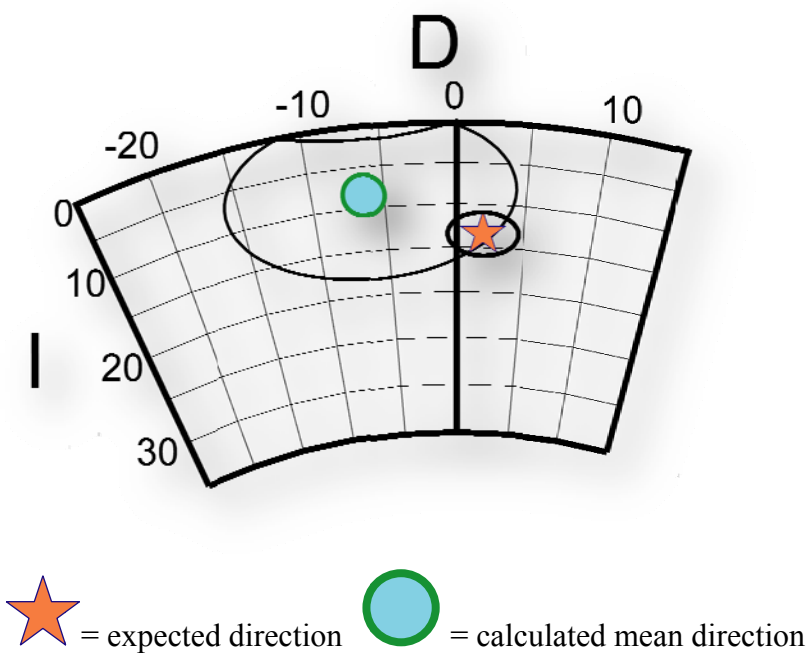

Fig.7.2 comparison of the overall mean direction (circular symbol) and the expected direction (star) from the theoretical apparent polar wander path curve for Africa (Besse and Courtillot 2003).

In fig.7.2 the two directions are within α_{95} of the calculatedmean, so the two directions are not distinguishable at the 5% significance level and as the α_{95} of calculated mean are large and Mc Fadden and Mc Elhinny, 1964 statistically analyzed and they are different.

Diriba A. Paleomagnetism and Tectonics of Northern Munesa, 2012. MSc thesis, Tel: +251-910-66-7446, email: nabekdiriba@hotmail.com, Addis Ababa; Ethiopia

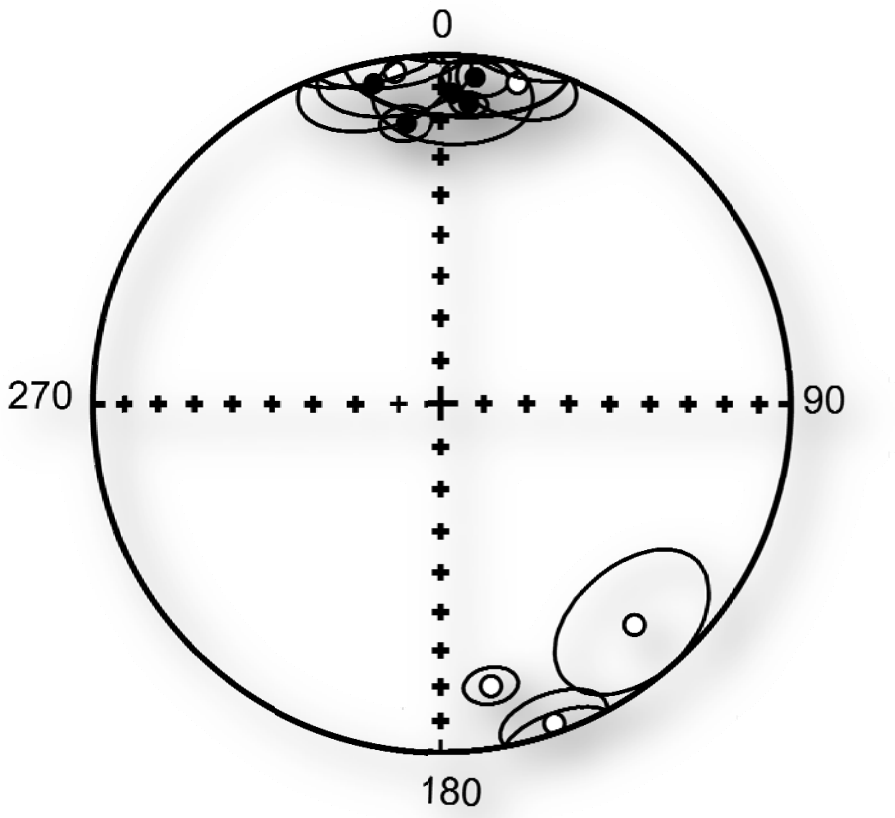

Figure 7.3 equal-area projections of site-mean ChRM directions from the rock unit of the area. Solid circles indicate NRM directions in the lower hemisphere of the equal-area projection, and open circles indicate directions in the upper hemisphere; the circle around each vector end points are α_{95} for each.

The normal and reversed polarities are 180 ° apart, and also they pass the paleomagnetic stability reversal test (McFadden & McElhinny 1988). When an overall mean direction is calculated for the 11 sites with stable polarities, excluding the one transitional, the following values are obtained: Ds = 354.1°, Is = 8.3°, N = 11, K = 22, α_{95} = 10°; with angular difference of -7 ± 8.24.

Because there was no tilting of all the young flows investigated in this study, there is no difference in the site mean directions in both geographic and tectonic coordinates.

Diriba A. Paleomagnetism and Tectonics of Northern Munesa, 2012. MSc thesis, Tel: +251-910-66-7446, email: nabekdiriba@hotmail.com, Addis Ababa; Ethiopia

8. Tectonic Rotation

The paleomagnetic observation on the 11 sites of Quaternary volcanic resulted in an overall mean direction of Dg=354.1°, Ig=8.3°, Ds = 354.1°, Is = 8.3°, N = 11, K = 22, α_{95} = 10° (see Table 7.1 and discussion above). When the obtained overall mean paleomagnetic direction is compared with the expected direction (Ds = 1.9 °, Is = 13.5 °, α_{95} = 2.5, K = 105.6, N = 32) calculated from the Apparent Polar Wander Path reference curve for Africa at 1.5 Ma (Besse & Courtillot 2003), they are not different (Fig. 7.2), as the confidence interval of the calculated direction is large the two directions are compared using Mc. Fadden and Mc. Elhinny, 1964 statistically analysis and they are different at $\alpha_{95}$and α_{99}as k1#k2. The small number of sites conducted which cause$\alpha_{95}$of calculated direction is large and as the area is at contact of central and rift margin there is indication of small rotation and the negative valueof angular difference (-7.8 ± 8.24) indicate small rotation to counter clock wise direction.

As Corti et al., 2012 suggested the boundary faults may be influenced by a local reorientation of the regional stress directions controlled by the reactivation of deep seated inherited fabrics.

The investigated region is located within and overlaps the < 1.9 my magmato-tectonic segments of Assela-Langano. Given the 20km overlap and right stepping nature of the individual fault and fissure belts lying within each magmato-tectonic segment, counterclockwise rotation of about 11 ° would be predicted if the oblique rifting model was responsible for the Pleistocene evolution of the MER (Boccaletti *et al.* 1992, 1999; Bonini *et al.* 1997). The paleomagnetic studies in this area indicate small detectable vertical axis rotation and therefore argue this model for rift formation and evolution.

Observations on recent structures in the rift indicated that, although shear surfaces are produced by cohesion less material such as pyroclastics fall deposits, most fractures open as Mode I cracks (tensile or opening mode) first and then evolve into Mode III cracks (one block move parallel to the crack parallel to the fracture front) (tearing mode) later (e.g. Accocella & Korme 2002). Thus, shear surfaces may not represent tectonic stresses, making it difficult to find true kinematic indicators on ignimbrites and basalts and explaining the contradictory kinematic results of Boccaletti *et al.* (1992) and Chorowicz *et al.* (1994).Numerical models of Buck (2004, 2006) show that the presence of magma at the lithosphere-asthenosphere boundary reduces the tectonic forces required to rift continental lithosphere, with progressive melt injection localizing strain. Keir *et al.* (2006) propose that magma injection to < 10 km subsurface beneath the magmatic segments triggers fault slip in the crust above the intrusions, leading to the formation of small offset faults. For example, Accocella and Korme (2002); Casey *et al. (*2006), field observation also show dykes reaching the surface, and open, magma-filled fissures in the magmatic segments. Thus, I suggest that strain is accommodated largely by movement along large offset fault border faults, or by large faults in the Quaternary magmatic segments rather than magma injection in to the crust.

Diriba A. Paleomagnetism and Tectonics of Northern Munesa, 2012. MSc thesis, Tel: +251-910-66-7446, email: nabekdiriba@hotmail.com, Addis Ababa; Ethiopia

9. Virtual Geomagnetic Polarity (VGP) and Paleosecular variation (PSV)

Table9.1 presents the VGPs of individual sites together with the mean paleomagnetic pole. A mean pole of,λ=85.9, ϕ=249.5, K=50.2 and α95=7.3 is calculated for the 11 sites considered. This value is statistically similar to the value λ=87.20, ϕ=217.10, and α95=4.00 of Kidane *et al*. 2003, for 'stable' part of Africa for the period ~2Ma. The site mean VGP distributions are shown in Fig.8.1 for the study area. As a site-mean VGP (table 8.1) is calculated from each site-mean ChRM direction (table 6.1) the mean pole position (paleomagnetic pole), λ=85.9, ϕ=249.5, K=50.2 and α95=7.3, is calculated from the set of VGP by fisher statistics, treating each VGP as a point on the unit sphere.

Because the age ranges of the studied lava flows is between 1.9Ma-0.025Ma and includes both reversed and normal polarities in different locations, the VGP scatter should reflect the Paleosecular variation of the geomagnetic field. The obtained VGP scatter values are in good agreement with the recent 0-5 Ma model of McFadden *et al.* (1990).

Table 9.1 site mean Virtual paleomagnetic poles (VGPs) for all analyzed sites and a mean paleomagnetic pole for 11 sites considered.

Site Name	**N**	**ϕ**	**λ**	**K**	**α95**
Mss1	8	329.5	82.5	2.8	5.3
Mss2	10	111.8	-69.5	4.7	9.4
Mss4	6	170.9	87.1	7.5	14.8
Mss5	5	168.2	72.7	5.3	10.5
Mss6	6	288.9	77.3	6.8	13.5
Mss7	5	200.8	81.5	9.3	18.7
MSS8	4	133.6	84.6	1.8	3.5
Mss9	9	119.1	11.1	7.1	13.3
Mss10	14	140.2	-79.9	2.8	5.4
Mss11	16	165.7	82.5	2.9	5.8
Mean VGP	9	249.5	85.9	50.2	7.3

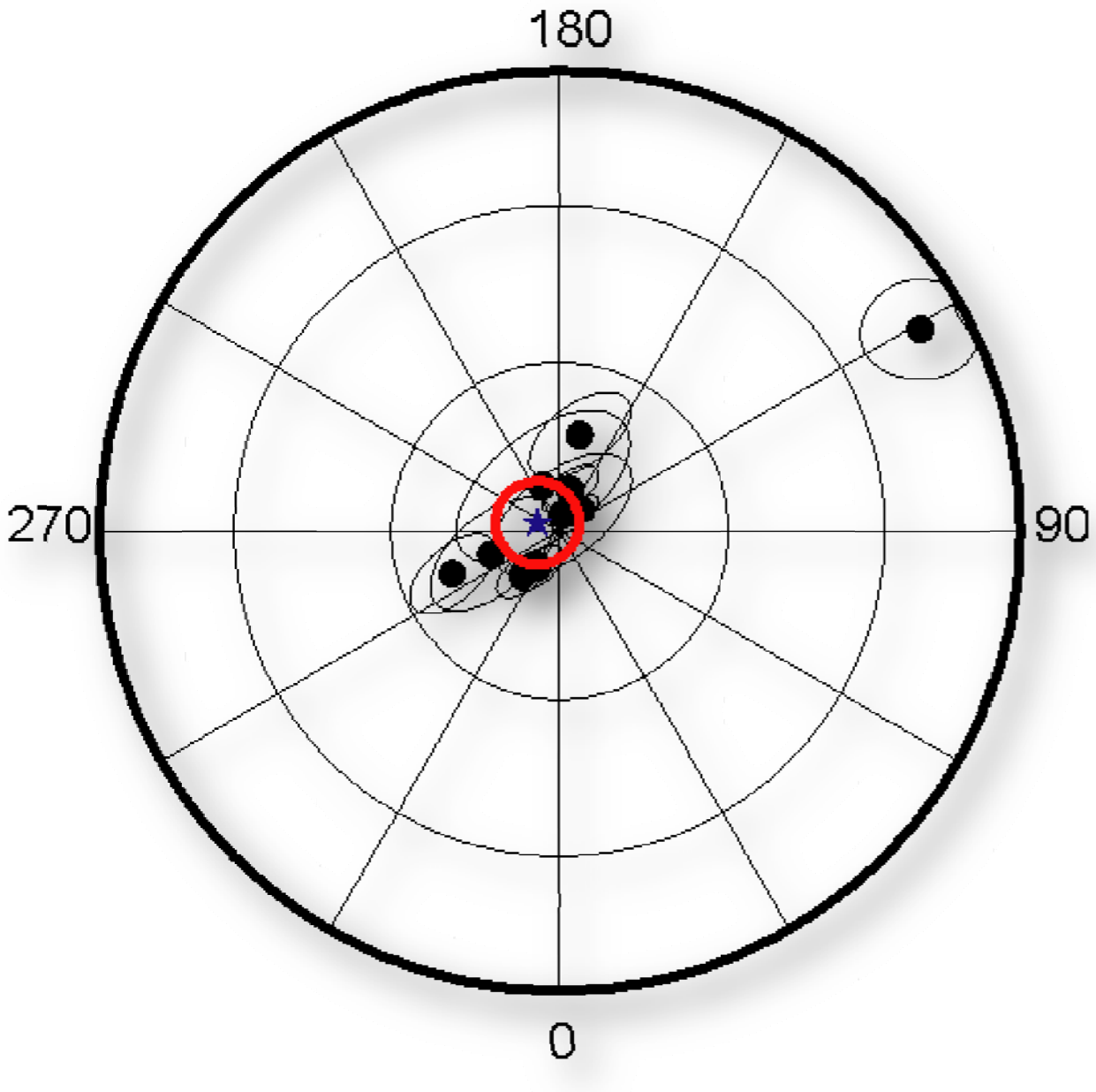

Fig.9.1 Stereographic projection of virtual geographic polarity(VGP)of the calculated mean, the star shows the mean VGP.

10. Conclusion and Recommendations

10.1 Conclusion

Generally at 11 paleomagnetic sites a total of 98 cores for paleomagnetic analysis were collected. The samples were oriented using both magnetic and sun compass. Mostly fissural basalt (mafic lava flow) and welded ignimbrite (felsic pyroclastics flows) are taken as paleomagnetic sites and there is very weak rhyolite with ash and obsidian. The site mean paleomagnetic directions for all the sampled sites of eastern part of the Langano-Ziway lakes are indicated in Fig. 4.4.

A paleomagnetic investigation involves numerous sites to collect numerous samples within a particular rock unit. The ChRM directions for the multiple specimens must be averaged, then site mean ChRM direction is calculated from the sample ChRM directions, and for each site-mean directions the site-mean VGP was calculated, and the site-mean VGP was averaged to yield either the average ChRM direction or a paleomagnetic pole position from the rock unit.

The sample collected from sites was thermally demagnetized following isolation of the ChRM by AF demagnetization to 20mT peak fields. Blocking temperatures were dominantly between 400^{o}Cand 580^{o}C, and AF demagnetization at 20 to 100mT interval. The Curie temperature determined on a sample was also 580^{o}c, indicating that magnetite is the dominant ferromagnetic mineral. In general, the observations indicate the low-stability NRM component removed by AF demagnetization to 20 mT is a secondary lightning-induced IRM. The high-stability ChRM isolated during AF demagnetization to peak fields ≥20 mT is a primary TRM acquired during original cooling of volcanic rocks. The acquisition curve indicate sharp increasing up to 200mT and saturated after 300mT, which is due to magnetite, some sulphide mineral also saturate at this magnetic field. To prove the ferromagnetic mineral thermal demagnetization are conducted and show the ferromagnetic mineral is magnetite.

Diriba A. Paleomagnetism and Tectonics of Northern Munesa, 2012. MSc thesis, Tel: +251-910-66-7446, email: nabekdiriba@hotmail.com, Addis Ababa; Ethiopia

The paleomagnetic observation from the 11 sites of Quaternary volcanic resulted in an overall mean direction of Dg=354.1°, Ig=8.3°, Ds = 354.1°, Is = 8.3°, N = 11, K = 22, α_{95} = 10°. When the obtained overall mean paleomagnetic direction is compared with the expected direction (Ds = 1.9 °, Is = 13.5 °, α_{95} = 2.5, K = 105.6, N = 32) calculated from the Apparent Polar Wander Path reference curve for Africa at 1.5 Ma (Besse & Courtillot 2003), it shows small counterclockwise rotation and it may be due to small number of paleomagnetic site, and they are statistically different were k1#k2.

The paleomagnetic studies in this area recommended there is small vertical axis rotation, as the area is at the contact of central and rift margins, and the strain is accommodated largely by movement along large offset fault border faults, or by large faults in the quaternary magmatic segmentsrather than by magma injection into the crust.

Diriba A. Paleomagnetism and Tectonics of Northern Munesa, 2012. MSc thesis, Tel: +251-910-66-7446, email: nabekdiriba@hotmail.com, Addis Ababa; Ethiopia

10.2 Recommendations

Due to the rough topography and road accessibility of the area detail investigations of structures and lithology, (as they are the basic features to conduct paleomagnetic sampling) were not conducted.

To use the results in the future studies the paleomagnetic results should be accompanied with good radiometric age data.

The paleomagnetic study of the whole of MER is required in order to explain regional deformation in the MER prior to advanceModeling.

Diriba A. Paleomagnetism and Tectonics of Northern Munesa, 2012. MSc thesis, Tel: +251-910-66-7446, email: nabekdiriba@hotmail.com, Addis Ababa; Ethiopia

11. References

1. Agostini et al., 2009. Evolution, Pattern, and Partitioning of deformation during oblique continent rifting: inferences from lithospheric scale centrifuge models. Vol. 10, No. 11, P. 1-23.
2. Abebe, B., 1993. Studio geologico-structurale Del Rift Etiopico a sud di Assela. Ph.D. Thesis. University of Frienze, Florence, Italy, pp. 153.
3. Acoccella, V., Korme, T., 2002. Holocene extension direction along the Main Ethiopian Rift, East Africa. Terra Nova 14 (3), 191–197
4. Acton, G.D., Tessema, A., Jackson, M., Bilham, R., 2000. The tectonic and geomagnetic significance of paleomagnetic observations from volcanic rocks from central Afar, Africa. Earth Planet. Sci. Lett. 180, 225–241.
5. Bastow, I., Stuart, G., Kendall, M., Ebinger, C., 2005. Upper mantle Seismic structure in a region of incipient continental break-up: northern Main Ethiopian Rift. Geophys. J. Int. 162, 479–493.
6. Benoit, M.H., Nyblade, A.A., Vandecar, J.C., Gurrola, H., 2003. Upper mantle P velocity structure and mantle transition zone thickness beneath the Arabian Shield. Geophys. Res. Lett. 30, 1153.
7. Besse, J., Courtillot, V., 1991. Revised and synthetic apparent polar wander paths of the African, Eurasian, North American and Indian plates, and true polar wander since 200 Ma. J. Geophys. Res. 96, 4029–4050.
8. Besse, J., Courtillot, V., 2003. Apparent and True Polar wander and the geometry of the geomagnetic field in the last 200 million years. J. Geophys. Res. 108 (B10), 2469, doi: 10.1029/2003JB002684.
9. Bilham, R., Bendick, R., Larson, K., Mohr, P., Braun, J., Tesfaye, S., Asfaw, L., 1999. Secular and tidal strain across the Main Ethiopian Rift. Geophys. Res. Lett. 26, 2789–2792.
10. Boccaletti, M., Getaneh, A., Tortorici, L., 1992. The Main Ethiopian Rift: an example of oblique rifting. Ann. Tecton. 6, 20–25.
11. Boccaletti, M.,Mammo,T., Bonini, M.,Abebe, B., 1994. Seismotectonics of East African Rift System: evidence of active oblique rifting. Ann. Tecton. 8, 87–99.

12. Boccaletti, M. et al., 1995. chemical variations in a bimodal magma system: the plio-quaternary volcanism in the dera Nazret area (MER,Ethiopia). Africa Geosciences Review, No. 1, PP., 37-60.
13. Boccaletti, M., Bonini, M., Mazzuoli, R., Abebe, B., Piccardi, L., Tortorici, L., 1998. Quaternary oblique extensional tectonics in the Ethiopian Rift (Horn of Africa). Tectonophysics 287, 97–116.
14. Bonini, M., Souriot, T., Boccaletti, M., Brun, J.P., 1997. Successive orthogonal and oblique extension episodes in a rift zone: Laboratory experiments with application to the Ethiopian rift. Tectonics 16, 347–362.
15. Butler, R.F. 1998. Paleomagnetism: Magnetic domains to geologic terranes.
16. Calais, E., Ebinger, C., Keir, D., Gloaguen, R., Mohammed, F., 2006. Strain accommodation in transitional rifts: Extension by magma intrusion and faulting in Ethiopian rift magmatic segments. In: Yirgu, G., Ebinger, C.J., Maguire, P.K.H. (Eds.), the Afar Volcanic Province within the East African Rift System, vol. 259. J. Geol. Soc., London, pp. 143–163.
17. Casey, M., Ebinger, C., Keir, D., Gloaguen, R.,Mohammed, F., 2006. Strain accommodation in transitional rifts: extension by magma intrusion and faulting in Ethiopian rift magmatic segments. In: Yirgu, G., Ebinger, C.J., Maguire, P.K.H. (Eds.), the Afar Volcanic Province within the East African Rift System, vol. 259. J. Geol. Soc., London, pp. 143–163.
18. Chorowicz, J., Collet, B., Bonavia, F.F., Korme, T., 1994. Northwest to north-northwest extension direction in the Ethiopian Rift deduced from the orientation of extension structures and fault slip analysis. Geol. Soc. Am. Bull. 105, 1560–1570.
19. Clifton, A.E., Schlisch, R.W., Withjack, M.A., Ackermann, R.V., 2000. Influence of rift obliquity on fault–population systematics results of experimental clay models. J. Struc. Geol. 22, 1491–1509.
20. Cogné, J.P., 2003. Paleomac, a Macintosh application for treating paleomagnetic data and making plate reconstructions. Geochem. Geophys. Geosyst. 4 (1), 1007, doi: 10.1029/2001GC000227.

Diriba A. Paleomagnetism and Tectonics of Northern Munesa, 2012. MSc thesis, Tel: +251-910-66-7446, email: nabekdiriba@hotmail.com, Addis Ababa; Ethiopia

21. Corti,G. 2006. Control of rift obliquity on the evolution segmentation of the MER.Vol. 1.
22. Corti, G. 2009. Continental rift evolution: from rift initiation to incipient break-up in the MER, east Africa.
23. Cox, A., 1969. Confidence limits for the precision parameter K. Geophys. J. R. Astron. Soc. 18, 545–549.
24. Di Paola, G.M., 1972. The Ethiopian Rift Valley (between 7◦ and 8◦40_ lat North). Bull. Volcanol. 35, 497–506.
25. Dugda, M.T. et al., 2006. New constraint on crustal structure in eastern afar from the analysis of receiver functions and surface wave dispersion in Djibouti. London. Vol. 259, p. 239-251.
26. Ebinger, C., Yemane, T., Harding, D., Tesfaye, S., Rex, D., Kelley, S., 2000. Rift deflection, migration, and propagation: Linkage of the Ethiopian and Eastern rifts, Africa. Geol. Soc. Am. Bull. 102, 163–176.
27. Ebinger, C.J., Casey, M., 2001. Continental breakup in magmatic provinces: An Ethiopian example. Geology 29, 527–530.
28. Fisher, R.A., 1953. Dispersion on a sphere, Proc, Roy. Soc. London, A. 217, 295–305.
29. Halls, H.C., 1976. A least-squares method to find a remanence direction from converging remagnetization circles. Geophys. J. R. Astron. Soc. 45, 297–304.
30. Halls, H.C., 1978. The use of converging remagnetization circles in Paleomagnetism. Phys. Earth Planet. Int. 16, 1–11.
31. Hofmann, C., Courtillot, V., Féraud, G., Rochette, P., Yirgu, G., Ketefo, E., Pik, R., 1997. Timing of the Ethiopian flood basalt event and implications for plume birth and global change. Nature 389, 838–841.
32. Keir, D., Ebinger, C., Stuart, G., Daly, E., Ayele, A., 2006. Strain accommodation by magmatism and faulting as rifting proceeds to breakup: Seismicity of the northern Ethiopian Rift. J. Geophys. Res. 111, B05314, doi: 10.1029/2005JB003748.

33. Keranen, K., Klemperer, S., Gloaguen, R., Eagle Working group, 2004. Imaging a protoridge axis in the Main Ethiopian Rift. Geology 39, 949–952.
34. Kenea, N.H., Ebinger, C.J., Rex, D.C., 2001. Late Oligocene volcanism and extension in the southern Red Sea Hills Sudan. J. Geol. Soc. London 158, 285–294.
35. Kidane, T., Carlut, J., Courtillot, V., Gallet, Y., Quidelleur, X., Gillot, P.-Y., Haile, T., 1999. Paleomagnetic and geochronological identification of the Reunion subchron in Ethiopian Afar. J. Geophys. Res. 104 (B5), 10,405–10,419.
36. Kidane, T., Courtillot, V., Manighetti, I., Audin, L., Lahitte, P., Quidelleur, X., Gillot, P. - Y., Gallet, Y., Carlut, J., Haile, T., 2003. New paleomagnetic and geochronological results from Ethiopian Afar: Block rotations linked to rift overlap and propagation and determination of a ~2 Ma reference pole for stable Africa. J. Geophys. Res. 108 (B2), 2102, doi: 10.1029/2001JB000645.
37. Kidane, T., Platzman, E., Ebinger, C., Abebe, B., Rochette, P., 2006. Paleomagnetic constrains on continental break-up processes: Observations from the Main Ethiopian Rift. In: Yirgu, G., Ebinger, C.J., Maguire, P.K.H. (Eds.), The Afar Volcanic Province within the East African Rift System, vol. 259. J. Geol. Soc., London, pp. 165–183.
38. Kidane, t. et al., 2009. Paleomagnetism of the Fantale-magmatic segment, MER: new evidence for counterclockwise block rotation linked to transtensional deformation. Phys. Earth planet. In.(2009). Doi. 10. 1016/j.pepi.2009.04.006
39. Kirschvink, J.L., 1980. The least squares line and plane and the analysis of paleomagnetic data. Geophys. J. R. Astron. Soc. 62, 699–718.
40. Korme, T., Chorowicz, J., Collet, B., Bonavia, F.F., 1997. Volcanic vents rooted on extension fractures and their geodynamic implications in the Ethiopian Rift. J. Volcanol. Geotherm. Res. 79, 205–222.
41. Kurz, t. et al., 2007. Deformation distribution and type in the MER: a remote sensing study. P. 100-114.

42. Mahatsente, R., Jentzsch, G., Jahr, T., 1999. Crustal structure of the Main Ethiopian Rift from gravity data: 3-dimensional modeling. Tectonophysics 313 (4), 363–382.
43. McFadden, P.L., McElhinny, M.W., 1990. Classification of the reversal test in Paleomagnetism. Geophys. J. Int. 103, 725–729.
44. McFadden, P., Merrill, L., McElhinny, M.W., Lee, M.W.S., 1991. Reversals of the Earth's magnetic field and temporal variations of the dynamo families. J. Geophys. Res. 96, 3923–3933.
45. McFadden, P.L., McElhinny, M.W., 1988. The combined analysis of remagnetization circles and direct observations in Paleomagnetism. Earth Planet. Sci. Lett. 87, 152–160.
46. Meyer,W., Pilger, A., Rosler, A., Stets, J., 1975. Tectonic evolution of the northern part of the Main Ethiopian Rift in Southern Ethiopian, "Afar depression of Ethiopia", in: A. Pilger, A. Rosler (eds.), IUGG Sci. Rep., Stuttgart, 14, pp. 352–362.
47. Mohr, P.A., 1962. The Ethiopian Rift System. Bull. Geophys. Obs. Addis Ababa Univ., 5, pp. 33-62.
48. Pik, R., Marty, B., Carignan, J., Lave, J., 2003. Stability of the Upper Nile drainage network (Ethiopia) deduced from (U-Th)/He thermo chronometry: Implications for uplift and erosion of the Afar plume dome. Earth Planetary Sci. Lett. 215, 73–88.
49. Pizzi A., Coltorti, M., Abebe, B., Disperati, L., Sacchi, G., Salvini, R., 2006. The Wonji fault belt (Main Ethiopian Rift): Structural and Geomorphological Constraints and GPS
50. Monitoring. In: Yirgu, G., Ebinger, C.J., Maguire, P.K.H. (Eds.), the Afar Volcanic Province within the East African Rift System, vol. 259. J. Geol. Soc. London, pp. 191–207.
51. Prévot, M., Grommé, S., 1975. Intensity of magnetization of subaerial and sub-marine basalts and its possible change with time. Geophys. J. R. Astr. Soc. 40, 207–224.

52. WoldeGabriel, G., Aronson, J.L., Walter, R.C., 1990. Geology, geochronology and rift basin development in the central sector of the Main Ethiopian Rift. Bull. Geol. Soc. Am. 102, 439–458.
53. Wolfenden, E., Ebinger, C., Yirgu, G., Renne, P., Kelley, S.P., 2005. Evolution of the southern Red Sea rift: Birth of a magmatic margin. Bull. Geolog. Soc. Am. 117, 846–864.
54. Williams, F.M., Williams, M.A.J., Aumento, F., 2004. Tensional fissures and crustal extension rates in the northern part of the Main Ethiopian Rift. J. African Earth Sci. 38, 183–197.

Index I: Data for sun angle

Site: mss1
Lat= 7¡39'50.70" (7.6641¡)
Lon= 38¡48'39.80" (38.8111¡)
Date (dd/mm/AZyear): 29/ 2/2011

Sample	Time	AzMag	AzSun	AzGeo	Decl
mss1-1	11:13	335.0	274.0	331.9	-3.1
mss1-2	11:18	318.0	324.0	23.3	65.3
mss1-3	11:21	356.0	298.0	358.0	2.0
mss1-4	11:23	327.0	264.0	324.5	-2.5
mss1-5	11:25	322.0	259.0	320.0	-2.0
mss1-6	11:27	318.0	253.0	314.5	-3.5
mss1-7	11:29	315.0	250.0	311.9	-3.1
mss1-8	11:31	296.0	230.0	292.3	-3.7

Site: mss2
Lat= 7¡51'40.20" (7.8612¡)
Lon= 38¡54'33.70" (38.9094¡)
Date (dd/mm/AZyear): 30/ 2/2011

Sample	Time	AzMag	AzSun	AzGeo	Decl
mss2-1	6:34	138.0	212.0	139.3	1.3
mss2-2	6:38	151.0	225.0	152.7	1.7
mss2-3	6:40	98.0	170.0	97.9	-.1
mss2-4	6:43	171.0	245.0	173.2	2.2
mss2-5	6:45	168.0	238.0	166.5	-1.5
mss2-6	6:48	164.0	232.0	160.8	-3.2
mss2-7	6:51	199.0	262.0	191.1	-7.9
mss2-8	6:53	159.0	220.0	149.4	-9.6
mss2-9	6:56	156.0	215.0	144.8	-11.2

Site: mss3
Lat= 8¡ 1'40.10" (8.0278¡)
Lon= 39¡ 2'40.90" (39.0447¡)
Date (dd/mm/AZyear): 30/ 2/2011

Sample	Time	AzMag	AzSun	AzGeo	Decl
mss3-1	8:22	240.0	277.0	226.2	-13.8
mss3-2	8:23	260.0	302.0	251.6	-8.4
mss3-3	8:24	273.0	306.0	256.0	-17.0
mss3-4	8:25	263.0	297.0	247.4	-15.6
mss3-5	8:27	311.0	358.0	309.2	-1.8
mss3-6	8:28	293.0	334.0	285.6	-7.4
mss3-7	8:29	296.0	333.0	285.1	-10.9
mss3-8	8:30	303.0	341.0	293.5	-9.5

Site: mss4
Lat= 7¡58'20.20" (7.9723¡)
Lon= 39¡ 3' .80" (39.0502¡)
Date (dd/mm/AZyear): 30/ 2/2011

Sample	Time	AzMag	AzSun	AzGeo	Decl
mss4-1	9:52	223.0	198.0	212.8	-10.2
mss4-2	9:55	218.0	191.0	208.4	-9.6
mss4-3	9:58	183.0	158.0	177.9	-5.1
mss4-4	9:59	220.0	190.0	210.8	-9.2
mss4-5	10: 2	204.0	173.0	196.2	-7.8
mss4-6	10: 4	236.0	202.0	226.8	-9.2
mss4-7	10: 6	229.0	194.0	220.3	-8.7
mss4-8	10: 8	224.0	188.0	215.8	-8.2

Site: mss5
Lat= 7¡58'11.00" (7.9697¡)
Lon= 39¡ 3'17.70" (39.0549¡)
Date (dd/mm/AZyear): 30/ 2/2011

Sample	Time	AzMag	AzSun	AzGeo	Decl
mss5-1	10:51	106.0	60.0	111.3	5.3
mss5-2	10:52	96.0	50.0	101.7	5.7
mss5-3	10:54	104.0	58.0	110.5	6.5
mss5-4	10:56	115.0	68.0	121.2	6.2
mss5-5	10:57	92.0	45.0	98.5	6.5
mss5-6	10:58	112.5	64.0	117.9	5.4
mss5-7	10:59	116.0	68.0	122.2	6.2

Site: mss6
Lat= 7¡57'33.90" (

7.9594¡)
Lon= 39¡ 3'22.50" (39.0562¡)
Date (dd/mm/AZyear): 30/ 2/2011

Sample	Time	AzMag	AzSun	AzGeo	Decl
mss6-1	11:55	327.0	261.0	328.2	1.2
mss6-2	11:57	339.5	273.0	340.5	1.0
mss6-3	11:58	333.0	266.0	333.7	.7
mss6-4	12: 2	306.0	238.0	306.3	.3
mss6-5	12: 3	308.0	240.0	308.4	.4
mss6-6	12: 5	331.0	262.0	330.7	-.3
mss6-7	12: 7	284.0	213.0	282.0	-2.0
mss6-8	12: 9	283.0	212.0	281.3	-1.7
mss6-9	12:12	292.0	221.0	290.7	-1.3

Site: mss7
Lat= 7¡57'21.00" (7.9558¡)
Lon= 39¡ 3'51.00" (39.0642¡)
Date (dd/mm/AZyear): 30/ 2/2011

Sample	Time	AzMag	AzSun	AzGeo	Decl
mss7-1	12:42	208.0	135.0	208.1	.1
mss7-2	12:44	221.0	147.0	220.3	-.7
mss7-3	12:46	206.0	133.0	206.5	.5
mss7-4	12:48	200.0	127.0	200.7	.7
mss7-5	12:49	204.0	131.0	204.7	.7
mss7-6	12:52	189.0	116.0	190.0	1.0
mss7-7	12:54	255.0	180.0	254.2	-.8
mss7-8	12:56	255.0	179.0	253.4	-1.6
mss7-9	12:58	261.0	186.0	260.5	-.5
mss7-1	12:59	264.0	189.0	263.6	-.4

Site: MSS8
Lat= 7¡57'21.00" (7.9558¡)
Lon= 39¡ 3'51.70" (39.0644¡)
Date (dd/mm/AZyear): 1/ 3/2011

Sample	Time	AzMag	AzSun	AzGeo	Decl
MSS8-	13:57	343.0	265.0	343.2	.2
MSS8-2	13:58	348.0	271.0	349.3	1.3
MSS8-3	13:59	352.0	275.0	353.3	1.3
MSS8-4	14: 0	346.0	268.0	346.4	.4
MSS8-5	14: 1	342.0	265.0	343.4	1.4
MSS8-6	14: 2	331.0	252.5	331.0	0.0
MSS8-7	14: 3	324.0	246.0	324.5	.5
MSS8-8	14: 5	325.0	247.0	325.6	.6
MSS8-8	14: 5	325.0	247.0	325.6	.6

Site: mss9
Lat= 7¡53'26.20" (7.8906¡)
Lon= 39¡58' 1.00" (39.9669¡)
Date (dd/mm/AZyear): 1/ 3/2011

Sample	Time	AzMag	AzSun	AzGeo	Decl
mss9-1	7:56	83.0	142.0	84.3	1.3
mss9-2	7:57	70.0	131.0	73.6	3.6
mss9-3	7:59	74.0	134.0	77.2	3.2
mss9-4	8: 1	79.0	138.0	81.7	2.7
mss9-5	8: 2	83.0	141.0	85.0	2.0
mss9-6	8: 3	89.0	147.0	91.3	2.3
mss9-7	8: 5	63.0	122.0	67.0	4.0
mss9-8	8: 6	65.0	125.0	70.3	5.3
mss9-9	8: 8	71.0	128.0	73.9	2.9

Site: mss10
Lat= 7¡52'36.00" (7.8767¡)
Lon= 38¡58'20.10" (38.9723¡)
Date (dd/mm/AZyear): 1/ 3/2011

Sample	Time	AzMag	AzSun	AzGeo	Decl
mss10-1	8:43	10.0	50.0	9.0	-1.0
mss10-2	8:44	4.0	44.0	3.6	-.4
mss10-3	8:45	6.0	51.0	11.1	5.1
mss10-4	8:46	4.0	54.0	14.7	10.7
mss10-5	8:47	6.0	68.0	29.2	23.2
mss10-6	8:48	24.0	68.0	29.8	5.8
mss10-7	8:49	23.0	70.0	32.4	9.4
mss10-8	8:50	24.0	58.0	21.0	-3.0

Site: mss11
Lat= 7¡51'26.50" (7.8574¡)
Lon= 39¡ 0'11.60" (39.0032¡)
Date (dd/mm/AZyear): 1/ 3/2011

Sample	Time	AzMag	AzSun	AzGeo	Decl
mss11-1	9:44	294.0	282.0	289.0	-5.0
mss11-2	9:46	326.0	280.0	288.8	-37.2
mss11-3	9:48	323.0	281.0	291.6	-31.4
mss11-4	9:50	347.0	283.0	295.4	-51.6
mss11-5	9:51	315.0	278.0	291.3	-23.7
mss11-6	9:53	290.0	266.0	281.0	-9.0
mss11-7	9:55	283.0	258.0	274.8	-8.2
mss11-8	9:57	285.0	260.0	278.4	-6.6
mss11-9	9:58	346.0	230.0	249.3	-96.7
mss11-10	10: 0	335.0	214.0	234.9	

*****

IndexII: Data arranged for Paleomac software package

Steps	X	y	z	M
NRM	-3.37	2.7	-3.07	0.5302
T150	-3.43	2.3	-3.03	0.5119
T200	-3.19	2.38	-2.94	0.4948
T250	-3.28	2.33	-2.91	0.4965
T300	-3.18	2.26	-2.8	0.4807
T350	-3.2	2.07	-2.83	0.475
T400	-3.14	2.07	-2.72	0.464
T430	-3.05	1.87	-2.54	0.4388
T460	-2.73	1.83	-2.43	0.4088
T490	-2.79	1.58	-2.39	0.4
T520	-2.71	1.48	-2.27	0.3836
T540	-2.6	1.59	-2.17	0.3747
T580	-2.27	1.44	-1.93	0.3311
T600	-2.07	1.7	-0.87	0.2817
T620	-1.468	0.861	-0.1161	0.2061

Mss4-2b

Steps	X	y	z	M
NRM	-3.08	2.14	-2.75	0.4651
M5	-3.15	2.18	-2.72	0.4702
M10	-3.11	1.96	-2.57	0.4489
M15	-2.5	1.84	-2.3	0.3866
M20	-2.13	1.55	-1.9	0.3244
M25	-1.588	1.374	-1.445	0.2549
M30	-1.269	1.261	-1.246	0.218
M40	-0.874	0.903	-0.91	0.1552
M60	-0.457	0.576	-0.533	0.09083
M80	-0.371	0.467	-0.435	0.0738
M100	-0.22	0.397	-0.28	0.05335

Mss4-2a

Steps	X	Y	Z	M
NRM	-3.72	2.74	-2.53	0.527
M5	-3.63	2.58	-2.49	0.5099
M10	-3.54	2.51	-2.35	0.4935
M15	-2.81	2.25	-2.06	0.4152
M20	-0.04	2.03	-1.66	0.2624
M25	-0.1668	0.1613	-0.1324	0.2672
M30	-0.1349	0.142	-0.106	0.2227

M40	-0.0815	0.1028	-0.0704	0.1489
M60	-0.0495	0.0694	-0.0502	0.09894
M80	-0.0376	0.0574	-0.0416	0.08019
M100	-0.0289	0.0496	-0.0333	0.06635

Mss4-4a

Steps	X	y	z	M
NRM	-0.404	1.64	-3.29	0.5458
T150	-0.387	1.87	-3.23	0.5382
T200	-0.395	1.76	-3.08	0.5309
T250	-0.39	1.84	-3.03	0.5272
T300	-0.39	1.61	-3	0.5176
T350	-0.381	1.31	-2.83	0.4925
T400	-0.355	1.34	-2.78	0.4705
T430	-0.334	1.52	-2.69	0.4556
T460	-0.336	1.5	-2.61	0.4508
T490	-0.32	1.29	-2.5	0.4259
T520	-0.301	1.32	-2.38	0.4058
T540	-0.262	1.14	-2.06	0.3524
T580	-0.236	1	-1.86	0.3171
T600	-0.1925	0.896	-1.478	0.2588
T620	-0.1925	0.896	-1.478	0.2588

Mss4-5b

Steps	X	Y	Z	M
NRM	-4.14	1.72	-3.62	0.576
M5	-4.04	1.79	-3.54	0.5667
M10	-3.7	1.61	-3.27	0.5189
M15	-3.12	1.2	-2.68	0.4289
M20	-2.26	1.04	-1.98	0.3178
M25	-1.582	0.641	-1.347	0.2175
M30	-1.2	0.439	-0.986	0.1614
M40	-0.772	0.266	-0.653	0.1046
M60	-0.571	0.0468	-0.588	0.09435
M80	-0.416	0.0418	-0.474	0.07566
M100	-0.302	0.0381	-0.441	0.06557
M100	-0.302	0.0381	-0.441	0.06557

Mss4-5a

Steps	x	Y	z	m
NRM	-2.69	2.97	-1.04	0.4142
M5	-2.79	2.99	-1.05	0.4223
M10	-2.48	2.83	-1.01	0.3892
M15	-2.2	2.64	-0.95	0.3569
M20	-1.84	2.25	-0.89	0.3041
M25	-1.52	2.01	-0.75	0.2627
M30	-1.27	1.743	-0.661	0.2256
M40	-0.916	1.333	-0.545	0.1707
M60	-0.605	0.959	-0.425	0.1211
M80	-0.463	0.715	-0.264	0.08916
M100	-0.321	0.602	-0.294	0.07427

Mss4-6a

Steps	x	y	z	m
NRM	-3.25	2.49	-1	0.4212
T150	-3.28	2.35	-1.06	0.4177
T200	-3.26	2.36	-1.01	0.4152
T250	-3.05	2.1	-0.98	0.3829
T300	-3.05	1.99	-0.94	0.3765

T350	-2.95	2.12	-0.91	0.3745
T400	-2.84	1.91	-0.86	0.3532
T430	-2.23	1.57	-0.7	0.2815
T460	-2.19	1.5	-0.67	0.2733
T490	-2	1.51	-0.65	0.2587
T520	-1.33	0.9	-0.25	0.1625
T540	-1.733	1.349	-0.0576	0.227
T580	-1.533	1.067	-0.0464	0.1924
T600	-1.411	1.011	-0.0451	0.1794
T620	-0.369	0.331	-0.0121	0.5102

Mss4-7b

Steps	X	y	z	M
NRM	-3.53	2.75	-2.36	0.506
M5	-3.49	0.305	-2.32	0.5182
M10	-3.57	0.326	-2.28	0.5341
M15	-3.25	0.317	-2.19	0.5044
M20	-3.03	0.309	-2.09	0.4806
M25	-2.63	0.275	-1.93	0.4268
M30	-2.29	0.227	-1.64	0.3615
M40	-1.674	0.1826	-1.272	0.2784
M60	-0.893	0.1075	-0.7	0.1563
M80	-0.57	0.0787	-0.466	0.1078
M100	-0.311	0.0583	-0.34	0.07431

Mss4-8a

NRM	X	y	z	M
T150	0.46	-5.87	-6.73	0.8941
T200	0.68	-5.94	-6.58	0.8895
T250	0.57	-5.49	-5.03	0.747
T300	0.42	-5.19	-4.81	0.7086
T350	0.66	-5.22	-4.11	0.6672
T400	0.58	-4.26	-2.85	0.516
T430	0.27	-3.69	-1.96	0.4188
T460	0.32	-3.59	-1.85	0.4056
T490	0.16	-3.38	-1.8	0.3832
T520	0.03	-2.12	-0.67	0.2248
T540	0.022	-2	-0.69	0.2131
T580	0.0163	-1.233	-0.351	0.1293
T600	0.0316	-1.153	-0.244	0.0122

Mss5-2b

steps	x	y	z	m
NRM	-0.53	-4.55	-4.24	0.6241
M5	-0.24	-4.39	-3.35	0.5533
M10	-0.14	-4.37	-1.91	0.477
M15	-0.03	-4.09	-1.23	0.4275
M20	0.11	-3.6	-0.88	0.3709
M25	-0.07	-0.07	-0.63	0.3186
M30	-0.01	-0.261	-0.47	0.2656
M40	0	-0.1964	-0.342	0.1993
M60	0.33	-0.1209	-0.179	0.1223
M80	0.24	-0.838	-0.099	0.08446
M100	0.19	-0.553	-0.076	0.05582

Mss5-4a

Steps	x	y	z	m
NRM	0.41	-6.08	-2.4	0.6547
M5	0.39	-5.79	-1.63	0.6024
M10	0.28	-5.33	-0.16	0.5341

M15	0.48	-4.96	0.21	0.4989
M20	0.47	-4.47	0.41	0.4516
M25	0.45	-3.89	0.49	0.3946
M30	0.42	-3.31	0.47	0.3374
M40	0.38	-2.36	0.37	0.2418
M60	0.135	-1.434	0.215	0.1456
M80	0.118	-0.954	0.197	0.09815
M100	0.082	-0.644	0.106	0.06575

Mss5-5a

Steps	X	y	z	M
NRM	-0.45	-4.4	-1.94	0.4827
M5	-0.48	-4.27	-1.58	0.4581
M10	-0.14	-4.14	-1.02	0.4269
M15	0.03	-3.88	-0.76	0.3953
M25	0.01	-2.99	-0.41	0.302
M30	0.006	-2.61	-0.33	0.2634
M40	0.0021	-1.913	-0.183	0.1922
M60	0.0027	-1.163	-0.09	0.1167
M80	0.00042	-0.752	-0.035	0.0754
M100	0.00031	-0.501	-0.004	0.0504

Mss5-6a

Steps	X	y	Z	M
NRM	-1.99	-9.19	-5.84	1.107
T150	-0.209	-9.44	-5.64	1.119
T200	-0.18	-8.98	-5.32	1.059
T250	-0.23	-8.39	-4.62	0.9853
T300	-0.175	-8.19	-4.12	0.9337
T350	-0.118	-7.55	-3.74	0.8507
T400	-0.101	-6.62	-3.04	0.7358
T430	-0.066	-6.35	-2.8	0.697
T460	-0.082	-6.08	-2.67	0.6691
T490	-0.0109	-5.8	-2.44	0.6383
T520	-0.0053	-5.02	-2.05	0.5447
T540	-0.0053	-4.57	-1.8	0.4945
T580	-0.0056	-4.28	-1.72	0.4647
T600	-0.0062	-3.67	-1.32	0.3948
T620	-0.0016	-2.18	-0.64	0.2278

Mss5-7b

Steps	x	y	z	m
NRM	0.33	1.89	2.89	0.03473
T150	0.46	1.83	2.6	0.03214
T200	0.25	1.83	2.73	0.03299
T250	0.34	1.82	2.87	0.0342
T300	0.45	1.58	2.62	0.03094
T350	0.38	1.72	2.58	0.03124
T400	0.3	1.41	2.23	0.02653
T430	0.23	1.34	2.01	0.02428
T460	0.166	1.227	1.926	0.02289
T490	0.0245	1.186	1.881	0.02237
T520	0.0223	1.209	1.827	0.02202
T540	0.0218	0.95	1.465	0.01759
T580	0.0086	0.402	0.608	0.00734
T600	0.0071	0.322	0.494	0.005941
T620	0.004	0.01	0.07	0.7985

Mss6-1b

Steps	x	y	z	m
NRM	0.46	1.91	3.09	0.03664

M5	0.5	2.02	3.13	0.03757
M10	0.47	1.91	3.02	0.03608
M15	0.42	1.85	2.85	0.03423
M20	0.42	1.69	2.65	0.0317
M25	0.29	1.56	2.46	0.02929
M30	0.3	1.49	2.25	0.02713
M40	0.287	1.259	1.811	0.02225
M60	-0.186	0.77	-0.22	0.02018
M80	0.097	0.504	0.0692	0.00862

Mss6-1a

Steps	X	y	Z	M
NRM	0.88	1.33	3.75	0.00073
T150	0.64	1.35	3.62	0.03913
T200	0.96	1.27	3.62	0.0395
T250	0.85	1.33	3.47	0.0381
T300	0.68	1.17	3.17	0.03451
T350	0.09	0.12	0.41	0.04321
T400	0.74	0.106	0.305	0.03313
T430	0.51	0.104	0.256	0.02813
T460	0.51	0.101	0.24	0.02651
T490	0.47	0.069	0.248	0.02613
T520	0.293	0.06	0.1581	0.01716
T540	0.269	0.0624	0.1607	0.01745
T580	0.261	0.0505	0.1285	0.01405
T600	0.181	0.0389	0.101	0.01097
T620	0.103	0.0148	0.0304	0.003531

Mss6-2b

Steps	X	y	z	M
NRM	0.73	1.34	3.44	0.03761
M5	0.66	1.23	3.4	0.03675
M10	0.63	1.24	3.23	0.03519
M15	0.66	1.18	3	0.03292
M20	0.57	1.1	2.74	0.03003
M25	0.46	0.97	2.49	0.0271
M30	0.42	0.93	2.23	0.02451
M40	0.379	0.708	1.781	0.01954
M60	0.196	0.463	1.198	0.013
M80	0.133	0.3	0.729	0.007995
M100	0.118	0.216	0.501	0.005581

Mss6-2a

Steps	x	y	z	m
NRM	0.63	1.5	3.85	0.04181
T150	0.72	1.77	3.71	0.04174
T200	0.54	1.61	3.63	0.04005
T250	0.63	1.59	3.44	0.03843
T300	0.6	1.49	3.25	0.03625
T350	0.71	1.55	3.14	0.03577
T400	0.54	1.47	2.93	0.0332
T430	0.62	1.27	2.63	0.0299
T460	0.62	1.16	2.31	0.02663
T490	0.26	1.09	2.79	0.03005
T520	-0.19	0.204	1.42	0.02494
T540	0.29	0.095	1.95	0.02185
T580	0.101	0.0273	0.535	0.006092
T600	0.076	0.247	0.499	0.005618
T620	-0.029	0	0.2	0.00035

Mss6-3b

Steps	X	y	z	M
NRM	0.45	2.13	2.13	0.04609
M5	0.35	2.09	0.397	0.04497
M10	0.043	1.98	0.374	0.04253
M15	0.045	1.79	0.344	0.03905
M20	0.029	1.57	0.311	0.03497
M30	0.022	1.21	0.25	0.02789
M40	0.0144	1.033	0.1905	0.02172
M60	0.007	0.683	0.1205	0.01385
M80	0.007	0.422	0.0808	0.009114

Mss6-3a

Steps	X	y	z	M
NRM	0	2.49	2.07	0.03237
M5	-0.08	2.46	2.03	0.03191
M15	-0.01	2.3	1.8	0.02922
M20	-0.006	2.16	1.67	0.02728
M25	-0.002	2.02	1.55	0.02544
M30	-0.00034	1.825	1.424	0.02314
M40	-8.8E-05	1.507	1.112	0.01875
M60	0.000068	1.05	0.715	0.01272
M80	0.000014	0.7	0.433	0.008236
M100	0.000006	0.503	0.281	0.005761

Mss6-4a

Steps	X	y	z	M
NRM	-1.26	8.2	2.67	0.0871
T150	-1.7	8.08	2.66	0.08672
T200	-1.37	7.73	2.49	0.08235
T250	-1.26	7.36	2.36	0.07836
T300	-1.29	7.45	2.42	0.07935
T350	-1.38	7.01	2.16	0.0746
T400	-1.71	6.72	2.17	0.07267
T430	-0.95	6.15	1.65	0.06434
T460	-0.101	5.84	1.72	0.06174
T490	-0.131	5.38	1.6	0.05762
T520	-0.123	5.22	1.57	0.05592
T540	-0.057	2.67	0.84	0.0286
T580	-0.014	0.39	0.3	0.005147
T600	-0.029	0.105	0.045	0.001176

Mss6-7b

Steps	X	y	z	m
NRM	-0.74	2.99	0.86	0.03196
M5	-0.88	2.91	0.77	0.0314
M10	-0.73	2.76	0.74	0.02954
M15	-0.085	2.51	0.64	0.02723
M20	-0.062	2.21	0.54	0.02362
M30	-0.0529	1.715	0.462	0.01853
M40	-0.041	1.348	0.358	0.01454
M60	-0.0208	0.84	0.249	0.00901
M80	-0.016	0.28	0.05	0.003271
M100	-0.0107	0.342	0.0095	0.003706

Mss6-7a

Steps	X	y	z	M
NRM	-0.35	2.81	1.03	0.03012
T150	-0.08	2.65	1.03	0.02843
T200	-0.37	1.99	0.91	0.02221
T250	-0.44	0.235	0.81	0.02523
T300	-0.32	0.23	0.67	0.02414
T350	-0.13	0.203	0.63	0.02127
T400	-0.0221	0.175	0.601	0.01864
T430	-0.0173	0.15	0.477	0.01583
T460	-0.0173	0.15	0.477	0.01583
T490	-0.0021	0.1642	0.36	0.01694
T520	-0.0009	0.139	0.023	0.01413
T540	0.0005	0.0327	0.107	0.003444
T580	0.0001	0.0377	0.09	0.003877
T600	0.0001	0.0288	0.067	0.00295
T620	-0.0029	0.0206	0.03	0.002101

Mss6-8b

Steps	x	y	z	m
NRM	-1.92	8.96	4.09	0.1003
T150	-0.268	8.78	3.91	0.09981
T200	-0.208	8.77	3.84	0.09796
T250	-0.186	8.4	3.82	0.09409
T300	-0.194	8.2	3.58	0.09161
T350	-0.184	8	3.46	0.08911
T400	-0.196	7.49	3.35	0.08433
T430	-0.227	6.89	3.07	0.07876
T460	-0.184	6.41	2.78	0.07227
T490	-0.181	6	2.49	0.06739
T520	-0.02	0.32	0.4	0.0546
T540	-0.0137	0.412	0.162	0.04638
T580	-0.0309	0.1161	0.0547	0.0132
T600	-0.0236	0.1086	0.0498	0.01218
T620	-0.0174	0.265	0.0121	0.003392

Mss6-9b

Steps	X	y	z	M
NRM	-0.68	2.23	0.66	0.0242
M5	-0.78	2.22	0.64	0.02438
M10	-0.61	2.13	0.62	0.02302
M15	-0.76	2.07	0.58	0.02277
M20	-0.491	1.926	0.505	0.0205
M25	-0.054	1.831	0.459	0.01963
M30	-0.0471	1.699	0.414	0.01811
M40	-4.15	1.499	0.293	0.01582
M60	-0.0326	1.137	0.174	0.01196
M80	-0.0268	0.914	0.106	0.009586
M100	-0.0112	0.709	0.039	0.007185

Mss6-8a

steps	X	y	z	m
NRM	-6.7	5.12	-11.98	0.01465
M5	-6.39	5.33	-11.96	0.01457
M10	-6.36	5.57	-11.42	0.01421
M15	-5.94	5.04	-10.58	0.01314
M20	-5.11	4.91	-9.73	0.01203
M25	-4.78	4.82	-8.85	0.01116
M30	-4.56	-4.56	-8.1	0.01018
M40	-3.55	3.83	-6.78	0.008556
M60	-2.87	2.77	-5.15	0.006518
M80	-1.74	2.24	-4.2	0.005071
M100	-1.71	1.37	-3.11	0.003806

Mss7-1a

Steps	X	y	z	M
NRM	-5.89	2	-7.97	0.01011
T150	-0.626	0.69	-7.33	0.009663
T200	-0.561	0.94	-7.3	0.009251
T250	-0.585	0.77	-7.14	0.009264
T300	-0.505	0.114	-6.34	0.008184
T350	-0.477	0.89	-5.99	0.007705
T400	-0.21	0.09	-0.41	0.004741
T430	-0.323	-0.37	-0.505	0.006004
T460	-0.281	0.77	-0.459	0.00544
T490	-0.467	0.166	-0.402	0.006382
T520	-0.3	-0.01	-0.46	0.005484
T540	-0.397	-0.036	-0.0513	0.00742
T580	-0.03	0.01	-0.02	0.00393
T600	0	0.025	-0.08	0.002621
T620	-0.0028	0.016	-0.078	0.00388

Mss7-3b

Steps	X	y	z	M
NRM	-1.16	-0.02	-1.7	0.02062
T150	-1.132	0.0092	-17.36	0.02074
T200	-1.14	0	-1.44	0.01838
T250	-1.048	0.00113	-1.621	0.01934
T300	-1.013	0.00196	-1.527	0.01843
T350	-0.998	0.00133	-1.478	0.01789
T400	-0.883	0.00146	-1.325	0.01599
T430	-0.79	0.003	-1.13	0.01375
T460	-0.0836	0.00131	-1.196	0.01465
T490	-0.061	0.00116	-1.136	0.01295
T520	-0.0794	0.00177	-1.018	0.01303
T540	-0.0575	0.001	-0.878	0.0105
T580	-0.03	0.004	-0.207	0.002095
T600	-0.03	-0.0006	-0.202	0.002144
T620	-0.011	-0.0007	-0.11	0.001347

Mss7-6b

Steps	x	y	z	m
NRM	-0.25	1.29	-0.13	0.01325
M5	-0.0513	1.268	-0.0156	0.01377
M10	-0.0527	1.225	-0.0147	0.01342
M15	-0.0504	1.131	-0.0017	0.0125
M20	-0.0418	1.069	-0.0015	0.01158
M30	-0.0294	0.848	-0.0002	0.009161
M40	-0.027	0.37	-0.0001	0.004757
M60	-0.0152	0.055	-0.0008	0.005756
M80	-0.0118	0.037	-0.0009	0.003983
M100	-0.0039	0.0307	-0.0005	0.003117

Mss7-7a

Steps	X	y	z	m
NRM	-4.49	10.39	-0.62	0.01133
M5	-4.42	10.21	-0.69	0.01114
M10	-4.52	9.61	-0.075	0.01064
M15	-4.53	9.37	-0.077	0.01044
M20	-3.91	8.63	-0.076	0.00951
M25	-3.29	8.02	-0.077	0.008702
M30	-2.78	7.2	-0.066	0.007748
M40	-2.78	6.13	-0.049	0.006754
M60	-1.75	4.82	-0.037	0.005145
M80	-1.34	3.87	-0.0063	0.004143
M100	-1.02	2.95	-0.005	0.003159

Mss7-8a

Steps	X	y	z	M
NRM	-0.23	1.42	0.02	0.01443
T150	-0.0644	1.437	0.0123	0.01579
T200	-0.0381	1.442	0.0123	0.01496
T250	-0.0585	1.2	0.0095	0.01339
T300	-0.047	0.99	0.002	0.01109
T350	-0.0351	0.1071	0.0081	0.0113
T400	-0.0344	0.0956	0.00108	0.01022
T430	-0.0305	0.0942	0.00122	0.00998
T460	-0.0234	0.0841	0.008	0.008768
T490	-0.0256	0.0719	0.0022	0.007638
T520	0.069	0.0538	0.0028	0.005432
T540	-0.0176	0.0632	0.00031	0.006567
T580	-0.029	0.0454	0.00021	0.00455
T600	-0.01	0.032	0.00019	0.003202
T620	-0.03	0.014	0.0001	0.001459

Mss7-10b

Steps	X	Y	z	M
NRM	4.68	5.13	9.55	1.181
M5	4.11	4.29	9.03	1.081
M10	3.26	3.44	8.25	0.9512
M15	2.7	2.94	7.11	0.8151
M20	2.04	2.23	5.55	0.6319
M25	1.55	1.63	3.98	0.4573
M30	1.04	1.14	2.78	0.3182
M40	0.557	0.744	1.444	0.1718
M60	0.216	0.503	0.57	0.07901
M80	0.16	0.34	0.221	0.04364
M100	0.086	0.361	0.17	0.04087

Mss8-1

STEPS	X	Y	Z	M
NRM	3.47	3.38	8.71	0.9962
M5	2.93	3.25	8.37	0.9441
M10	2.53	2.78	7.88	0.8729
M15	2.1	2.24	6.85	0.751
M20	1.83	1.81	5.36	0.5945
M25	1.26	1.22	3.84	0.4219
M30	0.81	0.83	2.76	0.2999
M40	0.513	0.547	1.429	0.1614
M60	0.145	0.36	0.558	0.068
M80	0.122	0.266	0.07	0.04718
M100	0.07	0.214	0.0149	0.02697

Mss8-2a

Steps	X	y	z	m
NRM	3.28	3.91	8.79	0.9822
T150	3.22	3.67	8.67	0.9952
T200	3.05	3.34	8.54	0.9663
T250	3.07	3.14	8.31	0.9401
T300	2.7	3.16	8.85	0.9776
T350	2.81	3.18	8.32	0.9342
T400	2.29	2.79	7.41	0.8239
T430	2.26	2.82	7.29	0.8136
T460	2.24	2.57	6.82	0.7623
T490	2.02	2.62	6.55	0.734
T520	2.37	2.66	6.4	0.7323
T540	2.09	2.26	6.04	0.6783
T580	2.11	2.2	5.64	0.6415
T600	1.96	2.22	5.48	0.6226
T620	1.57	1.63	4.21	0.4777

Mss8-4b

Steps	X	y	z	M
NRM	3.76	2.63	8.6	0.9746
M5	3.8	2.62	8.4	0.9586
M10	3.36	2.25	7.94	0.8907
M15	2.62	2.17	6.89	0.7686
M20	2.19	1.37	5.46	0.604
M25	1.65	1.15	4	0.4477
M40	0.716	0.671	1.579	0.1859
M60	0.294	0.336	0.71	0.08383
M80	0.214	0.229	0.354	0.04731
M100	0.136	0.217	0.167	0.03059

Mss8-4a

Steps	X	y	z	M
NRM	-16.33	0.13	19.14	2.516
T150	-16.12	0.1	19.04	2.497
T200	-15.45	-0.17	18.42	2.404
T250	-13.58	0.062	16.44	2.134
T300	-12.83	0.004	15.86	2.04
T350	-11.13	-0.001	13.7	1.765
T400	-9.91	0.00073	12.71	1.614
T430	-8.28	0.00075	10.74	1.358
T460	-7.34	0.000094	10.13	1.255
T490	-6.95	1.12E-05	9.63	1.193
T520	-6.11	1.05E-05	9.01	1.094
T540	-5.54	9.9E-06	8.34	1
T580	-4.42	1.05E-06	6.48	0.7909
T600	-3.9	1.04E-06	6.07	0.7287
T620	-1.16	3.1E-06	2.15	0.2464

Mss8-7b

Steps	x	y	z	m
NRM	1.33	1.43	8.86	0.9076
T150	1.3	0.214	8.65	0.9002
T200	1.22	0.161	7.95	0.8199
T250	1.18	0.138	7.28	0.7499
T300	1.01	0.102	6.67	0.6826
T350	0.98	0.07	6.3	0.6409
T400	0.78	0.061	5.12	0.5218
T430	0.65	0.047	4.47	0.4541
T460	0.78	0.046	4.41	0.4501
T490	0.82	0.027	4.03	0.412
T520	0.63	0.048	3.94	0.4018
T540	0.55	0.024	3.8	0.3843
T580	0.44	0.039	3.21	0.3265
T600	0.33	0.038	2.79	0.2832
T620	0.355	0.0192	1.781	0.1826

Mss9-1b

Steps	X	y	z	m
NRM	0.99	1.1	7.84	0.7975
M5	0.77	0.35	5.61	0.567
M10	0.176	-0.1417	1.536	0.2097
M15	0.094	-0.1529	0.512	0.1615
M20	0.068	0.167	0.332	0.1215
M25	0.037	-0.0814	0.257	0.08549
M30	0.02	-0.0618	0.184	0.06454
M40	0.0032	-0.0389	0.112	0.04059
M60	0.0021	-0.0251	0.061	0.02596
M80	0.0026	-0.0207	0.063	0.02179
M100	0.00102	-0.0195	0.047	0.02006

Mss9-1a

Steps	X	y	z	M
NRM	2.8	4.94	10.45	1.189
T150	2.62	4.83	10.3	1.168
T200	2.11	4.52	9.53	1.076
T250	2.6	3.76	8.88	0.9989
T300	2.1	3.56	7.82	0.88843
T350	1.83	3.37	7.61	0.8521
T400	1.79	2.77	6.79	0.7546
T430	1.32	2.39	5.66	0.6287
T460	1.27	2.16	5.42	0.5968
T490	1.3	1.89	5.05	0.5547
T520	1.21	1.19	3.73	0.4098
T540	0.86	1.19	3.72	0.3997
T580	0.109	1.08	3.45	0.3772
T600	0.173	0.2	0.736	0.07818
T620	0.049	0.062	0.7	0.01059

Mss9-3b

Steps	X	y	z	M
NRM	0.28	0.69	2.92	3.009
T150	0.31	0.66	2.87	2.964
T200	0.3	0.62	2.74	2.828
T250	0.27	0.55	2.48	2.558
T300	0.21	0.48	2.17	2.233
T350	0.21	0.48	2.13	2.197
T400	0.147	0.361	1.719	1.763
T430	0.169	0.345	1.656	1.7
T460	0.181	0.301	1.547	1.586
T490	0.113	0.27	1.345	1.377
T520	0.144	0.285	1.328	1.365
T540	0.168	0.275	1.288	1.327
T580	0.111	0.233	1.104	1.133
T600	0.087	0.173	0.906	0.9263
T620	0.083	0.131	0.618	0.6376

Mss9-4b

Steps	X	y	z	m
NRM	-0.16	0.48	2.07	2.137
M5	-0.151	0.324	1.614	1.653
M10	-0.062	-0.01	0.662	0.6647
M15	-0.066	-0.0135	0.1681	0.2169
M20	0.0082	-0.0105	0.00596	0.1213
M25	0.0072	-0.0074	0.003	0.07988
M30	0.0036	-0.0054	0.00233	0.05896
M40	0.00044	-0.0034	0.00149	0.03757
M60	0.00019	-0.0022	0.00099	0.02407
M100	0.000263	-0.0017	0.000743	0.01835

Mss9-4a

Steps	x	y	z	m
NRM	3.3	3.3	8.28	0.9504
T150	3.42	3.7	8.07	0.9512
T200	3.04	3.11	7.36	0.8545
T250	2.6	2.45	6.54	0.7454
T300	2.46	2.41	6.02	0.6933
T350	2.42	1.9	5.8	0.6566
T400	2.17	1.8	5.15	0.5873
T430	1.93	1.47	4.19	0.4845
T460	1.89	1.27	4.02	0.4621

T490	1.59	0.93	3.86	0.4275
T520	1.65	0.102	3.62	0.4111
T540	1.47	0.106	3.41	0.3865
T580	0.404	0.0222	0.813	0.09343
T600	0.339	0.0234	0.815	0.09134
T620	0.35	0.0143	0.79	0.08756

Mss9-5b

STEPS	X	Y	Z	M
NRM	3.16	3.86	7.94	0.9374
M5	2.22	2.08	5.53	0.6307
M10	0.587	-0.67	1.42	0.1676
M15	0.111	-0.1377	0.491	0.1466
M20	0.051	-0.1097	0.364	0.1157
M25	-0.016	-0.0824	0.243	0.08591
M30	0.026	-0.0609	0.164	0.06315
M40	-0.004	-0.0371	0.111	0.03869
M60	0.0019	-0.0241	0.061	0.02498
M80	0.0008	-0.022	0.064	0.02287
M100	0.00041	-0.0196	0.0517	0.02024

Mss9-5a

Steps	x	y	z	m
NRM	4.96	3.19	9.64	1.131
T150	0.543	3.87	9.25	1.141
T200	0.44	2.78	8.62	1.007
T250	0.392	2.49	7.85	0.9125
T300	0.353	1.72	7.21	0.8209
T350	0.33	1.47	6.21	0.7184

T400	0.257	0.79	5.15	0.5806
T430	0.246	0.46	4.49	0.5138
T460	0.248	0.53	4.29	0.4986
T490	0.217	0.29	3.86	0.4437
T520	0.204	0.1	3.78	0.4296
T540	0.189	0.14	3.51	0.3993
T580	0.156	0.03	2.89	0.3299
T600	0.107	0.018	2.15	0.2402

Mss9-6a

Steps	x	y	z	m
NRM	1.74	6.33	2.56	0.7044
M5	0.86	4.17	1.5	0.4515
M10	0.359	0.947	0.722	0.1244
M15	0.32	-0.535	0.498	0.07979
M20	0.136	-0.068	0.433	0.08177
M25	0.146	-0.0549	0.315	0.06497
M40	0.074	-0.0301	0.16	0.03491
M60	0.047	-0.0198	0.099	0.02265
M80	0.0353	-0.0157	0.01142	0.01975
M100	0.004	-0.0127	0.0083	0.01574

Mss9-7a

Steps	x	y	z	M
NRM	1.84	5.54	1.89	0.613
T150	1.81	5.55	1.83	0.6119
T200	1.43	4.91	1.8	0.542
T250	1.26	4.01	1.53	0.4472
T300	1.33	3.42	1.41	0.3933
T350	1.21	3.25	1.46	0.3764
T400	1.02	2.79	1.32	0.3248

T430	0.86	2.36	1.14	0.2757
T460	0.85	2.08	1.12	0.2516
T490	0.759	1.929	1.031	0.2315
T520	0.531	1.624	0.879	0.1921
T540	0.603	1.562	0.869	0.1887
T580	0.584	1.457	0.8	0.1762
T600	0.469	1.139	0.625	0.1381
T620	0.25	0.666	0.382	0.08073

Mss9-8b

Steps	X	y	z	M
NRM	2.83	5.13	2.07	0.6214
T150	2.51	5.02	1.95	0.5941
T200	2.38	3.95	1.88	0.4981
T250	2.25	3.57	1.8	0.4588
T300	1.9	2.89	1.59	0.3804
T350	1.8	2.47	1.56	0.3436
T400	1.68	2.24	1.46	0.3156
T430	1.497	1.559	1.308	0.2527
T460	1.339	1.243	1.239	0.2208
T490	1.22	1.165	1.151	0.2042
T520	1.26	0.92	1.02	0.1863
T540	1.071	0.847	1.055	0.1725
T580	0.96	0.733	0.922	0.152
T600	0.82	0.576	0.778	0.1269
T620	0.812	0.12	0.604	0.0102

Mss9-9b

Steps	x	y	Z	m
NRM	1.42	4.1	-6.58	0.07881
T150	1.12	4.25	-0.704	0.083
T200	1.33	3.98	-0.653	0.07759
T250	1.54	3.53	-0.568	0.06858
T300	0.18	2.49	-0.764	0.08041
T400	0.117	2.74	-0.538	0.0615
T430	0.111	2.48	-0.451	0.05264
T460	0.065	1.69	-0.293	0.03451
T490	0.0098	1.81	-0.243	0.03185
T520	0.0049	1.77	-0.334	0.0381
T540	0.00103	1.42	-0.287	0.03364
T580	0.000611	0.854	-0.1343	0.01705
T600	0.00054	0.67	-0.086	0.01214
T620	0.00043	0.14	-0.0133	0.004718

Mss10-1b

Steps	x	y	z	m
NRM	0.97	2.56	-6.21	0.06786
T150	0.85	2.56	-6.27	0.06822
T200	0.53	2.45	-6.07	0.06566
T250	0.75	1.9	-4.95	0.05354
T300	0.67	1.17	-4.4	0.04603
T350	0.85	1.51	-4.14	0.04493
T400	0.75	0.52	-3.37	0.03491
T430	0.4	0.148	-3.19	0.03539
T460	-0.231	0.0303	-0.708	0.08041
T490	0.05	0.0105	-0.205	0.02355
T520	0.01	0.008	-0.175	0.01931

T540	0.00794	0.00186	-0.1638	0.0183
T580	0.00439	0.000421	-0.0999	0.0117
T600	0.00262	0.000529	-0.0853	0.01037
T620	-0.0005	0.000216	-0.1	0.002429

Mss10-2b

Steps	X	Y	Z	M
NRM	0.91	1.68	-4.69	0.05064
M5	0.92	1.85	-4.91	0.05324
M10	0.75	0.203	-0.517	0.05607
M15	0.76	0.217	-0.499	0.05493
M20	0.091	0.206	-0.495	0.05443
M25	0.082	0.213	-0.48	0.05315
M30	0.062	0.203	-0.448	0.0496
M40	0.048	0.197	-0.402	0.04496
M60	0.048	0.16	-0.299	0.03426
M80	0.015	0.113	-0.214	0.0228
M100	0.0021	0.63	-0.1373	0.01525

Mss10-2a

Steps	X	y	Z	m
NRM	0.82	2.04	-6.22	0.06594
T150	0.49	1.98	-6.38	0.06696
T200	0.74	1.48	-6.14	0.06358
T250	0.77	1.64	-5.69	0.05966
T300	-0.2	1.57	-5.7	0.05914
T350	-0.1	1.53	-5.6	0.05805
T400	0.16	1.21	-4.8	0.04952
T430	0.18	1.31	-4.25	0.04453
T460	0.16	1.1	-4.31	0.04454
T490	0.4	1.05	-4.01	0.04162
T520	0	1.26	-3.63	0.03846
T540	0.034	0.51	-2.69	0.02763
T580	0.0417	0.498	-1.566	0.01695
T600	0.015	0.28	-0.52	0.006127
T620	-0.0256	-0.136	0.25	0.002915

Mss10-3b

Steps	x	y	z	m
NRM	0.84	1.49	-5.21	0.05483
M5	0.82	1.52	-5.39	0.095655
M10	0.78	1.61	-5.52	0.05805
M15	0.69	1.64	-5.48	0.05762
M20	0.72	1.63	-5.36	0.05644
M25	0.74	1.64	-5.12	0.05423
M30	0.64	1.59	-4.8	0.05093
M40	0.51	1.67	-4.4	0.04731
M60	0.39	1.24	-3.3	0.03543
M80	0.37	0.94	-2.37	0.02573
M100	0.187	0.647	-1.699	0.01827

Mss10-3a

Steps	X	y	z	M
NRM	0.01	0.25	-0.56	0.06128
T150	0.98	0.263	-0.531	0.06007
T200	0.71	0.281	-0.575	0.0644
T250	0.146	0.252	-0.532	0.06064
T300	0.117	0.236	-0.523	0.05858
T350	0.159	0.238	-0.497	0.05737
T400	-0.053	0.121	-0.468	0.0486
T430	0.0201	0.0315	-0.492	0.06175
T460	0.0104	0.0156	-0.331	0.03805
T490	0.0102	0.0136	-0.295	0.03404
T520	0.0104	0.0146	-0.287	0.03382
T540	-0.014	0.0121	-0.26	0.02869
T580	0.00981	0.00382	-0.1242	0.01628

Mss10-4b

Steps	*X*	*y*	*z*	*M*
NRM	1.37	2.55	-2.6	0.03892
M5	1.22	2.56	-2.7	0.0391
M10	1.31	2.6	-2.8	0.04041
M15	1.18	2.66	-2.82	0.04051
M20	1.11	2.48	-2.66	0.03806
M25	1.06	2.45	-2.59	0.03718
M30	1.07	2.44	-2.5	0.03657
M40	0.99	2.25	-2.23	0.0332
M60	0.691	1.761	-1.718	0.02556
M80	0.472	1.266	-1.271	0.01855
M100	0.269	0.996	-0.969	0.01416

Mss10-6a

Steps	*x*	*y*	*z*	*m*
NRM	1.37	3.73	-3.31	0.0517
T150	1.05	3.32	-3.6	0.05007
T200	1.07	3.39	-3.4	
T250	0.86	3.1	-2.87	0.04314
T300	0.36	3.04	-0.415	0.05152
T350	0.98	2.61	-0.261	0.03819
T400	0.84	2.7	-0.259	0.03836
T430	0.68	2.58	-0.15	0.03059
T460	0.664	1.985	-0.1959	0.02867
T490	0.66	0.208	-0.189	0.02886
T520	0.313	0.0908	-0.0717	0.01198
T540	0.226	0.0964	-0.0595	0.01155
T580	0.304	0.072	-0.053	0.00947
T600	-0.056	0.0295	-0.0177	0.003484

Mss10-7b

Steps	*x*	*y*	*z*	*m*
NRM	1.15	3.3	-3.14	0.04696
M10	1.19	3.49	-3.44	0.05041
M15	1.09	3.56	-3.41	0.05049
M20	1.15	3.54	-3.38	0.05023
M25	1.1	3.35	-3.24	0.04788
M30	0.96	3.25	-3.09	0.04589
M40	0.86	2.99	-2.76	0.04162
M60	0.63	2.44	-2.05	0.0325
M80	0.327	1.717	-1.602	0.02371
M100	0.305	1.197	-1.188	0.01714

Mss10-7a

Steps	*X*	*y*	*z*	*M*
NRM	1.37	2.55	-2.6	0.03892
M5	1.22	2.56	-2.7	0.0391
M10	1.31	2.6	-2.8	0.04041
M15	1.18	2.66	-2.82	0.04051
M20	1.11	2.48	-2.66	0.03806
M25	1.06	2.45	-2.59	0.03718
M30	1.07	2.44	-2.5	0.03657
M40	0.99	2.25	-2.23	0.0332
M60	0.691	1.761	-1.718	0.02556
M80	0.472	1.266	-1.271	0.01855
M100	0.269	0.996	-0.969	0.01416

Mss10-8a

Steps	*X*	*y*	*z*	*M*
NRM	-0.3	4.23	0.71	0.4297
T150	-0.25	4.11	0.72	0.4181
T200	0.01	3.88	0.8	0.3961
T250	-0.09	3.73	0.79	0.3814
T300	0.12	3.45	0.88	0.356
T350	0.23	3.14	1.05	0.3318
T400	0.28	3.14	0.84	0.3259
T430	0.27	2.83	0.78	0.2952
T460	0.18	2.53	0.71	0.2637
T490	-0.02	2.43	0.76	0.255
T520	-0.05	2.31	0.73	0.2425
T540	0.08	2.18	0.71	0.2291
T580	0.033	1.792	0.565	0.1879
T600	-0.027	0.486	0.152	0.05096
T620	0.041	0.477	0.148	0.05014

Mss11-1b

Steps	*x*	*y*	*z*	*m*
NRM	1.26	3.34	2.08	0.4134
T150	0.89	3.41	2.04	0.4073
T200	0.103	3.18	1.99	0.3896
T250	0.101	3.02	0.2	0.3761
T300	0.111	2.66	0.184	0.3423
T350	0.095	2.54	0.184	0.3281
T400	0.0102	2.27	0.18	0.3072
T430	0.0092	2.21	0.165	0.2909
T460	0.0093	1.97	0.159	0.2695
T490	0.00786	1.889	0.1539	0.256
T520	0.0078	1.754	0.145	0.2406
T540	0.00363	0.776	0.0678	0.1093
T580	0.0077	0.242	0.016	0.03004
T600	0.0084	0.237	0.0162	0.02993
T620	0.00117	0.228	0.0164	0.03047

Mss11-2b

Steps	*X*	*y*	*z*	*M*
NRM	1.48	3.4	2.42	0.4427
M5	1.51	3.06	2.38	0.4157
M10	1.59	2.33	2.28	0.635
M15	1.48	1.9	2.14	0.3225
M20	1.321	1.509	1.895	0.2759
M30	0.991	1.175	1.397	0.2077
M40	0.739	0.905	1.002	0.1539
M60	0.561	0.636	0.683	0.1089
M80	0.354	0.494	0.492	0.07823
M100	0.273	0.424	0.361	0.062

Mss11-2a

Steps	*X*	*y*	*z*	*M*
NRM	1.1	2.84	1.49	0.339
M5	1.08	2.72	1.45	0.3265
M10	1.09	2.12	1.39	0.2757
M15	0.1134	1.627	1.289	0.2365
M20	0.093	1.363	1.086	0.1976
M25	0.0803	1.124	0.901	0.165
M30	0.0665	0.887	0.789	0.1361
M40	0.051	0.754	0.554	0.1066
M60	0.0334	0.526	0.367	0.07229
M80	0.0266	0.442	0.257	0.05765
M100	0.021	0.361	0.199	0.04629

Mss11-3a

Steps	*X*	*y*	*z*	*M*
NRM	1.54	2.18	2.85	0.3907
M5	1.67	1.96	2.72	0.3745
M10	1.39	1.35	2.48	0.3143
M15	1.31	0.96	2.26	0.278
M20	1.19	0.73	1.97	0.2419
M25	0.984	0.549	1.674	0.2019
M30	0.854	0.492	1.396	0.1709
M40	0.634	0.371	1.06	0.129
M60	0.448	0.3	0.71	0.08913
M80	0.3	0.222	0.504	0.06268
M100	0.214	0.211	0.379	0.04836

Mss11-4a

Steps	*X*	*y*	*z*	*m*
NRM	-0.11	3.63	1.35	0.3874
T150	0.03	3.52	1.32	0.3761
T200	-0.05	3.37	1.37	0.3638
T250	0.0149	3.06	1.33	0.3654
T300	0.016	2.85	1.32	0.3143
T350	0.006	2.71	1.3	0.301
T400	-0.004	2.48	1.23	0.2766
T430	0.0013	2.08	1.1	0.2357
T460	0.0021	2.03	1.09	0.2316
T490	0.00208	1.869	1.04	0.2148
T520	-0.0051	1.75	0.77	0.1976
T540	0.00167	1.215	0.729	0.1426
T580	0.00258	1.144	0.703	0.1367
T600	0.00263	1.147	0.684	0.1361
T620	0.0087	0.586	0.354	0.6906

Mss11-5b

Steps	*X*	*y*	*z*	*M*
NRM	-1.51	5.59	0.19	0.579
T150	-1.33	5.34	0.2	0.5508
T200	-1.01	5.11	0.33	0.5221
T250	-0.93	4.91	0.47	0.5021
T300	-0.11	4.51	0.055	0.4674
T350	-0.099	4.33	0.058	0.4477
T400	-0.061	3.98	0.063	0.407
T430	-0.066	3.64	0.063	0.3752
T460	-0.073	3.47	0.063	0.3603
T490	-0.071	3.29	0.067	0.3435
T520	-0.056	2.78	0.058	0.2892

T540	-0.049	2.72	0.063	0.2837
T580	-0.0255	1.962	0.042	0.2022
T600	-0.0329	1.851	0.0412	0.1925
T620	-0.0265	1.162	0.0237	0.1215

Mss11-6b

Steps	*X*	*y*	*z*	*M*
NRM	-1.38	6	0.35	0.6171
M5	-1.37	5.74	0.55	0.5922
M10	-0.8	4.95	0.098	0.5112
M15	-0.43	4.28	0.116	0.4451
M20	-0.37	3.71	0.111	0.3888
M25	-0.31	3.23	0.094	0.3374
M30	-0.29	2.85	0.078	0.297
M40	-0.24	2.21	0.057	0.2292
M60	-0.125	1.593	0.0355	0.1636
M80	-0.112	1.189	0.0233	0.1217
M100	-0.059	0.954	0.1	0.09612

Mss11-6a

Steps	*X*	*y*	*z*	*m*
NRM	-1.21	4.09	0.1	0.4271
M5	-1.06	3.87	0.22	0.4017
M10	-0.56	3.24	0.054	0.3329
M15	-0.21	2.7	0.063	0.278
M20	-0.22	2.32	0.055	0.2391
M25	-0.11	1.918	0.0456	0.1975
M30	-0.032	1.675	0.0343	0.1711
M40	-0.006	1.263	0.0277	0.1295
M60	-0.0034	0.908	0.0149	0.09208
M80	0.0004	0.72	0.008	0.0725
M100	-0.0003	0.568	0.0041	0.057

Mss11-7a

Steps	*x*	*y*	*z*	*m*
NRM	-1.79	5.03	-0.22	0.5345
T150	-1.82	4.76	-0.16	0.5094
T200	-1.54	4.72	0.03	0.4963
T250	-1.34	4.2	0.16	0.4409
T300	-1.49	4.08	0.19	0.4347
T350	-1.17	3.85	0.24	0.4032
T400	-1.09	3.51	0.31	0.3689
T430	-1.03	3.2	0.35	0.3381
T460	-0.94	3.03	0.39	0.3199
T490	-0.99	2.88	0.36	0.3068
T540	-0.67	2.44	0.38	0.256
T580	-0.605	1.953	0.323	0.207
T600	-0.301	1.277	0.202	0.1328
T620	-0.263	0.921	0.15	0.09696

Mss11-8b

Steps	*x*	*y*	*z*	*M*
NRM	1.18	3.29	4.01	0.5317
T150	1.07	3.3	3.94	0.5246
T200	1.12	3.08	3.77	0.4993
T250	1.11	2.65	3.61	0.4609
T300	0.92	2.46	3.48	0.4362
T350	0.79	2.31	3.32	0.4128
T400	0.79	2.13	3.14	0.3875
T430	0.8	1.63	2.9	0.342
T460	0.69	1.52	2.62	0.311
T490	0.68	1.45	2.52	0.2985

T520	0.73	1.23	2.42	0.2805
T540	0.62	1.07	2.1	0.2438
T580	0.508	0.936	1.772	0.2067
T600	0.364	0.607	1.129	0.1332
T620	0.246	0.45	0.757	0.9145

Mss11-9b

Steps	*X*	*y*	*z*	*M*
NRM	0.65	3.69	3.15	0.4897
T150	0.51	3.75	3.04	0.4855
T200	0.46	3.46	2.99	0.4595
T250	0.59	2.98	2.78	0.4123
T300	0.38	2.85	2.73	0.3967
T350	0.48	2.62	2.63	0.3742
T400	0.33	2.2	2.67	0.348
T430	0.39	1.97	2.27	0.3035
T460	0.46	0.205	2.78	0.3486
T490	0.39	0.182	2.06	0.2773
T520	0.304	0.1602	1.928	0.2524
T540	0.245	0.1416	1.787	0.2293
T580	0.276	0.1202	1.464	0.1915
T620	0.1	0.0393	0.551	0.6838

Mss11-10b

Steps	x	y	z	m
NRM	-1.95	5.96	4.15	7.516
m15	141.9	-96.6	-0.9	171.7
m50	232	-97	-7	251.3
m66	263	-58	-8	269.1
m83	254	-111	-4	277.4
m168	283	18	-11	284
m253	251	139	-10	286.8
m337	282	-78	-5	293
m504	281	71	-6	289.5
m666	282	42	-5	285.4
m831	288	-8	-2	288.5
m994	288	-27	-1	289.6
m1154	278	-90	0	291.7

Mss2-3ca

steps	*x*	*y*	*z*	*m*
NRM	-0.3	3.35	4.52	5.629
m15	121	-11.3	7.8	121.8
m50	360	145	19	388
m66	491	12	21	491.8
m83	545	-70	13	549.2
m168	630	-27	23	631.2
m253	627	156	22	646.5
m337	642	-130	22	655.2
m504	652	-32	20	653.2
m666	650	40	21	652
m831	652	-8	30	652.3
m994	621	-250	20	670.1
m1154	623	-175	19	647.4

Mss1-6ct

Steps	*x*	*y*	*z*	*M*
NRM	25.8	-17	27.2	41.18
m15	-18.1	-137.1	18.6	139.5
m50	245	-41	-21	249.1
m66	259	-54	-22	265.9

m83	272	-8	-27	273.3
m168	283	-2	-27	284.6
m253	286	-23	-26	287.9
m337	285	45	-31	290.2
m504	288	8	-28	289.5
m666	283	52	-29	289.4
m831	286	7	-26	287.6
m994	283	53	-27	289.5
m1154	285	24	-26	287.2

Mss2-5ca

steps	*X*	*y*	*z*	*M*
NRM	-11.6	-26.9	15.8	33.26
m15	99.9	-5.4	16.2	101.4
m50	342	-33	35	345.8
m66	407	-132	43	429.9
m83	439	-164	49	471.6
m168	536	-46	48	539.9
m253	517	-221	59	565.3
m337	550	-107	55	563.1
m504	560	-30	54	563.3
m666	561	-25	59	564.5
m831	563	-17	54	565.4
m994	549	-161	63	575.6
m1154	560	84	52	568.9

Mss3-1ca

steps	*X*	*y*	*z*	*m*
NRM	6.33	-11.09	5.55	13.93
m15	83.4	25.3	-7.6	87.48
m50	294	75	24	304.8
m66	371	33	1	372.4
m83	405	2	-10	404.8
m168	463	-47	-39	466.9
m253	-291	38.2	75	485.8
m337	480	34	-47	483.4
m504	483	-37	7	484.4
m666	486	-22	-17	486.9
m831	466	-159	-4	492.2
m994	475	-157	4	500.1
m1154	470	-133	-62	492.1

Mss3-7ca

Steps	*x*	*y*	*z*	*m*
NRM	-0.197	0.223	-0.176	0.3459
m15	1.376	0.192	0.17	1.4
m50	17.84	1.22	6.18	18.92
m66	237	-63	6.4	25.3
m83	27.3	-2.7	7.4	28.38
m168	31.3	-11.7	7.9	34.37
m253	-31.8	-9.4	-7.1	33.89
m337	30.4	-14.2	8.3	34.54
m504	33.6	2.2	8.4	34.68
m666	33.1	-6.4	8.6	34.84
m831	33.8	-5.5	8.5	35.26
m994	33.8	6.8	7.4	35.3
m1154	33.1	7	7.7	34.66

Mss4-1ca

steps	*x*	*y*	*z*	*m*
NRM	-0.09	-0.41	-0.168	0.4521
m15	0.35	0.829	-0.247	0.9329
m50	15.89	-1.51	-1.74	16.06
m66	22.3	-1.5	1	22.36
m83	26.7	-1.9	1.4	26.81
m168	36.1	2.9	3	36.36
m253	-23.4	-30.5	-2.8	38.51
m337	38.5	-8	6.2	39.84
m504	39.8	-5.3	-1.3	40.13
m666	40.3	-4.7	4	40.81
m831	36.8	12.9	2.4	39.03
m994	40.2	-4	7.3	41.08
m1154	39.9	-4	-1.1	40.12

Mss5-7ca

steps	*x*	*y*	*z*	*m*
NRM	0.0045	0.0184	0.0302	0.03568
m15	0.0122	0.0854	0.0292	0.09105
m50	0.59	-0.075	0.034	0.5955
m66	0.862	0.214	0.031	0.8887
m83	1.083	0.164	0.031	1.096
m168	1.575	0.284	0.052	1.601

m253	1.737	-0.068	0.028	1.738
m337	1.747	-0.14	0.052	1.754
m504	1.777	-0.006	0.037	1.778
m666	1.793	0.1	0.044	1.796
m831	1.679	0.616	0.056	1.789
m994	1.815	-0.144	0.048	1.821
m1154	1.768	0.5	0.065	1.839

Mss6-1ca

steps	*X*	*y*	*z*	*m*
NRM	0.0065	0.0139	0.0326	0.03605
m15	0.0417	0.093	0.0257	0.1051
m50	0.732	0.087	0.064	0.7402
m66	1.001	0.162	0.082	1.017
m83	1.24	0	0.101	1.244
m168	1.719	0.017	0.135	1.724
m253	-0.294	1.842	-0.201	1.876
m337	1.86	0.019	0.145	1.866
m504	1.901	-0.175	0.153	1.915
m666	1.913	-0.255	0.174	1.938
m831	1.89	-0.542	0.172	1.974
m994	1.902	-0.408	0.193	1.955
m1154	1.956	-0.08	0.171	1.966

Mss6-3ca

steps	*X*	*y*	*z*	*m*
NRM	-0.032	0.1353	0.0541	0.1492
m15	0.636	0.232	0.051	0.6787
m50	6.19	3.04	-0.01	6.892
m66	9.09	1.16	0.07	9.161
m83	10.26	-3.57	0.05	10.87
m168	13.56	3	0.03	13.89
m253	14.48	-0.16	-0.05	14.48
m337	14.63	-1	0.03	14.66
m504	14.77	1.3	0.1	14.83
m666	13.69	6.26	-0.01	15.05
m831	14.89	-1.43	0.1	14.96
m994	14.14	-4	0.11	14.7
m1154	14.96	-0.06	0.12	14.97

Mss6-9ca

steps	*x*	*y*	*z*	*m*
NRM	-0.00679	0.00233	-0.0103	0.01256
m15	-0.0566	-0.0171	-0.0232	0.06347
m50	-0.398	-0.031	-0.114	0.4147
m66	0.488	0.095	0.094	0.5056
m83	0.586	0.048	0.154	0.6078
m168	0.813	-0.031	0.165	0.8298
m253	0.38	0.813	0.068	0.9
m337	0.896	-0.108	0.252	0.9369
m504	0.953	-0.089	0.195	0.9771
m666	0.983	0.041	0.202	1.004
m831	0.984	0.158	0.198	1.016
m994	1.016	-0.065	0.209	1.039
m1154	0.995	0.236	0.211	1.044

Mss7-3ca

steps	*X*	*y*	*z*	*m*
NRM	-0.00431	0.00921	-0.0015	0.01028
m15	0.0354	0.0188	-0.0026	0.04011
m50	-0.398	-0.138	-0.007	0.4217
m66	576	-0.07	-0.15	0.5759
m83	0.711	-0.006	-0.006	0.7108
m168	1.151	-0.239	-0.033	1.176
m253	-1.31	0.116	-0.027	1.315
m337	1.363	-0.136	-0.001	1.37
m504	1.399	0.124	-0.015	1.405
m666	1.162	0.803	-0.006	1.412
m831	1.407	0.152	-1	1.415
m994	1.392	-0.339	-0.029	1.433
m1154	1.408	0.294	-0.021	1.439

Mss7-7ca

steps	*x*	*y*	*z*	*m*
NRM	-0.0044	0.00805	0.00043	0.00919
m15	0.0197	0.036	0.0004	0.04107
m50	0.287	0.092	0.002	0.3017
m66	0.303	0.267	0	0.4039
m83	0.5	0.016	0.003	0.5005

m168	0.676	0.075	0.02	0.6801
m253	0.742	-0.06	0.008	0.7446
m337	0.756	0.024	0.008	0.7569
m504	0.768	0.055	0.01	0.7701
m666	0.572	0.558	0.016	0.7996
m831	0.785	0.035	0.016	0.7856
m994	0.792	0.055	0.015	0.794
m1154	0.793	0.061	0.019	0.7955

Mss7-9ca

steps	*X*	*y*	*Z*	*m*
NRM	0.416	0.204	0.978	1.082
m15	1.12	3.45	0.88	3.727
m50	9.8	-37.1	0.1	38.42
m66	47.7	-8.4	1.2	48.45
m83	50.7	-20.1	1.6	54.55
m168	63.1	13.3	2.3	64.49
m253	-60.3	-27	-3	66.12
m337	65.1	-9.1	1.8	65.8
m504	66.6	-5.2	1.7	66.85
m666	63.9	20.4	2.4	67.09
m831	66.5	9.1	2.5	67.17
m994	67.6	1	2.6	67.64
m1154	67.3	-6.2	2.5	67.67

Mss8-3ca

steps	*X*	*y*	*z*	*m*
NRM	0.217	0.419	0.435	0.6416
m15	-3.05	1.61	-0.26	3.46
m50	26.9	-2.6	6	27.69
m66	32.1	-5.6	8.9	33.8
m83	34.1	-12.9	7.6	37.25
m168	37.1	9.4	14.6	40.93
m253	40.8	-2	10.8	42.26
m337	38.7	-19	7	43.66
m504	40.2	-4.9	11.5	42.06
m666	40.3	-5	12.1	42.37
m831	-10.1	8.7	8.8	43.28
m994	38.1	5.8	14.7	41.22
m1154	40.6	-1.7	12.5	42.5

Mss8-7ca

steps	*x*	*y*	*z*	*m*
NRM	0.142	0.55	0.189	0.5988
m15	1.458	1.153	0.152	1.865
m50	9.32	1.46	0.38	9.445
m66	10.26	3.77	0.11	10.93
m83	11.87	-0.35	0.38	11.88
m168	12.45	4.8	0.43	13.35
m253	12.73	-3.62	0.49	13.24
m337	13.28	1.09	0.6	13.33
m504	12.62	4.31	0.39	13.35
m666	10.02	9.44	0.38	13.77
m831	13.56	1.49	0.48	13.65
m994	13.72	3.27	0.5	14.11
m1154	13.55	2.99	0.76	13.9

Mss9-8ca

steps	*x*	*y*	*z*	*m*
NRM	0.0096	0.0325	-0.0687	0.07662
m15	0.838	-0.277	0.057	0.8841
m50	6.91	0.38	1.05	6.997
m66	9.47	-0.92	1.41	9.615
m83	11.45	-0.88	1.79	11.62
m168	16.4	-1.11	1.95	6.56
m253	17.77	-1.04	2.74	18.01
m337	18.18	-2.04	2.81	18.51
m504	18.61	-1.84	2.89	18.92
m666	17.7	-6.97	2.77	19.23
m831	18.61	-5.14	1.4	19.36
m994	18.99	0.39	-0.98	19.02
m1154	18.23	-4.75	3.01	19.08

Mss10-4ca

steps	*X*	*y*	*z*	*m*
NRM	0.0212	0.0477	-0.0541	0.07516
m15	0.964	0.896	-0.025	1.316
m50	7.71	-0.09	-0.08	7.713
m66	10.26	-0.78	-0.08	10.29
m83	12.39	0.08	-0.07	12.39

m168	17.17	-0.51	-0.09	17.18
m253	18.68	-0.71	-0.08	18.69
m337	19.14	-0.55	-0.19	19.15
m504	19.47	-2.77	0.05	19.67
m666	19.73	0.94	-0.04	19.75
m831	19.43	-4.29	-0.09	19.9
m994	19.81	-0.19	-0.02	19.81
m1154	19.8	-0.63	0.02	19.81

Mss10-6ca

steps	*X*	*y*	*z*	*m*
NRM	0.033	0.0845	-0.0877	0.1262
m15	0.764	-1.069	0.054	1.315
m50	9.4	0.83	0.94	9.488
m66	12.55	1.42	0.34	12.63
m83	14.6	-4.73	1.1	15.39
m168	19.17	3.55	0.23	19.5
m253	20.4	1.9	0.6	20.47
m337	20.9	0.2	0.7	20.96
m504	20.6	4.5	0	21.1
m666	21.2	-3.5	1.3	21.51
m831	20.2	6.2	2	21.1
m994	21.3	0.7	0.9	21.35
m1154	21.3	3.2	0.8	21.55

Mss10-7ca

steps	*X*	*y*	*z*	*m*
NRM	0.0126	0.0319	-0.0321	0.047
m15	-0.347	0.656	-0.046	0.7432
m50	5.48	0.44	0.08	5.503
m66	7.42	0.36	0.03	7.429
m83	8.92	-1.09	0.12	8.988
m168	12.49	0.18	0.18	12.49
m253	13.47	-0.88	0.21	13.5
m337	13.66	-1.88	0.26	13.79
m504	13.96	-1.84	0.24	14.08
m666	13.71	-3.7	-1.3	14.26
m831	14.22	-1.47	0.12	14.3
m994	14.34	-1.41	0.07	14.41
m1154	14.22	-1.61	0.14	14.31

Mss10-8ca

steps	*X*	*y*	*z*	*m*
NRM	-0.133	0.592	0.045	0.6088
m15	-0.629	-0.281	0.003	0.6893
m50	12.18	-1.65	0.66	12.31
m66	16.22	4.05	0.76	16.73
m83	19.79	-1.17	1.06	19.86
m168	24.3	-9	1.4	25.94
m253	27.2	2.1	2.2	27.39
m337	27.2	4.7	2.1	27.68
m504	26.1	8.5	2	27.48
m666	26	10.3	2.5	28.1
m831	-0.1	-4.3	0.9	4.35
m994	25.6	-12.5	1.5	28.5
m1154	27.3	-6.1	2.2	28.05

Mss11-6ca

steps	*X*	*y*	*z*	*m*
NRM	-0.214	0.486	-0.025	0.5313
m15	-0.39	-0.416	-0.061	0.5737
m50	10.83	-0.99	0.74	10.9
m66	13.58	5.91	1.17	14.86
m83	17.67	-0.9	1.33	17.74
m168	21.6	2.6	1.8	21.82
m253	24.7	-2.5	2	24.89
m337	25.1	-2.6	2	25.36
m504	25.3	-3.9	2	25.71
m666	25.6	1.4	1.9	25.71
m831	25.3	2.5	2.1	25.49
m994	25.9	-1.1	2.1	26.02
m1154	25.7	-2.5	2.3	25.96

Mss11-8ca

steps	*X*	*y*	*z*	*m*
NRM	0.135	0.343	0.418	0.5576
m15	1.186	0.123	0.402	1.258
m50	13.06	-1.96	0.57	13.21
m66	17.09	2.18	0.82	17.24

m83	19.92	-1.87	0.94	20.03
m168	24	-33	1.1	24.21
m253	25.4	-1.7	0.9	25.43
m337	25.5	1.8	1.4	25.63
m504	25.2	5.7	1.5	25.89
m666	26.1	2.6	1.3	26.22
m831	26.1	-1.1	1.3	26.16
m994	26	-5.3	1.3	26.53
m1154	25.6	6.3	1.3	26.37

Mss11-9ca

m300	11.22	-3.46	-0.31	117.4
m350	9.4	-3.26	-0.26	99.58
m400	7.47	-2.5	-0.16	78.73
m430	6.09	-1.79	-0.27	63.53
m460	3.94	-1.35	-0.1	41.69
m490	2.63	-0.79	-0.11	27.49
m520	2.41	-0.81	-0.12	25.51
m540	2.09	-0.81	0.1	22.5
m560	1.071	-0.358	-0.079	11.32
m580	0.888	-0.31	-0.064	9.433
m600	0.1809	-0.518	-0.0114	1.886
m620	0.449	-0.097	0	0.4594

Mss2-3ct

Steps	*X*	*y*	*z*	*m*
NRM	2.78	-0.9	0	291.7
T150	1.961	-0.667	-0.51	207.2
T200	1.504	-0.467	-0.44	157.6
T250	1.35	-0.481	-0.37	143.4
T300	1.122	-0.346	-0.31	117.4
T350	0.94	-0.326	-0.26	99.58
T400	0.747	-0.25	-0.16	78.73
T430	0.609	-0.179	-0.27	63.53
T460	0.394	-0.135	-0.1	41.69
T490	0.263	-0.079	-0.11	27.49
T520	0.241	-0.0081	-0.12	25.51
T540	0.209	-0.0081	0.1	22.5
T560	0.1071	-0.0826	11.32	
T580	0.0888	-0.0031	-0.064	9.433
T600	0.01809	-0.0052	-0.0114	1.886
T620	0.00449	-0.0009	-0.016	0.4594

Mss1-6ct

Steps	*x*	*y*	*z*	*m*
NRM	2.85	0.24	-0.26	287.2
m150	1.984	0.102	-0.205	199.7
m200	1.729	0.099	-0.176	174.1
m250	1.397	0.031	-0.145	140.4
m300	1.157	0.073	-0.128	116.6
m350	0.893	0.067	-0.093	90.01
m400	0.723	0.03	-0.086	72.81
m430	0.572	0.048	-0.071	57.82
m460	0.449	-0.021	-0.052	45.27
m490	0.34	0	-0.048	34.32
m520	0.282	-0.01	-0.038	28.42
m540	0.226	-0.05	-0.006	22.63
m560	0.1154	-0.014	-0.0016	11.65
m580	0.0901	-0.0435	-0.0032	10.48
m600	0.024	0.0092	-0.0031	0.2592
m620	0.0235	0.0097	-0.0031	0.2563

Mss2-5ct

Steps	*X*	*y*	*z*	*m*
NRM	2.78	-9	0	291.7
m150	19.61	-6.67	-0.51	207.2
m200	15.04	-4.67	-0.44	157.6
m250	13.5	-4.81	-0.37	143.4

Steps	*x*	*y*	*z*	*m*
NRM	5.6	0.84	0.52	568.9
m150	4.92	0.47	0.45	496.6

m200	4.56	0.44	0.42	460.4
m250	4.29	0.42	0.37	432.5
m300	4	0.44	0.37	403.8
m350	3.51	0.32	0.32	354.2
m400	3.21	0.43	0.31	325.3
m430	2.78	0.38	0.27	281.5
m460	2.35	0.25	0.23	237.6
m490	2.04	0.3	0.19	206.8
m520	1.348	0.181	0.125	136.5
m540	0.209	0.026	0.023	21.18
m560	0.1248	0.013	0.0137	12.62
m580	0.1208	0.0116	0.0112	12.19
m600	0.47	0.0057	0.0044	4.753
m620	0.345	-0.0018	0.0027	3.467

Mss3-1ct

Steps	*x*	*y*	*z*	*m*
NRM	3.31	0.7	0.77	34.66
m150	2.94	0.5	0.66	30.5
m200	2.78	0.55	0.6	29.01
m250	2.53	0.5	0.56	26.39
m300	2.33	0.32	0.47	24
m350	2.14	0.48	0.48	22.47
m400	1.836	0.368	0.406	19.16
m430	1.73	0.391	0.402	18.19
m460	1.41	0.272	0.316	14.7
m490	1.372	0.345	0.325	14.52
m520	1.233	0.284	0.278	12.95
m540	0.804	0.149	0.176	8.368
m560	0.782	0.142	0.163	8.113
m580	0.596	0.122	0.124	6.212
m600	0.534	0.101	0.112	5.547
m620	0.304	0.066	0.068	3.184

Mss4-1ct

Steps	*X*	*y*	*z*	*m*
NRM	4.7	-1.33	-0.62	492.1
m150	3.85	-0.92	-0.56	399.6
m200	3.76	-1.16	-0.47	395.8
m250	3.49	-1.06	-0.43	367.1
m300	3.12	-0.74	-0.41	323.6
m350	3.03	-0.86	-0.38	317.2
m400	2.64	-0.69	-0.34	275
m430	2.48	-0.52	-0.29	255.4
m460	2.15	-0.55	-0.27	223.4
m490	1.649	-0.426	-0.203	171.5
m520	1.276	-0.386	-0.182	134.6
m540	0.823	-0.255	-0.109	86.89
m560	0.1332	-0.345	-0.135	13.83
m580	0.0624	-0.119	-0.059	6.384
m600	0.0296	-0.053	-0.029	3.021
m620	0.01911	-0.0267	-0.0186	1.939

Mss3-7ct

Steps	*x*	*y*	*z*	*m*
NRM	3.99	-0.4	-0.11	40.12
m150	3.4	-0.47	-0.09	34.29
m200	3.03	-0.5	-0.03	30.73
m250	2.69	-0.4	-0.05	27.18
m300	2.31	-0.32	-0.03	23.37
m350	1.932	-0.252	-0.23	19.48
m400	1.543	-0.189	-0.23	15.54
m430	1.383	-0.116	-0.08	13.88
m460	1.106	-0.122	-0.22	11.13
m490	1.044	-0.142	-0.19	10.54
m520	0.915	-0.134	-0.2	9.246
m540	0.825	-0.101	-0.15	8.313
m560	0.46	-0.079	-0.14	4.67
m580	0.452	-0.06	-0.15	4.562
m600	0.338	-0.049	-0.1	3.422
m620	0.1374	-0.0266	-0.02	0.1399

Mss5-7ct

Steps	*X*	*y*	*z*	*m*
NRM	17.68	5	0.65	1.839
m150	15.3	3.63	0.47	1.573
m200	14.3	3.9	0.3	1.482
m250	13.2	2.99	0.27	1.353
m300	11.55	2.67	0.29	1.186
m350	10.8	2.69	0.23	1.114
m400	8.94	2.26	0.27	0.9224
m430	7.74	1.75	0.29	0.7937
m460	7.03	1.54	0.27	0.7206
m490	5.71	1.43	0.18	0.5893
m520	5.12	0.97	0.19	0.5212
m540	4.11	0.97	0.11	0.4229
m560	2.19	0.43	0.09	0.2239
m580	1.916	0.407	0.61	0.1959
m600	0.682	0.13	0.24	0.06948
m620	0.404	0.055	0.15	0.04077

Mss6-1ct

Steps	*X*	*y*	*z*	*m*
NRM	19.56	-0.8	1.71	1.966
m150	17.13	-0.46	1.24	1.718
m200	15.71	-0.4	1.17	1.575
m250	13.62	-1.34	0.93	1.372
m300	12.6	-1.39	0.86	1.271
m350	10.81	-0.57	0.7	1.085
m400	8.56	-0.49	0.71	0.8605
m430	7.99	-0.63	0.67	0.8043
m460	7.09	-0.75	0.6	0.7158
m490	4.76	-0.48	0.42	0.4798
m520	4.66	-0.49	0.38	0.4705
m540	4.02	-0.2	0.34	0.4041
m560	1.241	-0.063	0.119	0.1248
m580	1.166	-0.098	0.105	0.1174
m600	0.754	-0.036	0.072	0.07581
m620	0.547	-0.061	0.049	0.05522

Mss6-3ct

Steps	*x*	*y*	*z*	*m*
NRM	14.96	-0.06	0.12	14.97
m150	13.23	0.9	0.09	13.26
m200	11.9	0.13	-0.03	11.9
m250	11.15	0.64	0.07	11.16
m300	10.12	-0.18	0.01	10.13
m350	7.94	0.31	0.08	7.944
m400	6.56	0.17	-0.04	6.562
m430	5.65	0.27	0.01	5.652
m460	4.9	0.38	-0.02	4.916
m490	3.74	0.42	0.01	3.768
m520	3.26	0.26	-0.02	3.267
m540	2.37	0.26	0	2.387
m560	1.512	0.115	0.05	1.517
m580	1.463	0.053	0.02	1.464
m600	1.532	0.0186	0.27	0.1544
m620	1.504	0.0101	0.21	0.1508

Mss6-9ct

Steps	*x*	*y*	*z*	*m*
NRM	9.95	2.36	2.11	1.044
m150	8.66	1.98	1.69	0.9038
m200	7.22	1.62	1.41	0.7535
m250	6.13	1.64	1.17	0.6449
m300	5.06	1.08	1.02	0.5277
m350	4.54	1.07	0.89	0.4746
m400	4.04	0.97	0.8	0.4228
m430	3.7	0.81	0.74	0.3861
m460	3.43	0.68	0.69	0.3564
m490	3.06	0.74	0.63	0.3216
m520	2.22	0.43	0.46	0.2308
m540	2.06	0.46	0.42	0.2151
m560	1.834	0.413	0.377	0.1917
m580	1.847	0.332	0.367	0.1912
m600	1.518	0.35	0.331	0.1593
m620	0.765	0.147	0.162	0.7959

Mss7-3ct

Steps	*X*	*y*	*z*	*m*
NRM	14.08	2.94	-0.21	1.439
m150	11.08	1.96	-0.25	1.125
m200	8.89	1.82	-0.24	0.9075
m250	7.57	1.57	-0.17	0.7736
m300	5.72	0.94	-0.17	0.58
m350	4.29	0.73	-0.09	0.4348
m400	4.03	0.78	-0.06	0.4103
m430	3.67	0.38	-0.01	0.3685
m460	3.19	0.45	-0.03	0.3224
m490	2.99	0.49	-0.03	0.3028
m520	2.36	0.43	-0.01	0.2401
m540	1.779	0.287	0.35	0.1803
m560	1.543	0.15	-0.02	0.155
m580	1.533	0.164	-0.09	0.1541
m600	1.393	0.181	-0.031	0.1405
m620	0.982	0.11	0.07	0.09877

Mss7-7ct

Steps	*x*	*y*	*z*	*m*
NRM	13.55	2.99	0.76	13.9
m150	11.26	1.85	0.51	11.42
m200	10.83	1.98	0.37	11.01
m250	9.84	1.19	0.24	9.918
m300	9.04	0.81	0.32	9.078
m350	8.05	0.95	0.12	8.107
m400	6.67	0.94	0.13	6.74
m430	5.83	0.84	0.34	5.896
m460	5.65	0.85	0.16	5.712
m490	5.13	0.89	0.19	5.215
m520	3.88	0.53	0.23	3.923
m540	3.49	0.65	0.16	3.555
m560	3.08	0.55	0.09	3.134
m580	3.08	0.55	0.03	3.131
m600	1.115	0.225	0.044	1.139
m620	1.055	0.185	0.023	1.072

Mss9-8ct

Steps	*X*	*y*	*z*	*m*
NRM	4.06	-0.17	1.25	42.5
m150	3.52	-0.16	1.09	36.93
m200	3.09	-0.19	0.88	32.15
m250	2.56	-0.08	0.75	26.71
m300	2.14	-0.08	0.67	22.42
m350	1.901	-0.135	0.576	19.91
m400	1.517	-0.107	0.472	15.93
m430	1.418	-0.45	0.443	14.86
m460	1.299	-0.068	0.406	13.63
m490	1.123	-0.038	0.332	11.72
m520	1.098	-0.058	0.337	11.5
m540	1.029	-0.059	0.303	10.74
m560	0.874	-0.035	0.291	9.214
m580	0.867	-0.035	0.263	9.069
m600	0.651	-0.023	0.191	6.791
m620	0.562	-0.032	0.177	5.896

Mss8-7ct

Steps	*x*	*y*	*z*	*m*
NRM	18.23	-4.75	3.01	19.08
m150	15.6	-4.21	2.44	16.34
m200	14.27	-4.01	2.24	14.99
m250	12.04	-3.2	1.84	12.59
m300	10.36	-2.9	1.72	10.9
m350	8.97	-2.48	1.37	9.404
m400	6.91	-2.02	1.15	7.292
m430	5.36	-1.45	0.87	5.624
m460	4.87	-1.6	0.79	5.187
m490	3.83	-1	0.6	3.999
m520	3.35	-0.94	0.56	3.522
m540	2.71	-0.72	0.44	2.841
m560	1.333	-0.381	0.227	1.404
m580	0.242	-0.073	0.045	0.2568
m600	0.204	-0.052	0.037	0.2142
m620	0.0954	-0.0256	0.0183	0.1005

Mss10-4ct

Steps	*X*	*y*	*z*	*m*
NRM	19.8	-0.63	0.02	19.81
m150	17.05	-1.37	0	17.11
m200	15.16	-0.53	-0.04	15.17
m250	12.14	-0.76	0.04	12.16
m300	10.46	-1.06	-0.06	10.51
m350	9.1	-1.01	-0.03	9.161
m400	6.85	-0.65	0.02	6.882
m430	6.24	-0.54	-0.01	6.264
m460	5.31	-0.53	0.02	5.338
m490	4.42	-0.28	0.06	4.432
m520	3.3	-0.35	0.04	3.317
m540	1.768	-0.191	0.38	1.779
m560	1.198	-0.088	0.04	1.202
m580	0.437	-0.018	0.06	0.4373
m600	0.1005	-0.079	0.016	0.1009
m620	0.0967	-0.038	0.014	0.09682

Mss10-6ct

Steps	*X*	*y*	*z*	*m*
NRM	2.13	0.32	0.08	21.55
m150	18.82	1.42	0.65	18.89
m200	16.85	1.61	0.48	16.93
m250	15.84	0.81	0.44	15.87
m300	14.15	0.71	0.39	14.17
m350	11.93	1.33	0.35	12.01
m400	8.88	0.58	0.27	8.902
m430	7.6	0.82	0.34	7.655
m460	7.44	0.66	0.29	7.48
m490	6.74	0.85	0.23	6.797
m520	4.8	0.3	0.18	4.811
m540	4.48	0.28	0.15	4.489
m560	2.28	0.11	0.09	2.28
m580	2.2	0.21	0.09	2.213
m600	0.356	0.042	0.019	0.359
m620	0.34	0.03	0.016	0.3415

Mss10-7ct

Steps	*x*	*y*	*z*	*m*
NRM	14.22	-1.61	0.14	14.31
m150	12.15	-1.37	0.16	12.23
m200	11.14	-0.91	0.05	11.18
m250	9.73	-0.99	0.1	9.777
m300	8.22	-1.01	-1.01	8.286
m350	7.01	-0.76	0.05	7.054
m400	5.69	-0.61	0.11	5.726
m430	4.89	-0.57	0.09	4.923
m460	4.22	-0.57	0.11	4.257
m490	3.78	-0.43	0.06	3.804
m520	2.89	-0.36	0.04	2.912
m540	1.879	-0.215	0.37	1.891
m560	0.315	-0.25	0.07	0.3162
m580	0.31	-0.054	0.07	0.3143
m600	0.291	-0.049	0.05	0.2948
m620	0.1751	-0.161	0.026	0.1758

Mss10-8ct

Steps	*x*	*y*	*z*	*m*
NRM	2.73	-0.61	0.22	28.05
m150	2.32	-0.51	0.16	23.79
m200	2.24	-0.43	0.14	22.8
m250	19.78	-3.64	1.47	20.16
m300	17.2	-4.1	1.24	17.73
m350	15.32	-3	1.08	15.65
m400	12.43	-2.36	0.87	12.69
m430	11.81	-2.52	0.84	12.1
m460	10.5	-2.14	0.62	10.73
m490	9.5	-1.89	0.54	9.702
m520	8.09	-1.45	0.57	8.24
m540	6.89	-1.35	0.52	7.035
m560	3.25	-0.62	0.21	3.312
m580	2.08	-0.51	0.15	2.143
m600	2.03	-0.43	0.15	2.083
m620	1.689	-0.32	0.121	1.723

Mss11-6ct

Steps	*X*	*y*	*z*	*m*
NRM	2.57	-0.25	0.23	25.96
m150	2.18	-0.25	0.19	22.05
m200	19.51	-2.53	1.62	19.74
m250	18.39	-2.45	1.46	18.61
m300	15.64	-2.37	1.38	15.87
m350	13.96	-1.43	1.16	14.08
m400	11.78	-1.53	1.01	11.92
m430	10.67	-1.57	0.86	10.82
m460	9.5	-1.57	0.75	9.659
m490	8.16	-1.09	0.59	8.251
m520	7.04	-1.02	0.53	7.136
m540	5.96	-0.57	0.45	6.008
m560	3.56	-0.46	0.29	3.607
m580	3.47	-0.47	0.25	3.515
m600	2.52	-0.29	0.21	2.549
m620	1.593	-0.135	0.141	1.605

Mss11-8ct

Steps	*x*	*y*	*z*	*m*
NRM	2.56	0.63	0.13	26.37
m150	2.21	0.5	0.11	22.68
m200	17.82	3.85	0.96	18.26
m250	16.45	3.4	1.01	16.83
m300	14.53	3.61	0.9	15
m400	10.87	2.47	0.5	11.16
m430	10.5	2.14	0.65	10.73
m460	9.53	2.34	0.59	9.832
m490	8.81	2.07	0.55	9.062
m520	7.6	1.77	0.41	7.817
m540	6.6	1.42	0.37	6.763
m580	4.01	0.79	0.18	4.094
m600	2.97	0.76	0.11	3.064
m620	2.14	0.47	0.12	2.191

Mss11-9ct

ACKNOWLEDGEMENT

I grateful to my advisor, Dr. Tesfaye Kidane, for a clear and precise training in the field sampling, sample treatment and data analysis back in the laboratory and for his continuous support passing throughout the study.

I also thank the Addis Ababa University, Earth Science Department for funding part of this work and for letting me use the facility of paleomagnetic laboratory for free, especially Dr.Tigistu Haile. I would like to thank Dr. Bekele Abebe, Ato Bayisa, Ato Marawi, and all staff members of Earth Science Department for providing the necessary materials for this study.

I am also grateful to Pr. Yo.ichiro Otofuji, Dr. Ishikawa Naoto and An, Geri, and Gain, for sharing their experience during preliminary works in the Kesem area.

I am very much grateful to my family; Dad, Mom, Dame, Dare, Hawi, Tare, and Tigist whenever I need you.